PH.D. PROGRAM
MEDITERRANEA UNIVERSITY OF REGGIO CALABRIA

DEPARTMENT OF CIVIL ENGINEERING, OF ENERGY, OF ENVIRONMENT AND OF MATERIALS (DICEAM)

PH.D. IN
CIVIL ENGINEERING,
ENVIRONMENT AND SECURITY

XXXI CYCLE

Title

Influence of Celerity and Force Changes In Pressure Pipes – Physical And Numerical Modelling of Transient Flow Phenomena

PH.D. STUDENT:
Pierfabrizio Puntorieri

TUTOR:
Prof. Giuseppe Barbaro

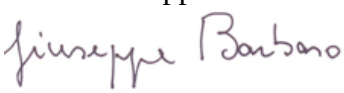

COORDINATOR:
Prof. Felice Arena

Acknowledgments

Heartfelt thanks - not just a routine thank-you – to: Prof. Giuseppe Barbaro, Dr. phd Agnieszka Malesińska, Prof. Didia Covas, Dr. phd Nuno Martins, Prof. Felice Arena, my co-workers from the University, Ylenia Albanese, Family and my co-workers from S.I.R. Cal. Srl for their support.

Chapter 1
INTRODUCTION

INTRODUCTION AND AIMS

Transient flow is the transition from one steady state to another steady state in a fluid flow system. Transient flow occurs in all fluids, confined and unconfined by Batterton (2006). A transition is caused by a disturbance to the flow. In a confined system, such as a water pipeline, an abrupt change to the flow that causes large pressure fluctuations is called water hammer. The name comes from the hammering sound that sometimes occurs during the phenomenon, Psrmiakian (1963).

The water hammer is a phenomenon generated when there is a change in the flow regime in a pressurized pipe, causing the acceleration and deceleration of particles in the flow inside the pipe system.

The water hammer has always been an area of study that has captivated the minds of researchers due to its complex and challenging phenomena.

It has been known to cause serious ruptures and losses in pipe systems. For these reasons, there are extensive studies in the literature related to water hammer, for example, in Shamloo H. (2015), (Libraga 2011) and Bruce (1995.).

THE ESSENCE OF THE WATER HAMMER PHENOMENON

The earliest study of the water-hammer made by Euler (1759) when he attempted a solution of the phenomena of flow of blood through the arteries. Lagrange in 1966 obtained solutions for the movement of incompressible fluids and compressible fluids in his work Lagrange (1788), After Cauchy became interested on the differential on a sound analytical basis, described in Cauchy (1890). During the summer and the winter Joukowski and Frizell in two different places they worked to study the pressures generated by the phenomenon of the water-hammer, certainly the most valuable studies for the understanding of this phenomenon with the contribution of Allevi (1902), described by Wood (1970).

Up to the present day with great researchers such as: Wood, Libraga, Betterton, Covas, Brunone.

The disturbance that spreads in the form of a pressure wave occurs in transient fluid flow conditions, described by Wylie (1993). The water hammer phenomenon happens when there are strong pressure oscillations in a pipe that is operating under pressure described by Libraga (2011). This is due to rapid changes in fluid flow rate forced in a short period of time. Physically, flows occurring in the form of hydraulic shock are caused by inertia of the mass of the fluid moving in the pipeline, where the flow rate changes suddenly. Rapid changes in the velocity and volume stream of flowing fluid leads to a local change in the proportion of kinetic and potential energy to the total energy of the section, which is expressed in a pressure increase or decrease in the stream. A rapid reduction of kinetic energy is observed in conditions of very rapid flow rate deceleration, which causes a sudden increase in potential energy, which in turn is manifested by a high-pressure increase. The course of water hammer phenomenon is significantly affected by fluid susceptibility to the compressibility and elasticity of the pipeline walls, i.e. their sensitivity to elastic strains due to hydrodynamic pressure changes in the pipeline. In extreme cases, this sudden pressure increase may cause an excessive amount of critical tensile stress in the pipeline walls, Meniconi S. (2012).

Water hammer is associated with an increase in pressure referred to as “positive impact”, which is accompanied by a sudden pressure drop called “negative impact”. The pressure gains for positive and negative water hammer phenomenon are calculated according to the formula of Joukowky-Allievi:

$$\Delta p = \pm \rho c \Delta v$$

Equation 1

where:
Δp = maximum pipe pressure increase in water hammer phenomenon [F/L2],
ρ = fluid density [M/L3],
c = the speed of propagation of the pressure wave, which is called celerity [L/T],
Δv = change in velocity [L/T].
Dimensions: F=Force, L=Length, M=Mass, T=Time.
For both positive and negative water hammer, two cases are possible:

- when $t_z < T$, where t_z = time of total valve opening, T = total time of wave propagation from the valve and back, then a straight surge will be observed in the pipe;
- when $t_z > T$, then a non-straight surge will be noted in the pipe.

Equation 1 is commonly known as the Joukowsky equation, but it is sometimes called either the Joukowsky–Frizell or the Allievi equation. Its first explicit statement in the context of water hammer is usually attributed to Joukowsky (1898).
Frizell (1898) and Allievi (1902), unaware of the achievements by Joukowsky and Frizell, also found Equation 1, but they did not provide any experimental validation. Anderson (2000) noted that Rankine (1870) had already derived Equation 1 in a more general context than water hammer.
Kries (1883) derived Equation 1 mentioning, without any particular reference, its existence in the theory of shock waves, but at the same time stating that it had not been validated by experiments, something that he would subsequently do.
There is a parallel between the contemporaries, Joukowsky (1847–1921) and Kries (1853–1928). Both are famous because of their work in other fields: Joukowsky in aerodynamics and Kries in physiology. Both of their investigations on water hammer are impressive because of their clarity and maturity in terms of their theoretical and experimental aspects.
The transient event of water hammer was difficult to capture in their day. Joukowsky measured fast waves in long steel pipes, and Kries measured slow waves in short rubber hoses; so their test systems had relatively large times L/c, where L/length of the tube Tijsseling (2007).
Contemporary analysis of water hammer phenomenon is most often based on the results obtained from the numerical solution of mathematical models. Most of these methods have their origin in differential equations of motion and continuity. In order to model the

water hammer phenomenon in conduits it is required to solve a set of momentum and continuity equations. The motion and continuity equations form a set of non-linear, hyperbolic, partial differential equations which cannot be solved by hand. A numerical method with an initial condition and two boundary conditions are needed. For a water distribution system, there are many more parameters needed for solving the water hammer problem. In a water distribution system, every branch of the system requires an additional boundary condition. External boundary conditions take on the form of a driving head, or a flow leaving the system. Internal boundary conditions arise in the form of nodal continuity, energy loss between points, head across valves, pumps, and more. The complexity of the problem requires the use of modelling software Batterton (2006).

Differential equations of motion and continuity are adopted in a simplified form, i.e. average flow parameters are "constant" and their derivatives are equal to zero, and the friction is reduced to a linear function. This results in a special solution of equations whose results are algebraic equations with respect to the parameters of pipelines and boundary conditions. Taking into account the impact of the enclosure on the solution, i.e. a valve, pump, or change in pipe diameter, it is possible to achieve a solution, i.e. a description of the phenomenon for a typical fluid transport system, without the necessity to refer to differential equations. It should be noted that by applying an equation reduced to a linear form to describe the phenomenon, the superposition principle can be used even for complex water supply or heating systems.

In the simplified equations of motion and continuity, pressure changes p are presented in the form of pressure head changes $H = p/\gamma$, and the equations have the following form (Wylie 1993).

$$\frac{\partial H}{\partial x} + \frac{1}{gQ}\frac{\partial Q}{\partial t} + \frac{\lambda Q^n}{2gDA^n} = 0$$

Equation 2

$$\frac{\partial Q}{\partial x} + \frac{gA}{c^2}\frac{\partial H}{\partial t} = 0$$

Equation 3

where H = piezometric head [m] of the liquid column, Q = volumetric flow rate [m^3/s], λ = multiplication factor of the friction element [-], n = power exponent [-], D = pipeline inner diameter [m], A = pipeline cross-sectional area [m^2], c = celerity [m/s], and g = acceleration due to gravity [m/s^2].

OBJECTIVE EXPERIMENTAL CAMPAIGN

The objective of the present work is to deepen the phenomena of unsteady flow and provide models for the study of the variables that come into play in the phenomenon of water hammer.
In the first phase of the research a deepening of the water hammer phenomenon was carried out, subsequently the fundamental parameters of this phenomenon were analysed (displacements, forces, celerity).
With this work, already illustrated and examined by various researchers during international conferences, we want to provide a simple but functional method of calculating the displacements and celerities during the water hammer phenomenon.
Specifically, it is very interesting to validate the model for the calculation of the equivalent celerity. There are several software models that model the phenomenon of water hammer but, all these software consider, in situations of conduct with different characteristics, a single celerity.
Chapter four shows how important it is, from the physical point of view, to homogenize celerity for pipes with different characteristics (diameter, material ...).
For these reasons this work is innovative and of useful application in the field of research, design, and verification of networks subject to the water hammer phenomenon.
All the numerical models were compared with physical modelling carried out in research laboratories, as shown below.
The present work is the result of three years of experimentation in two different laboratories.

1) The first experimentation was carried out at the Laboratory of Hydraulics and Environment at the Department of Civil Engineering, Architecture and Georesources, in the Instituto Superior Técnico, Lisbon, Portugal.
2) The second and third experiments were carried out at the Warsaw University of Technology, Warsaw, Poland.

The experiment conducted in Lisbon had the objective of understanding, through experimentation, the transient flow phenomena using measurements carried out in the laboratory pipe-rig, and confirming that the classic water hammer theory is not always valid in the presence of cavitation Puntorieri (2017).

The first experiment conducted at the Warsaw University had as its objective the study of water hammer phenomena on a physical model in combinations of two and three pipelines connected in series. The combined pipelines were made of steel and polypropylene. Pipelines made of one material type were connected in series in different configurations of diameter ratios and lengths of connecting sections. The obtained results were used to verify the value of the equivalent celerity calculated from equations derived using linear analysis of natural vibrations of the system. For verification of the equations, an algorithm in MATLAB has been developed that allows one to easily calculate the equivalent celerity, ce, for N pipelines connected in series with varying diameter, length and material composition, described by Malesinska A. (2018).

The second experiment conducted at the Warsaw University had as its objective to measure dynamic forces and associated displacements recorded on the model caused by transient flow conditions. For measured forces, the displacements of the pipe were also calculated by using the oscillation motion equations. Force measurements and displacement analysis were carried out in laboratory using the model of a simple fire protection system equipped with three nozzles. The measurement results and calculations were used to calibrate a mathematical model created using MATLAB software, by Malesinska A. (2018).

Chapter 2

EXPERIMENTAL STUDY OF THE TRANSIENT FLOW WITH CAVITATION IN A COPPER PIPE SYSTEM

This thesis presents the results of measurements carried out in the laboratory pipe-rig, confirming that the classic water hammer theory is not always valid in the presence of cavitation.

Three initial discharges are analysed with different closure positions, in steady state conditions. To improve the results of the numerical modelling, the valve manoeuvres need to be adjusted to fit the experimental data.

This research analyses the behaviour of the system, in steady state flow, for different positions of the valve closure and compares collected data for different transient events. The aim of the research is to show the steady and dynamic behaviour of the system due to the valve closure, described by Puntorieri (2017).

This work was presented at the WIT Transactions on Engineering Sciences conference in Tallin (2017) and published in the International Journal of Civil Engineering and Technology (2017).

EXPERIMENTAL FACILITY

This section presents a description of the experimental system and of the experimental programs carried out in a pipe-rig, assembled in the Laboratory of Hydraulics and Environment at the Department of Civil Engineering, Architecture and Georesources, in the Instituto Superior Técnico, Lisbon, Portugal, Puntorieri (2017).

The pipe system comprises a 15.22 m of copper pipe with an internal diameter of 20 mm and a wall thickness of 1 mm. Figure 1 presents the schematic of the pipe rig. The system operates at an approximately constant piezometric head, maintained by a pump with a nominal flow rate of Q=55 l/min at the upstream end, followed by a 60 L hydropneumatic vessel Figure 2. At the downstream end, a valve setup is positioned: first a pneumatic actuated spherical valve, the one that generates the water hammer, followed by a manually controlled spherical valve to control the flow rate, which is measured by a rotameter positioned after the valves setup. After the rotameter, the flow goes through a plastic pipe to a free surface storage tank that continuously supplies the system pump. Two pressure transducers are installed in the system: at the upstream of the pneumatic valve (PT1), and at the pipe mid-section (PT2). The pressure transducers (WIKA S-10) have a nominal pressure of 25 bars and a span of 0.5%.

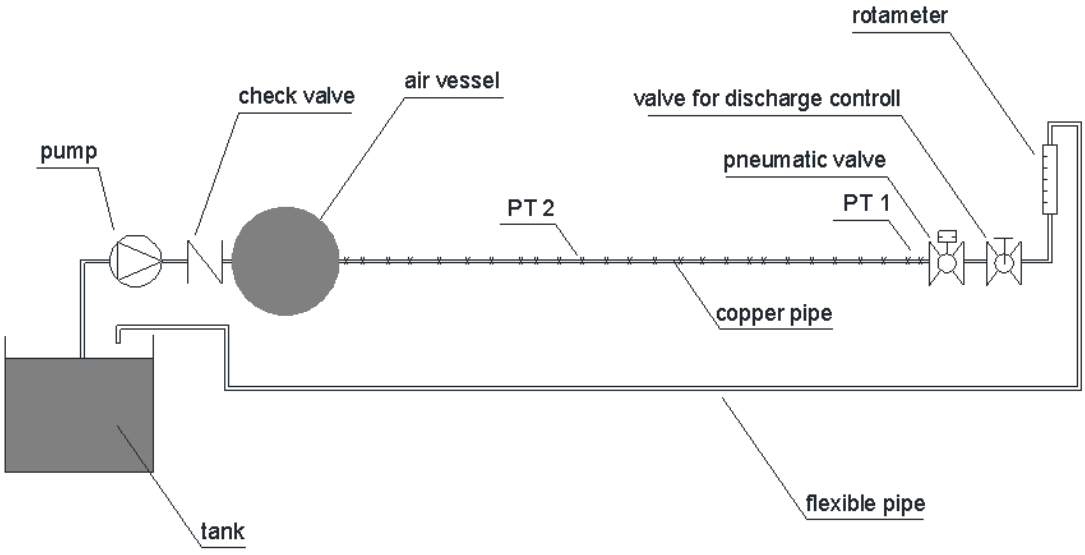

Figure 1 Schematic of the copper pipe system

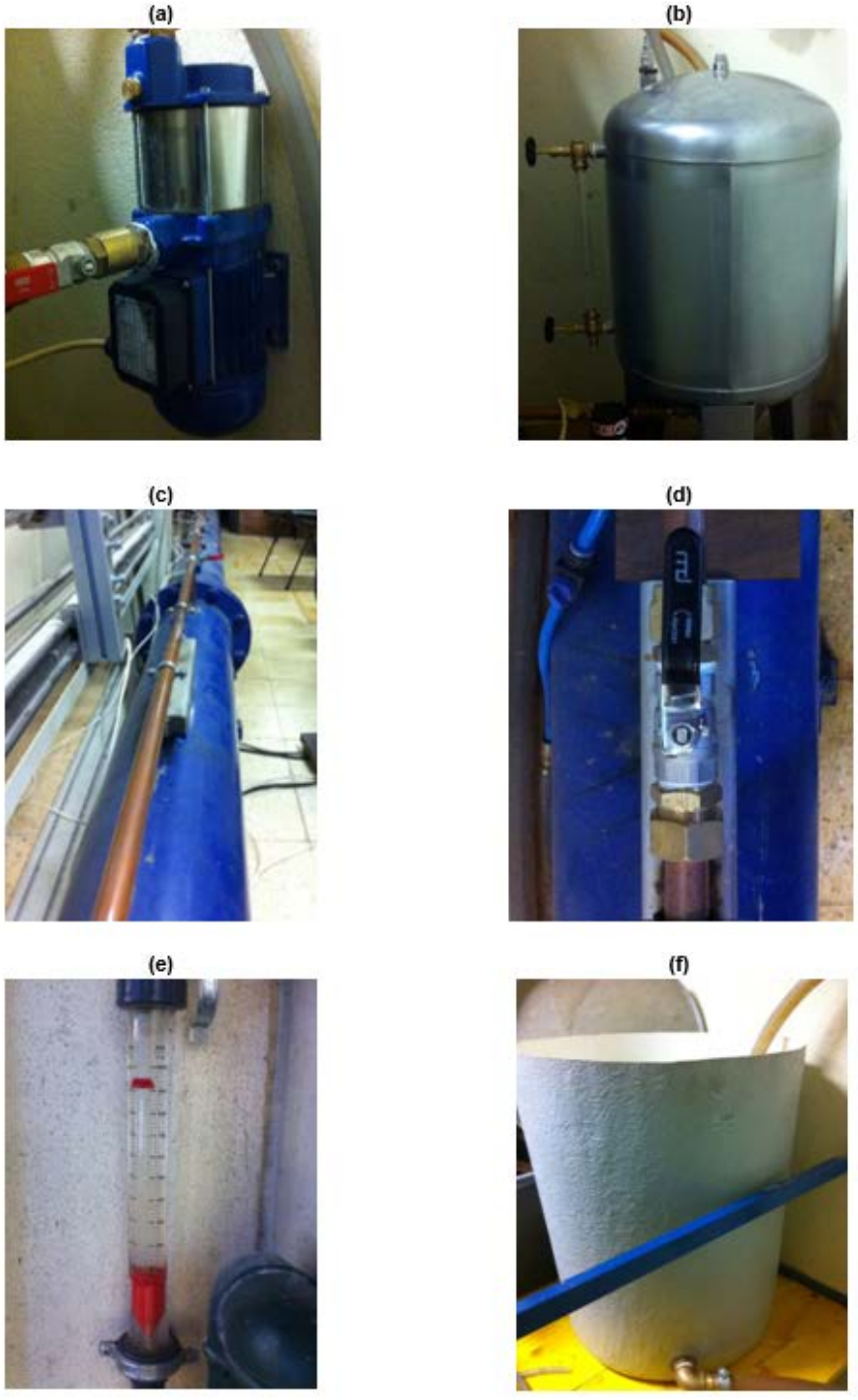

Figure 2 Schematic of the copper pipe system Copper-pipe facility: (a) Pump: (b) air vessel; (c) copper pipes; (d) manual ball valve; (e) rotameter; (f) tank.

The data acquisition signal converts all signals into numerical data using the digital oscilloscope (PicoScope™). The oscilloscope is then connected to a computer to storage.

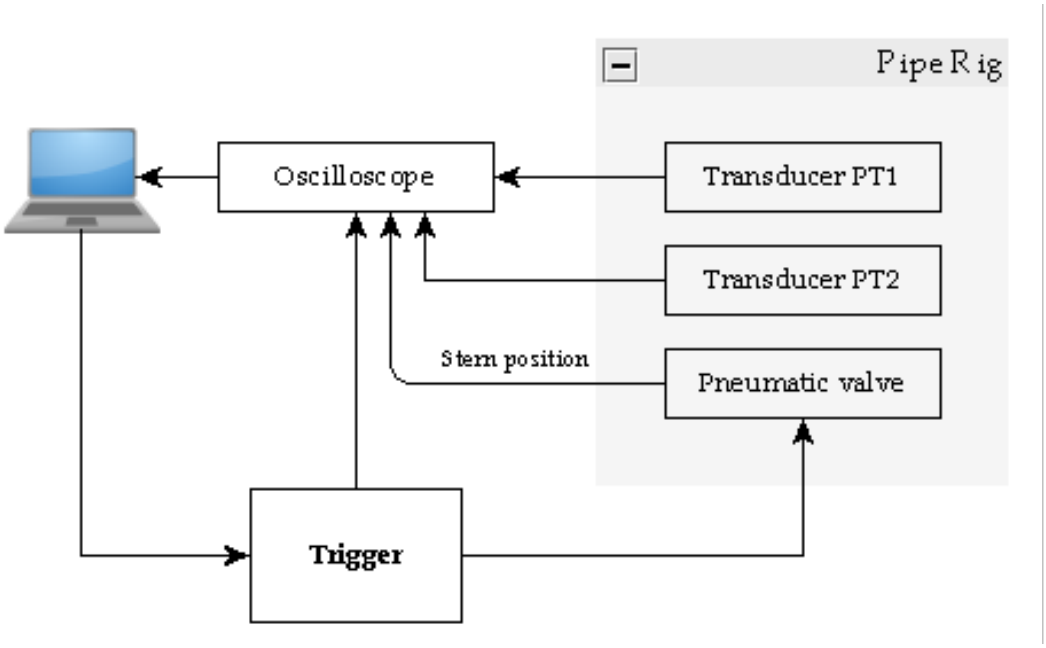

Figure 3 Scheme of the data acquisition system

ROTAMETER CALIBRATION

A rotameter is a device that measures the flow rate of a liquid in a closed tube. Before running the water hammer tests, the rotameter was tested and a calibration curve was obtained. For this purpose, the flow rate was measured in the flowmeter for different discharges and compared with the flow manually measured by the volumetric method. The volumetric method consists of measuring the time required for filling a container of known volume (11,43 litres).

Table 1 Summary of the rotameter calibration tests

		h (m)	time (s)	Ø sup	Ø inf	V (m^3)	V (l)	Q (m^3/s)	Q (l/h)	Δ
Test 1	1.1	0.23	350.0000	0.2772	0.225	0.0114	11.43	3.27E-05	117.57	17.57%
100	1.2	0.23	365.0000	0.2772	0.225	0.0114	11.43	3.13E-05	112.74	12.74%
l/hr	1.3	0.23	359.0000	0.2772	0.225	0.0114	11.43	3.18E-05	114.62	14.62%
Test 2	2.1	0.23	268.0000	0.2772	0.225	0.0114	11.43	4.27E-05	153.54	2.36%
150	2.2	0.23	263.0000	0.2772	0.225	0.0114	11.43	4.35E-05	156.46	4.31%
l/hr	2.3	0.23	265.0000	0.2772	0.225	0.0114	11.43	4.31E-05	155.28	3.52%
Test 3	3.1	0.23	212.0000	0.2772	0.225	0.0114	11.43	5.39E-05	194.10	-2.95%
200	3.2	0.23	215.0000	0.2772	0.225	0.0114	11.43	5.32E-05	191.39	-4.30%
l/hr	3.3	0.23	214.0000	0.2772	0.225	0.0114	11.43	5.34E-05	192.29	-3.86%
Test 4	4.1	0.23	174.0000	0.2772	0.225	0.0114	11.43	6.57E-05	236.49	-5.40%
250	4.2	0.23	174.0000	0.2772	0.225	0.0114	11.43	6.57E-05	236.49	-5.40%
l/hr	4.3	0.23	176.0000	0.2772	0.225	0.0114	11.43	6.49E-05	233.80	-6.48%
Test 5	5.1	0.23	148.0000	0.2772	0.225	0.0114	11.43	7.72E-05	278.03	-7.32%
300	5.2	0.23	147.0000	0.2772	0.225	0.0114	11.43	7.78E-05	279.93	-6.69%
l/hr	5.3	0.23	144.0000	0.2772	0.225	0.0114	11.43	7.94E-05	285.76	-4.75%
Test 6	6.1	0.23	131.0000	0.2772	0.225	0.0114	11.43	8.73E-05	314.12	-10.25%
350	6.2	0.23	131.0000	0.2772	0.225	0.0114	11.43	8.73E-05	314.12	-10.25%
l/hr	6.3	0.23	130.0000	0.2772	0.225	0.0114	11.43	8.79E-05	316.53	-9.56%
Test 7	7.1	0.23	116.0000	0.2772	0.225	0.0114	11.43	9.85E-05	354.73	-11.32%
400	7.2	0.23	116.0000	0.2772	0.225	0.0114	11.43	9.85E-05	354.73	-11.32%
l/hr	7.3	0.23	116.0000	0.2772	0.225	0.0114	11.43	9.85E-05	354.73	-11.32%
Test 8	8.1	0.23	101.0000	0.2772	0.225	0.0114	11.43	1.13E-04	407.42	-9.46%
450	8.2	0.23	102.0000	0.2772	0.225	0.0114	11.43	1.12E-04	403.42	-10.35%
l/hr	8.3	0.23	101.0000	0.2772	0.225	0.0114	11.43	1.13E-04	407.42	-9.46%
Test 9	9.1	0.23	92.0000	0.2772	0.225	0.0114	11.43	1.24E-04	447.27	-10.55%
500	9.2	0.23	91.0000	0.2772	0.225	0.0114	11.43	1.26E-04	452.19	-9.56%
l/hr	9.3	0.23	91.0000	0.2772	0.225	0.0114	11.43	1.26E-04	452.19	-9.56%
Test 10	10.1	0.23	83.0000	0.2772	0.225	0.0114	11.43	1.38E-04	495.77	-9.86%
550	10.2	0.23	84.0000	0.2772	0.225	0.0114	11.43	1.36E-04	489.87	-10.93%
l/hr	10.3	0.23	84.0000	0.2772	0.225	0.0114	11.43	1.36E-04	489.87	-10.93%
Test 11	11.1	0.23	78.0000	0.2772	0.225	0.0114	11.43	1.47E-04	527.55	-12.07%
600	11.2	0.23	79.0000	0.2772	0.225	0.0114	11.43	1.45E-04	520.88	-13.19%
l/hr	11.3	0.23	79.0000	0.2772	0.225	0.0114	11.43	1.45E-04	520.88	-13.19%
Test 12	12.1	0.23	71.0000	0.2772	0.225	0.0114	11.43	1.61E-04	579.57	-10.84%
650	12.2	0.23	72.0000	0.2772	0.225	0.0114	11.43	1.59E-04	571.52	-12.07%
l/hr	12.3	0.23	72.0000	0.2772	0.225	0.0114	11.43	1.59E-04	571.52	-12.07%

		h (m)	time (s)	Ø sup	Ø inf	V (m^3)	V (l)	Q (m^3/s)	Q (l/h)	Δ
Test 13	13.1	0.23	67.0000	0.2772	0.225	0.0114	11.43	1.71E-04	614.17	-12.26%
700	13.2	0.23	68.0000	0.2772	0.225	0.0114	11.43	1.68E-04	605.13	-13.55%
l/hr	13.3	0.23	66.0000	0.2772	0.225	0.0114	11.43	1.73E-04	623.47	-10.93%
Test 14	14.1	0.23	62.0000	0.2772	0.225	0.0114	11.43	1.84E-04	663.70	-11.51%
750	14.2	0.23	63.0000	0.2772	0.225	0.0114	11.43	1.81E-04	653.16	-12.91%
l/hr	14.3	0.23	62.0000	0.2772	0.225	0.0114	11.43	1.84E-04	663.70	-11.51%
Test 15	15.1	0.23	57.0000	0.2772	0.225	0.0114	11.43	2.01E-04	721.92	-9.76%
800	15.2	0.23	59.0000	0.2772	0.225	0.0114	11.43	1.94E-04	697.44	-12.82%
l/hr	15.3	0.23	58.0000	0.2772	0.225	0.0114	11.43	1.97E-04	709.47	-11.32%
Test 16	16.1	0.23	54.0000	0.2772	0.225	0.0114	11.43	2.12E-04	762.02	-10.35%
850	16.2	0.23	55.0000	0.2772	0.225	0.0114	11.43	2.08E-04	748.17	-11.98%
l/hr	16.3	0.23	55.0000	0.2772	0.225	0.0114	11.43	2.08E-04	748.17	-11.98%
Test 17	17.1	0.23	51.0000	0.2772	0.225	0.0114	11.43	2.24E-04	806.85	-10.35%
900	17.2	0.23	52.0000	0.2772	0.225	0.0114	11.43	2.20E-04	791.33	-12.07%
l/hr	17.3	0.23	51.0000	0.2772	0.225	0.0114	11.43	2.24E-04	806.85	-10.35%
Test 18	18.1	0.23	50.0000	0.2772	0.225	0.0114	11.43	2.29E-04	822.98	-13.37%
950	18.2	0.23	50.0000	0.2772	0.225	0.0114	11.43	2.29E-04	822.98	-13.37%
l/hr	18.3	0.23	50.0000	0.2772	0.225	0.0114	11.43	2.29E-04	822.98	-13.37%
Test 19	19.1	0.23	47.0000	0.2772	0.225	0.0114	11.43	2.43E-04	875.51	-12.45%
1000	19.2	0.23	47.0000	0.2772	0.225	0.0114	11.43	2.43E-04	875.51	-12.45%
l/hr	19.3	0.23	47.0000	0.2772	0.225	0.0114	11.43	2.43E-04	875.51	-12.45%

Rotameter measurements are plotted with volumetric measurements in Table 1 for a flow rate range from 100-1000 l/h. The correlation coefficient (R2) was calculated and the regression curve was obtained Figure 3.

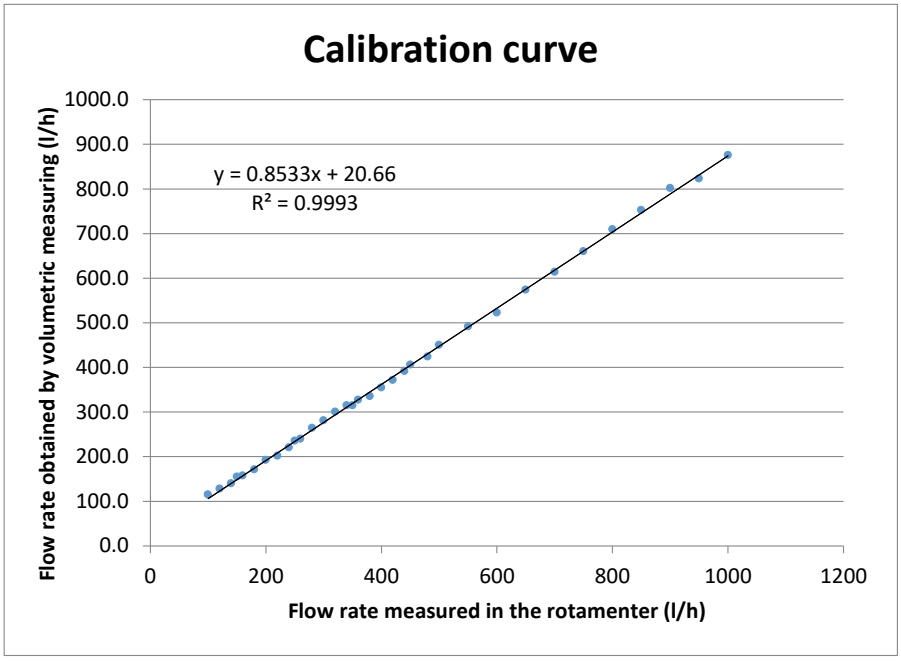

Figure 4 Calibration curves obtained by the relationship between the flow rate measured in the rotameter and the flow rate by volumetric measuring.

The relative error is positive for flow rates lower than 400 l/h and negative for higher flow rates. This error varies between 15% and -15%, tending to be constant for flow rates higher than 500 l/h Figure 4 and Figure 5.

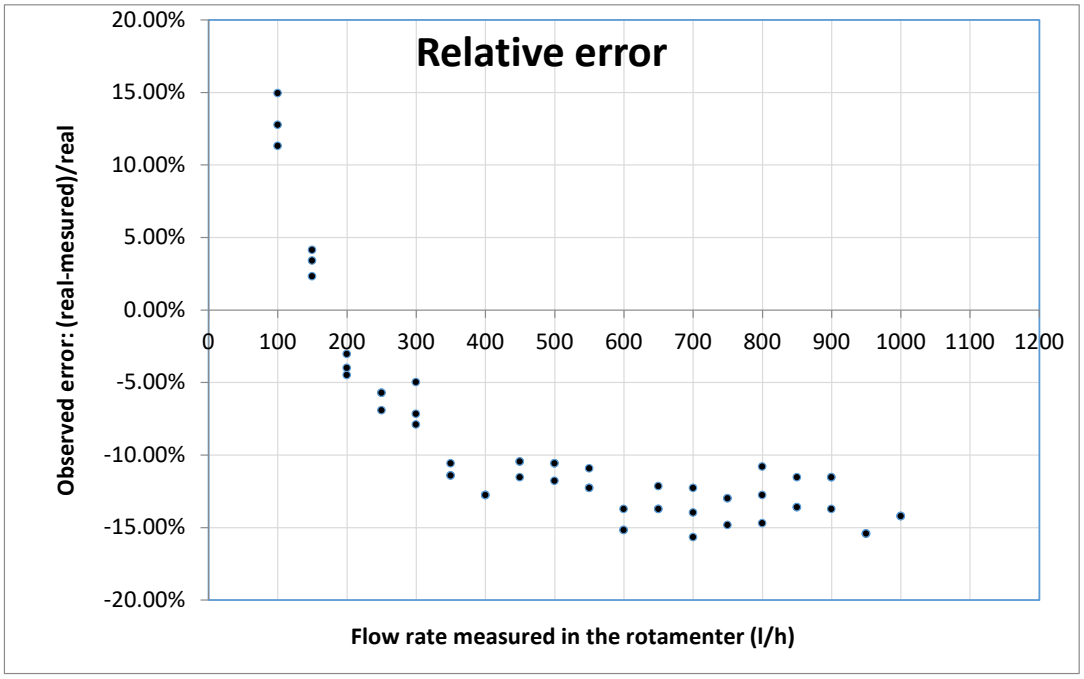

Figure 5 Chart representing the relative error between the flow rate measured in the rotameter and the flow rate by volumetric measurement.

TRANSIENT DATA COLLECTION

The instrumentation used for the measurement of the piezometric head time variation was composed of: two pressure transducers, an oscilloscope (Picoscope 3424) and a laptop computer. Seventeen tests have been carried out for different initial discharges and, for each discharge, the tests were repeated 20 times for obtaining the time-average. The water hammer was generated by instantaneous closure of the downstream end valve. Table 2 presents data obtained from the transient tests, namely the discharges and the corresponding maximum, minimum and amplitude of variation of the piezometric head, ΔHexp (which is the difference between the maximum piezometric head and the steady state one). Two values of celerity, the theoretical and the experimental, are also presented. The relative error between observed and theoretical Joukowsky overpressure, ΔHJ, are also presented.

Table 2 Table list of tests

Q	**Hsteady state**	**Hmax**	**Hmin**	**ΔH_{exp}**	**Celerity theor.**	**Celerity exp.**	**Joukowsky overpressure, ΔH_J**	**Relative Error**
[L/h]	[m]	[m]	[m]	[m]	[m/s]	[m/s]	[m]	[%]
115	47.03	61.31	32.11	14.28	1270	1242.45	12.89	9.7%
155	46.95	65.70	27.28	18.74	1270	1255.26	17.55	6.3%
192.6	**46.02**	**68.66**	**21.92**	**22.64**	**1270**	**1255.26**	**21.81**	**3.6%**
235.6	46.74	74.67	17.58	27.93	1270	1255.26	26.68	4.5%
281.2	46.56	80.26	11.44	33.70	1270	1255.26	31.85	5.5%
314.9	46.44	84.90	6.72	38.46	1270	1255.26	35.67	7.3%
354.7	46.27	89.62	1.19	43.35	1270	1255.26	40.18	7.3%
406.1	46.01	94.61	-4.05	48.60	1270	1255.26	45.99	5.4%
450.6	45.94	99.24	-7.62	53.30	1270	1255.26	51.03	4.3%
491.8	45.57	102.60	-9.27	57.03	1270	1255.26	55.70	2.3%
523.1	45.70	135.44	-9.97	89.74	1270	1255.26	59.24	34.0%
574.2	46.17	152.52	-10.07	106.35	1270	1255.26	65.03	38.9%
614.3	46.29	174.60	-10.21	128.31	1270	1255.26	69.57	45.8%
614.3	46.47	174.68	-10.26	128.21	1270	1255.26	26.68	79.2%
709.6	**47.00**	**172.51**	**-10.21**	**125.51**	**1270**	**1255.26**	**80.37**	**36.0%**
752.8	47.48	167.84	-10.29	120.35	1270	1035.05	70.30	41.6%
801.7	47.65	160.17	-10.19	112.52	1270	1014.67	73.39	34.8%

The celerity was measured experimentally as:

$$\boldsymbol{c_{exp} = \frac{4L}{T}}$$

Equation 4

The celerity was measured experimentally as:

$$\boldsymbol{\Delta H_{Joukowsky} = \frac{c_{exp}\Delta v}{g}}$$

Equation 5

where T= the wave period, L = the pipe length, g = the gravitational acceleration, Δv = the mean velocity variation. In conclusion, the relative error was found using the following equation Eq. (3):

$$\boldsymbol{RE = \frac{\left(H_{max} - H_{steady}\right) - \Delta H_{Joukowsky}}{H_{max} - H_{steady}}}$$

Equation 6

The following are graphs: Time history of the piezometric head from a range of 115 l/h up to a range of 801.7 l/h.

In particular, two cases are chosen to illustrate the phenomenon of the water hammer with and without cavitation: tests with discharges of 192.6 L/h and of 709.6 L/h (from Figure 6 to Figure 22). These tests were chosen to represent two different situations: a transient test without cavitation and a test with cavitation. In the first case, see Figure 6, it can be seen that at time t=0.2 s, the maximum values of the two pressure signals collected at two different locations (PT1 and PT2) are almost overlapped while in the second test, see Figure 16, two additional pressure peaks appear in the transient phase (Christopher E. 1998). As mentioned previously, this is due to the phenomenon of cavitation. For this setup, cavitation occurs for initial steady-state discharges higher than 523.1 L/h; after this value the R.E. increases. This confirms that the classic water hammer theory is not always valid in the presence of cavitation, given from Soares (2015) and Gale (2008).

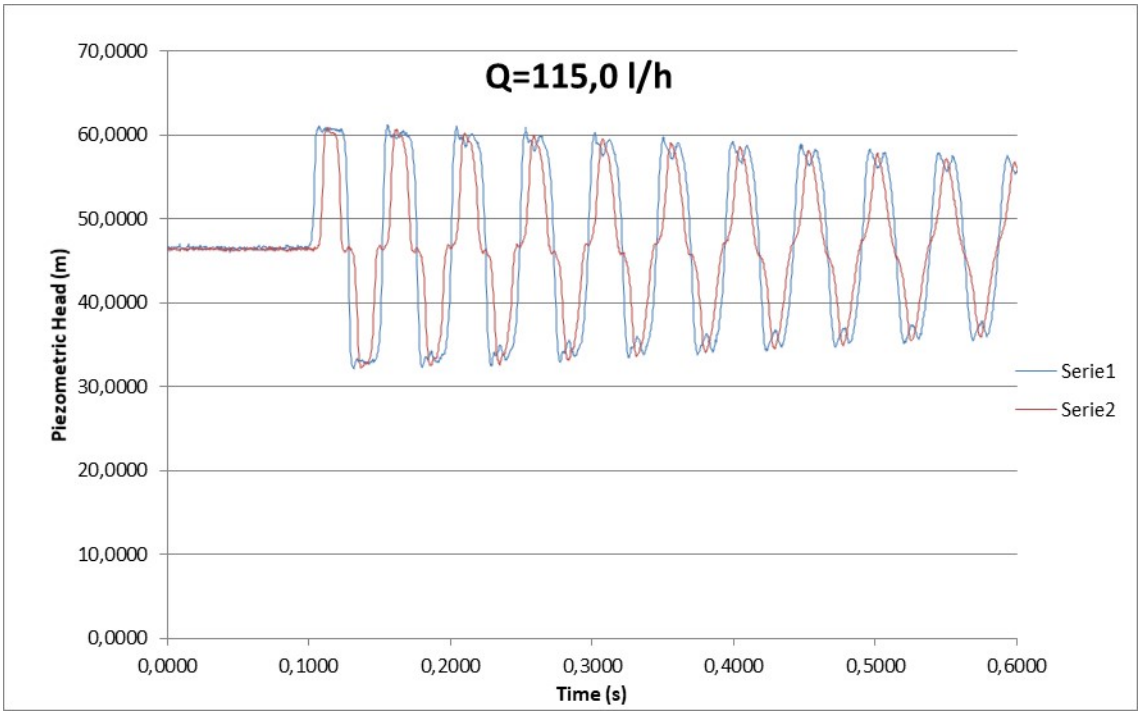

Figure 6 Time history of the piezometric head for Q0=115.0 l/h.

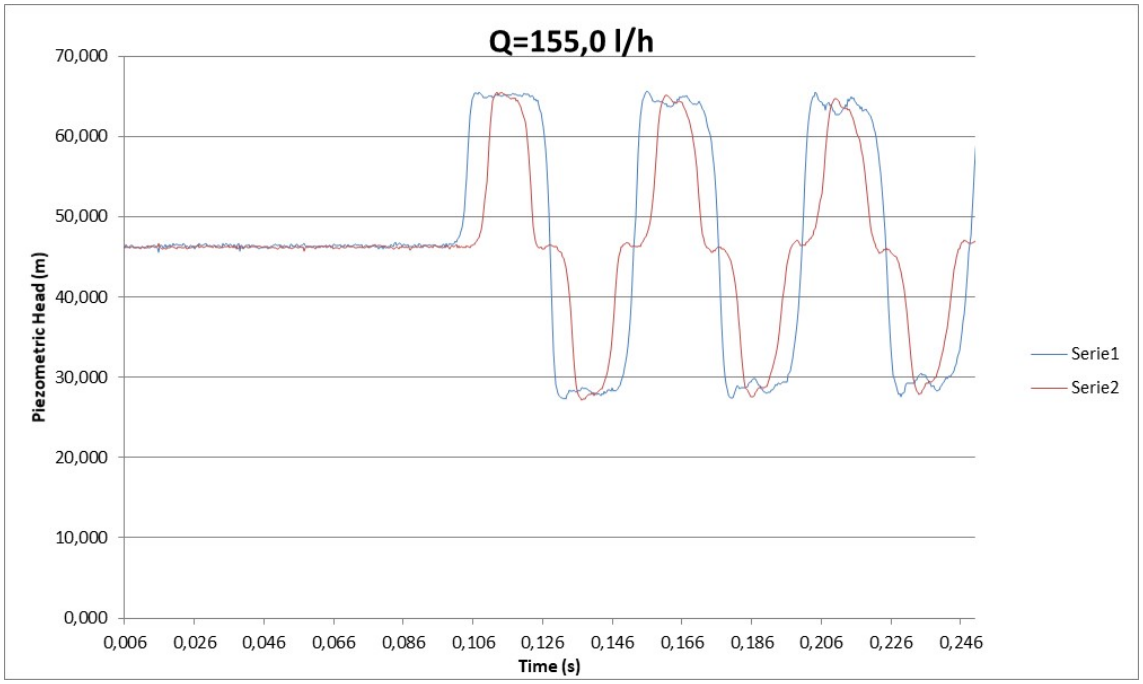

Figure 7 Time history of the piezometric head for Q0=155.0 l/h

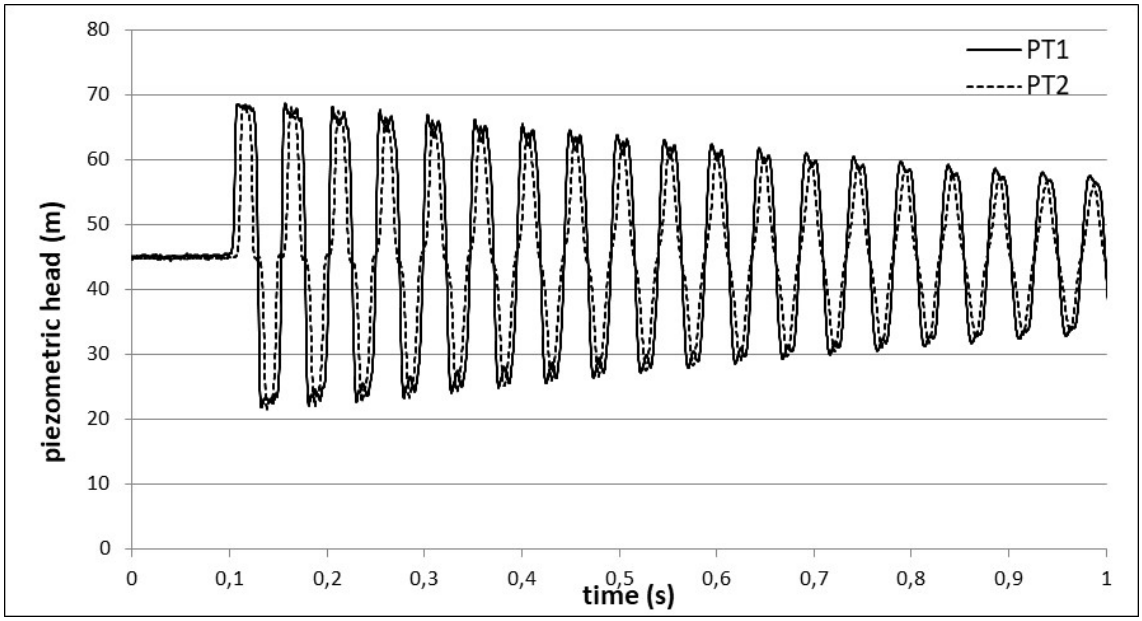

Figure 8 Time history of the piezometric head for Q0=192.6 l/h

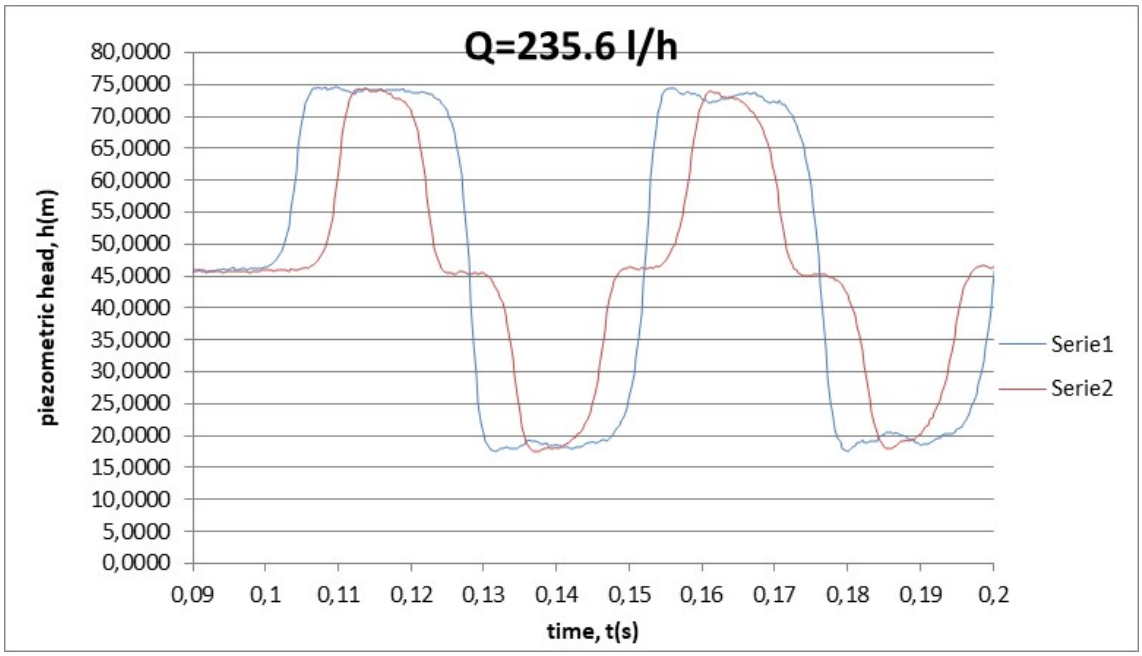

Figure 9 Time history of the piezometric head for Q0=235.6 l/h

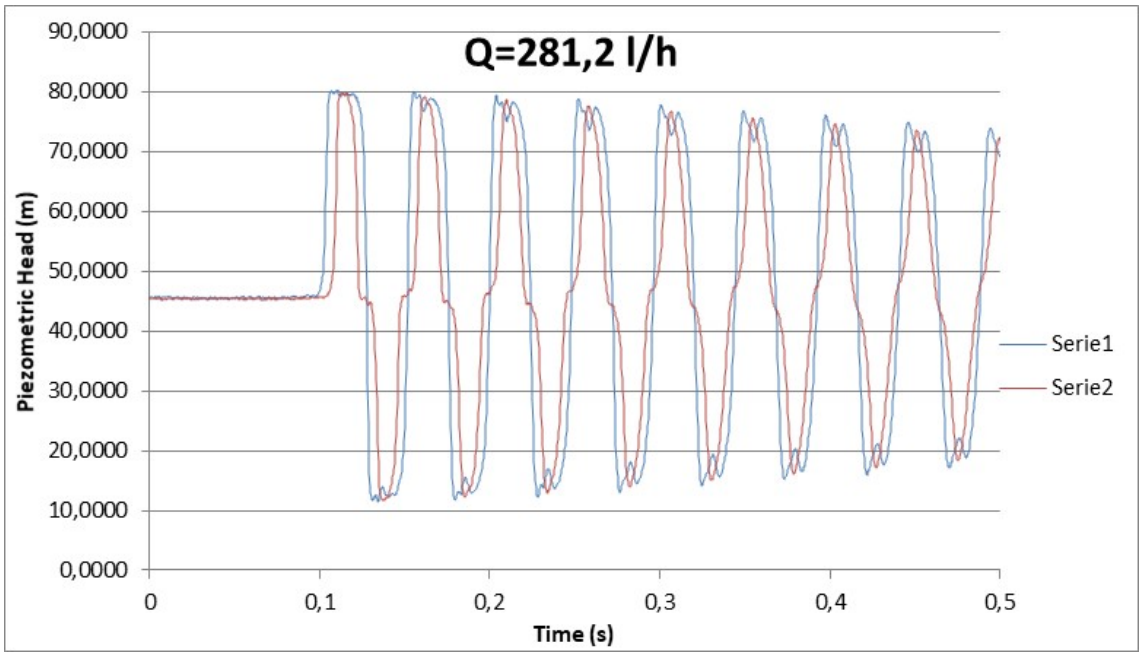

Figure 10 Time history of the piezometric head for Q0=281.2 l/h

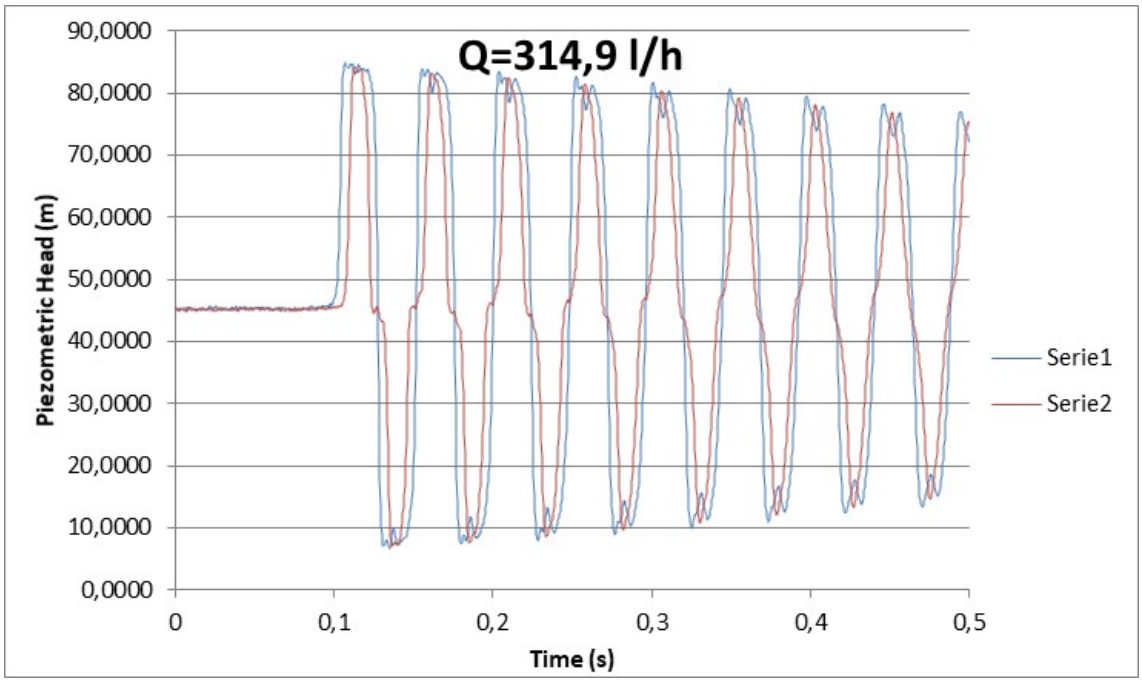

Figure 11 Time history of the piezometric head for Q0=314.9 l/h

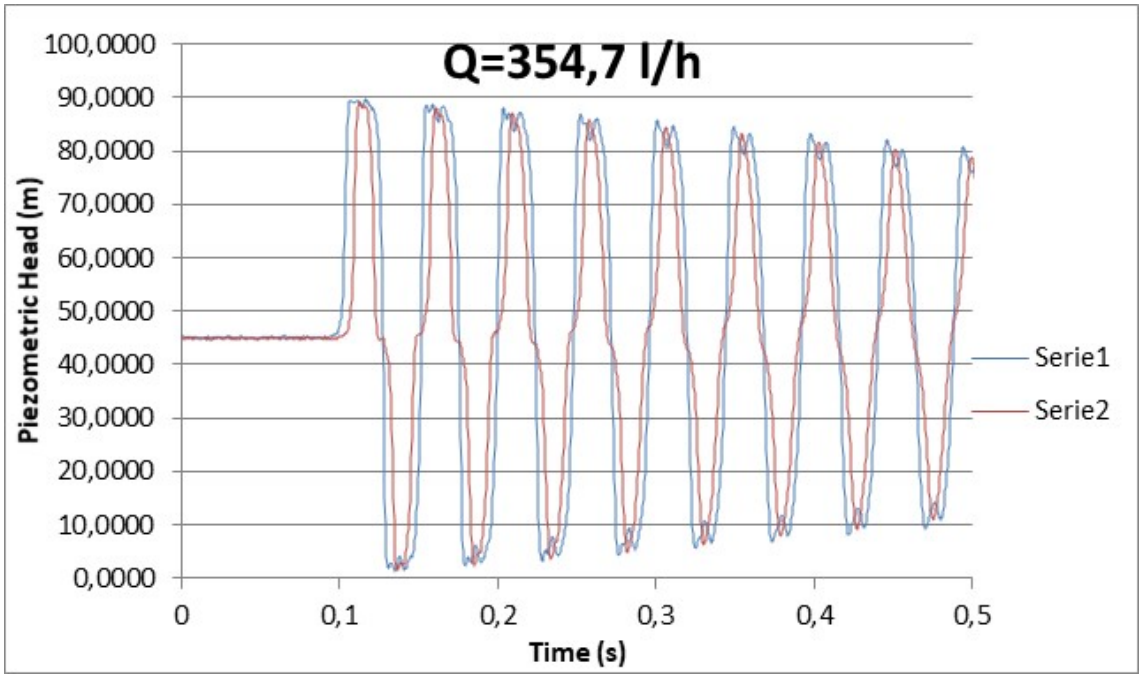

Figure 12 Time history of the piezometric head for Q0=354.7 l/h

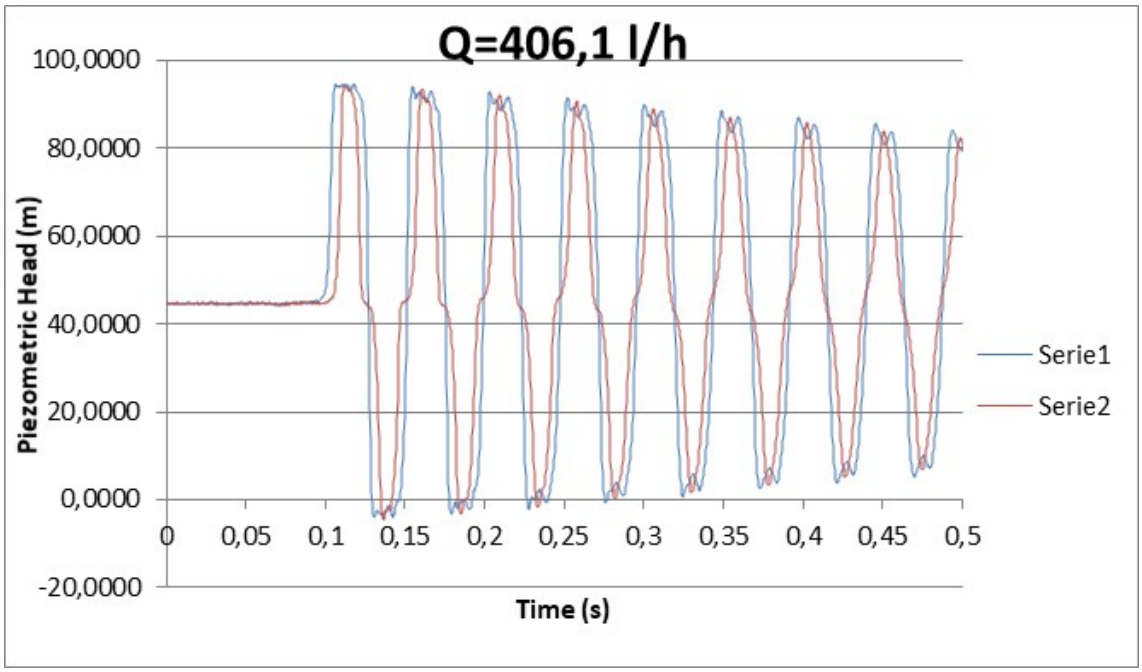

Figure 13 Time history of the piezometric head for Q0=406.1 l/h

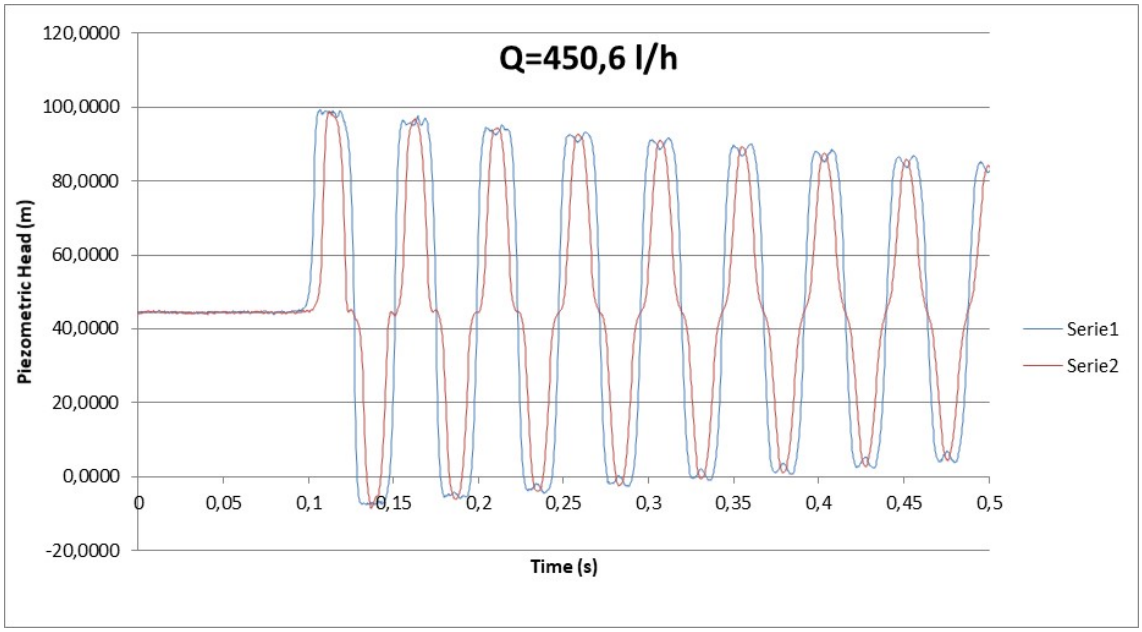

Figure 14 Time history of the piezometric head for Q0=450.6 l/h

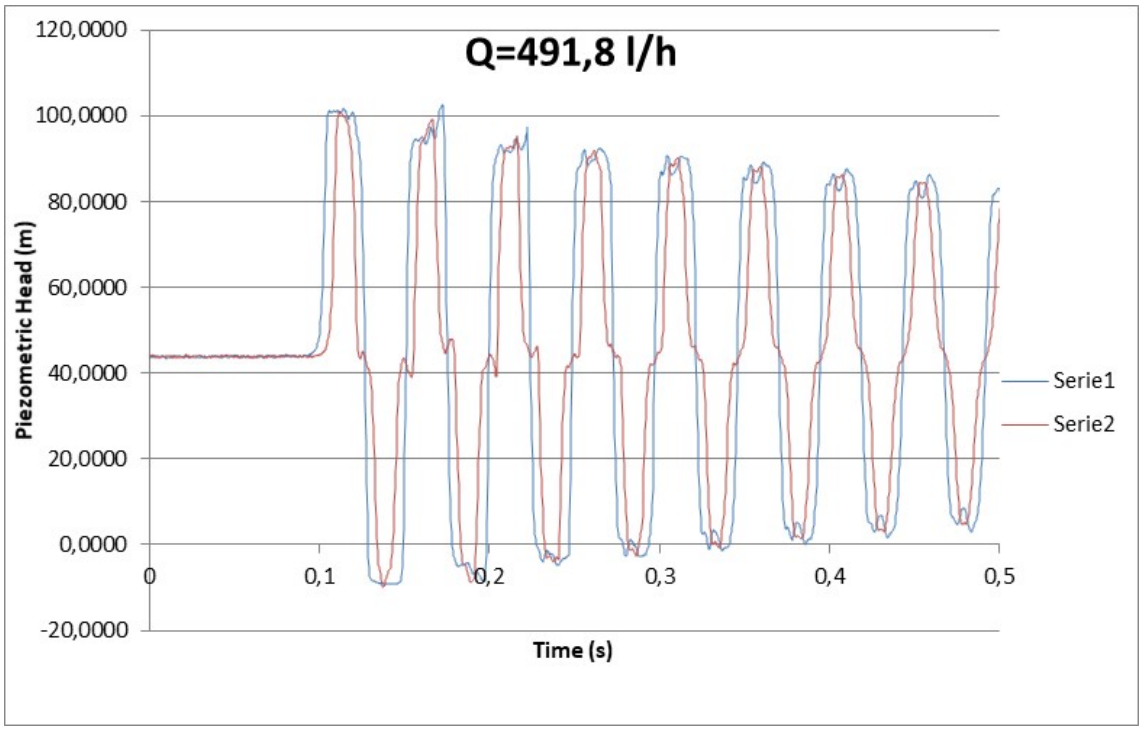

Figure 15 Time history of the piezometric head for Q0=491.8 l/h

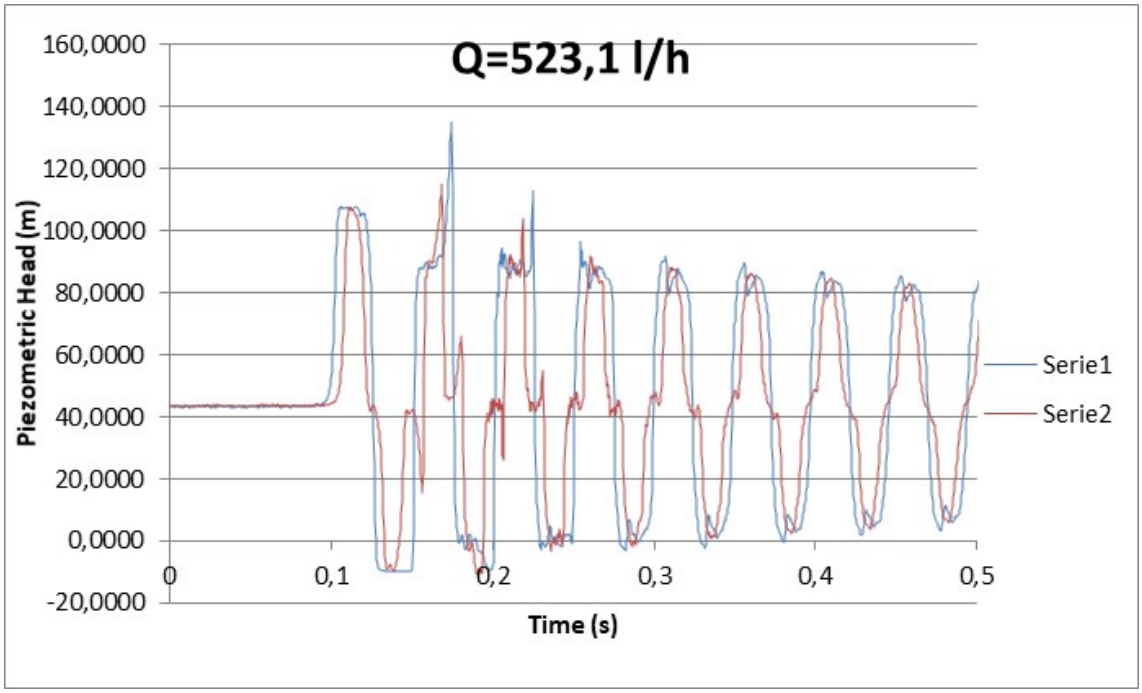

Figure 16 Time history of the piezometric head for Q0=523.1 l/h

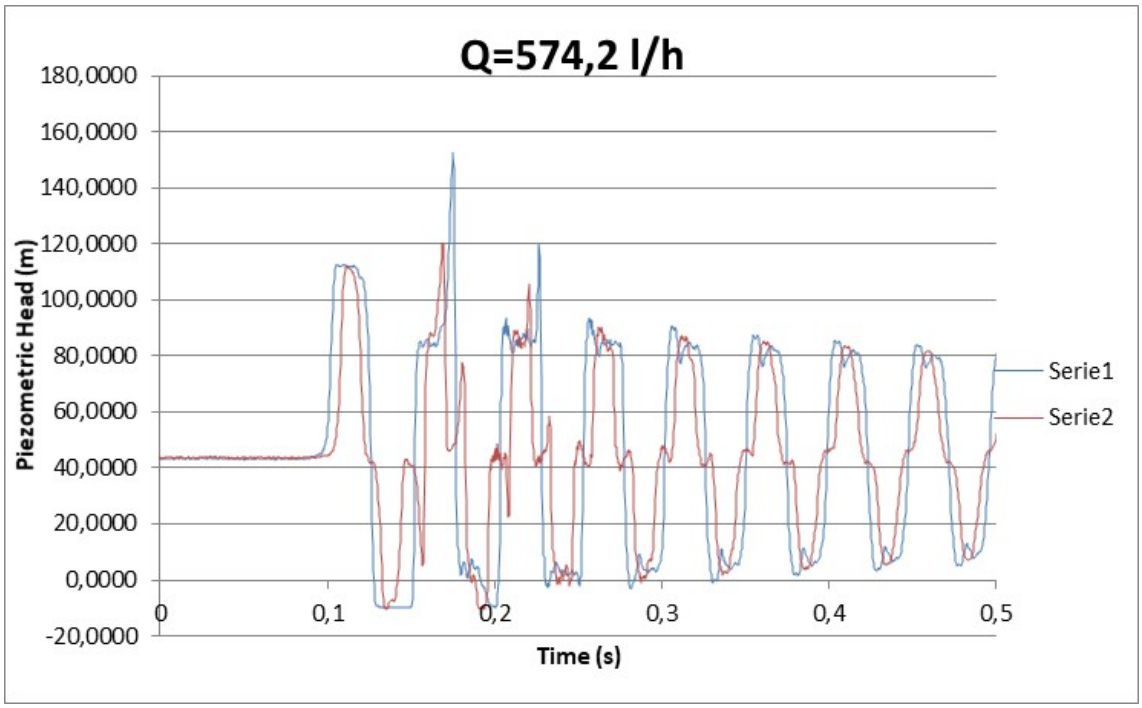

Figure 17 Time history of the piezometric head for Q0=574.2 l/h

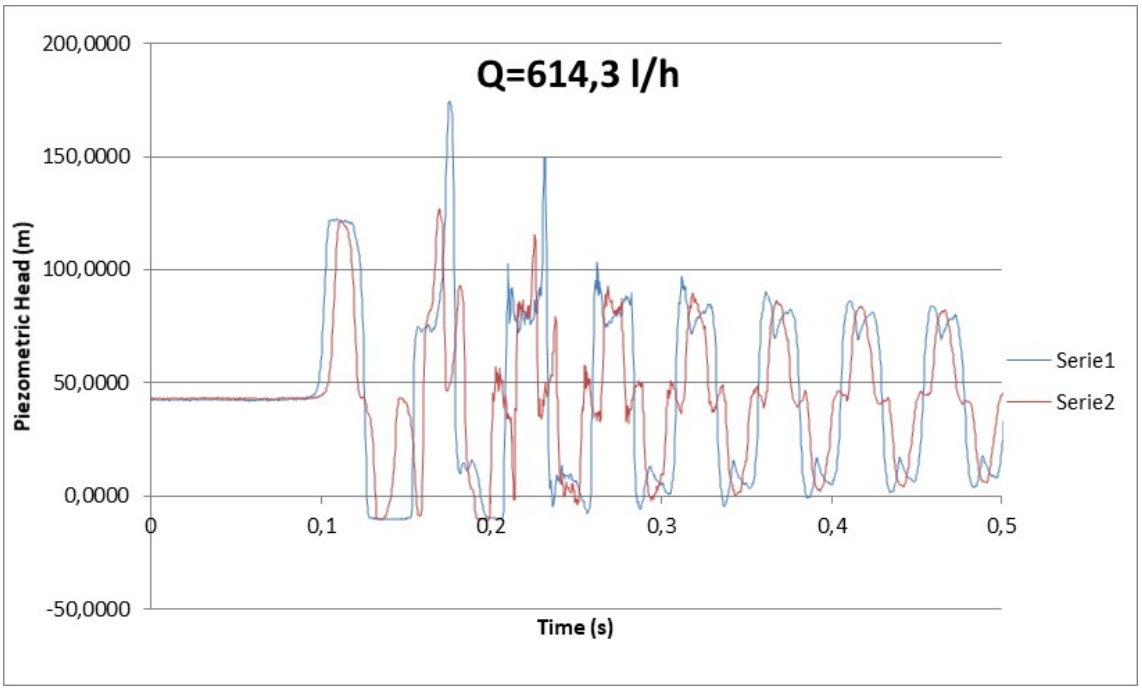

Figure 18 Time history of the piezometric head for Q0=614.3 l/h

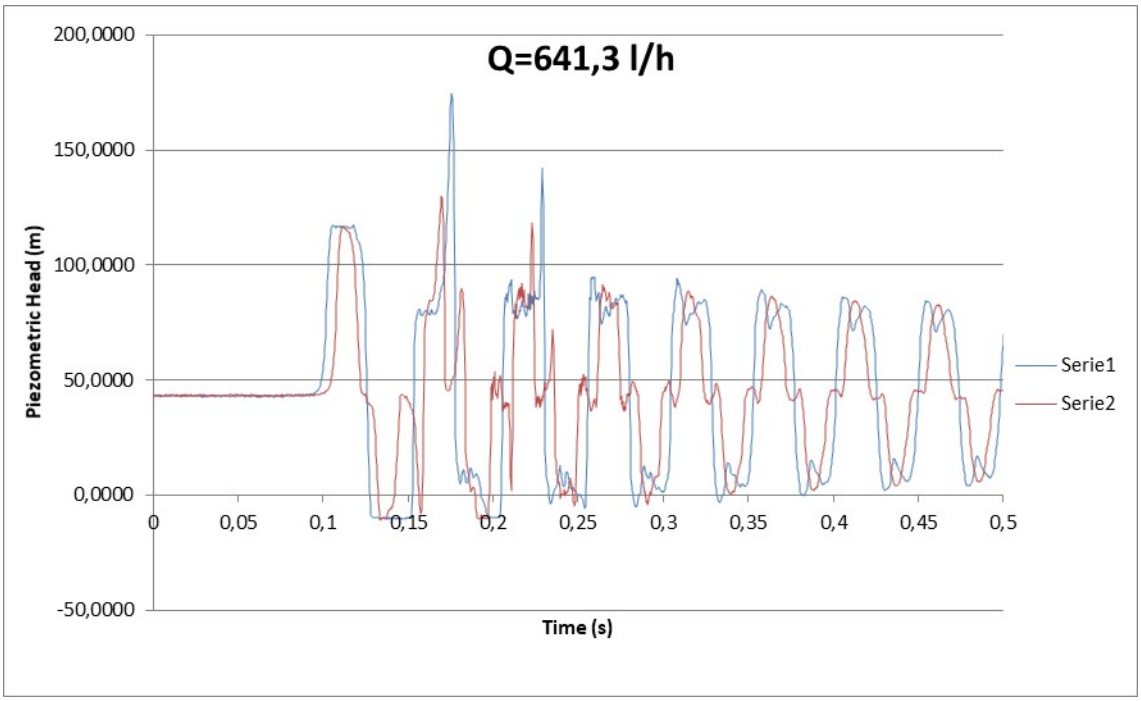

Figure 19 Time history of the piezometric head for Q0=641.3 l/h

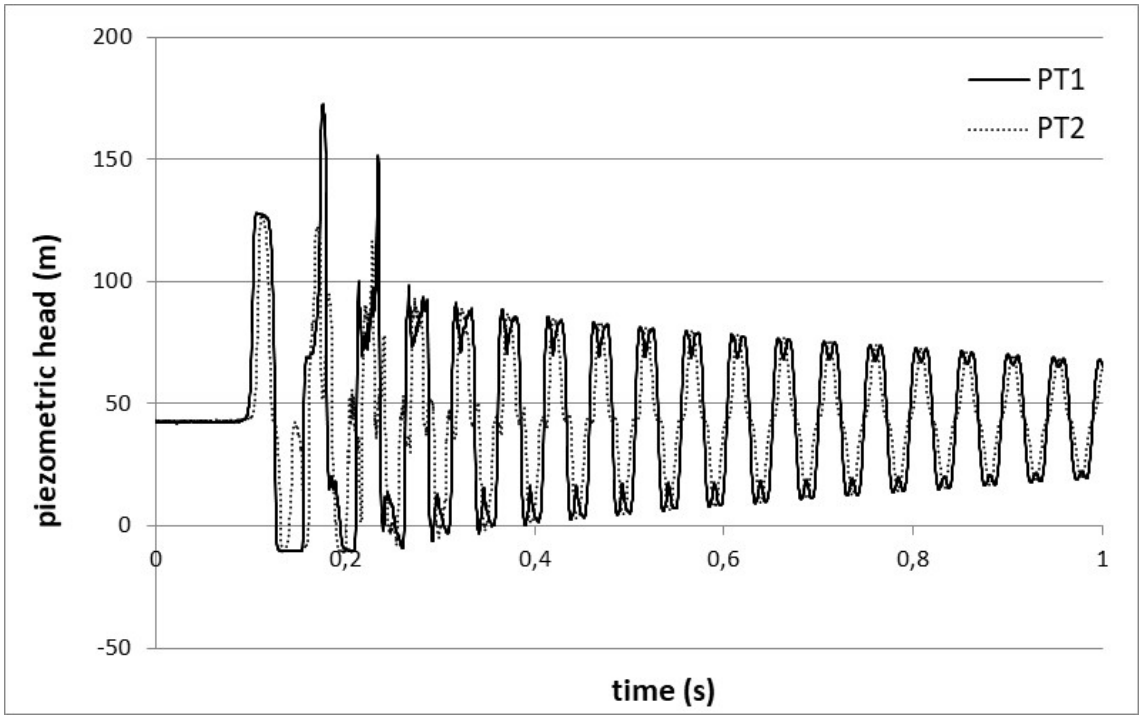

Figure 20 Time history of the piezometric head for Q0=709.6 l/h

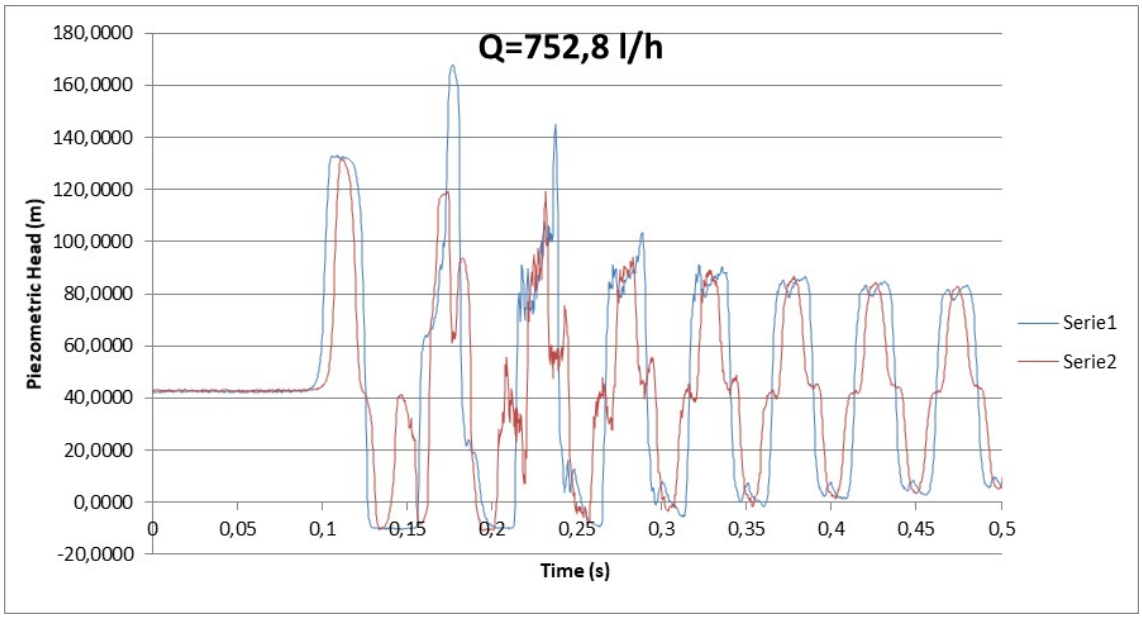

Figure 21 Time history of the piezometric head for Q0=752.8 l/h

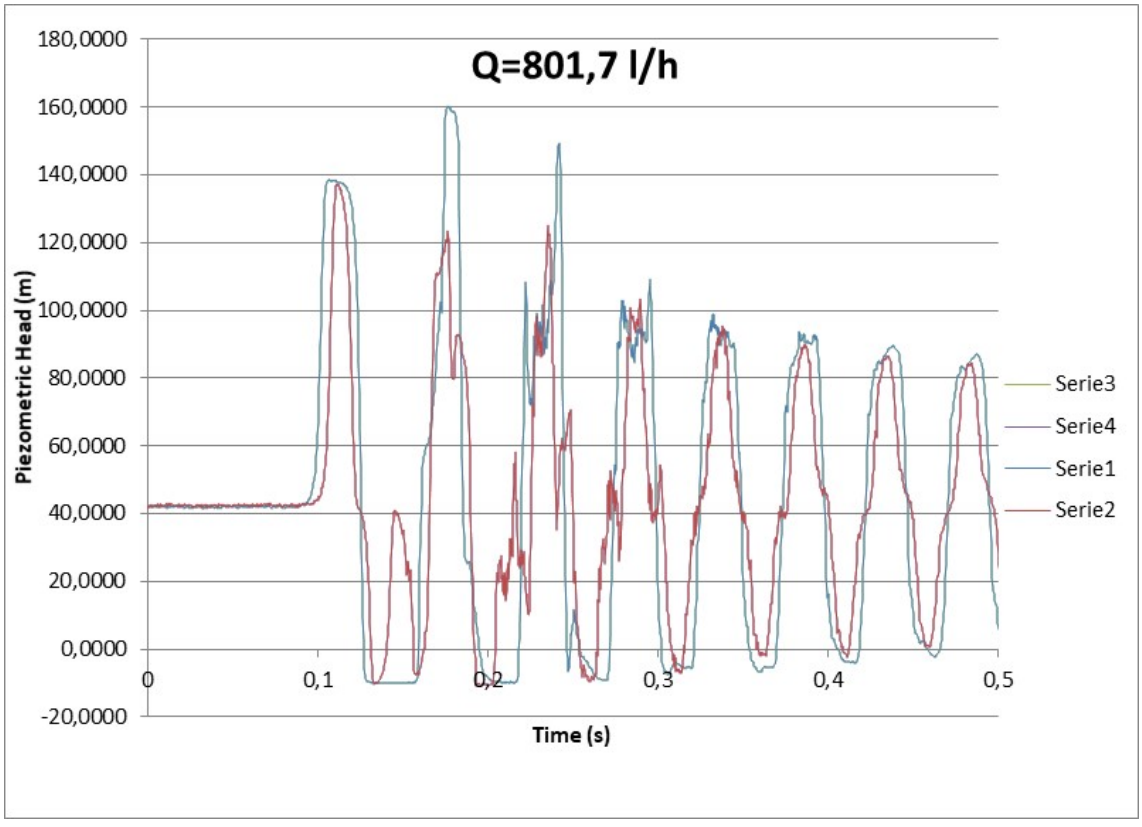

Figure 22 Time history of the piezometric head for Q0=801.7 l/h

Chapter 3

DISPLACEMENTS OF THE PIPE SYSTEM CAUSED BY A TRANSIENT PHENOMENON USING THE DYNAMIC FORCES MEASURED IN THE LABORATORY

A severe form of water hammer is called surge, which is a slow-motion mass oscillation of water caused by internal pressure fluctuations in a system, described by Shamloo H (2015). This can be pictured as a slower “wave” of pressure arising within the system. If not controlled, it can yield the following results: damage to pipes, fittings, and valves, which in turn causes leaks and life shortening of the system Given by Malesinszka A. (2015).

This work was published in the journal Measurement and Control (United Kingdom) (2018).

INTRODUCTION

This thesis shows the use of equations describing the movement of suspended mass focused on the beam to calculate the displacement of the pipelines under the action of dynamic forces. This approach will allow the calculation, as far as possible, of the actual displacement of the pipeline in the direction of flow change. This is very important information for designers calculating and selecting parameters of fixed points Ghidaoui M. (2005).

One of the factors that affect the reliability of an installation is its proper fastening to the structure of the building or other supporting components. This is especially important for installations which are exposed to dynamic loads. An example of an installation with the necessary high reliability exposure to dynamic loads is a fire protection system. The selection of fastening elements for such an installation depends on the force that the fastener can carry. Unfortunately, it is usually assumed that the force is applied statically. Therefore, it is important to implement numerical models for the calculation of the displacements for the dynamic system, and to compare them with physical models.

The measurements made, (in order to calculate the parameters of the pipe-water system), are necessary to calculate displacements based on the equation using the natural frequency for the entire system (i.e. the walls of the pipe and water filling the pipe). Such approach allows the impact on displacement to take in account not only the coefficient of elasticity of the pipe walls, but also the bulk modulus of the water filling the pipe. Considering the mutual influence of both coefficients of elasticity (by calculating the natural frequency of oscillations) will allow a more accurate description of the phenomenon. The described problem does not finish solving the whole task. Currently, further research is planned to confirm the validity of the assumptions made, as well as to conduct measurements for pipes of various materials, with different wall thicknesses and the proportions of wall thickness and inside diameter, as well as for liquids with different densities, descibed by Edwards JE (2015). Such an examination will allow for the development of a computational scheme, which in a simple way will allow, for example, engineers to calculate real ranges of displacements of pipe systems caused by transient phenomena. This knowledge, in turn, will allow adequate protection of pipe systems against damage, thanks to the appropriate pipe support selection.

EXPERIMENTAL FACILITY IN LABORATORY

This thesis presents and improves in detail the study which was presented in a simple form by Malesinszka (2015). The draft of the test stand concerned the simple scheme of a fire protection system, consisting only of the distribution pipe and one straight pipe (made up of three different diameters), armed with three nozzles. A simple geometric scheme allowed for an initial analysis and identification of phenomena accompanying the hydraulic shock wave propagation. The pipe system was designed in accordance with applicable standards. A scheme of the designed installation is presented in Figure 23 and Table 3.

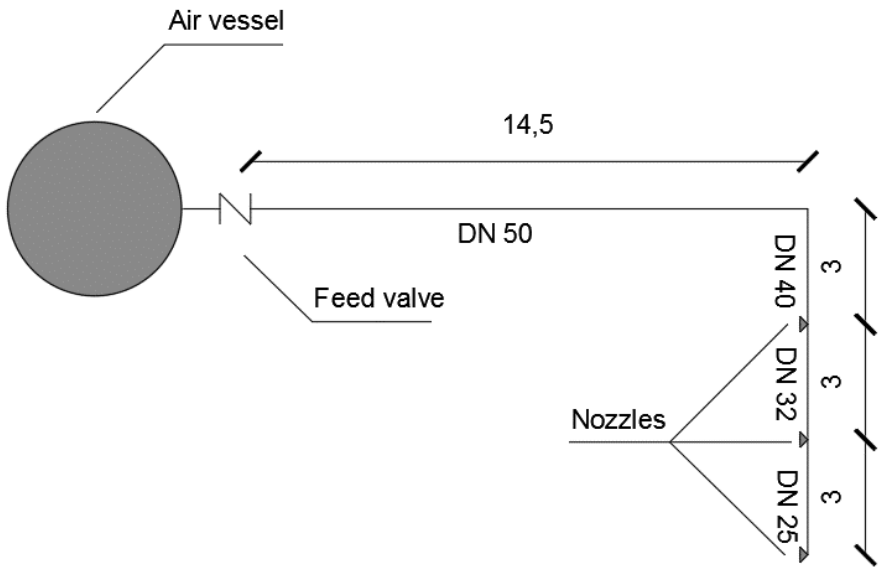

Figure 23 Scheme of the laboratory test stand.

A system of steel of various outer diameters D_0 and wall thickness e was used in the experiment.

Table 3 Properties of steel pipes used in the experiment.

No	Nominal diameter *DN* [mm]	Outer diameter D_0 [mm]	Wall thickness *e* [mm]	Individual celerity c_i [m/s]	Pipe length *L* [m]
1	50	60.3	3.65	1280	14.5
2	40	48.3	3.25	1280	3.0
3	32	42.3	3.25	1280	3.0
4	25	33.7	3.25	1280	3.0

The installation system that was accepted for the study was not filled with water. It was a model of an air system device used to protect the space of construction objects from the risk of frost or water evaporation. The installation system was equipped with three upright nozzles. The nozzles were placed one on each section of constant diameter *DN40*, *DN32* and *DN25*. The test stand for the water hammer analysis was constructed to perform the experiments, using the measuring system and recording of fast-changing pressure values.

The model was supplied with water via a pressure increasing station Figure 24 and Figure 25. The water in the tank was refilled from a water supply system. Permanent steady flow conditions established in the model of the system were made possible by the use of a water-air tank which had a capacity of 300 dm^3. The model was connected to the compressor, allowing an increase in the initial pressure in the system to the value of 5.5 bar, see Figure 25.

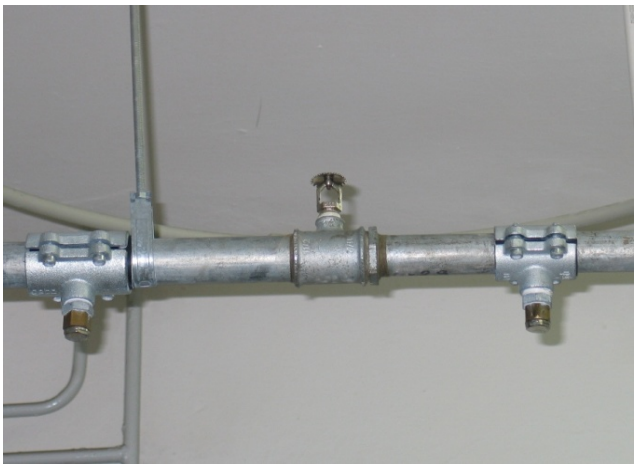

Figure 24 Upright nozzle installed in the pipe

Figure 25 Pressure increasing station with the compressor.

The measurement and analysis of the results was for a simple water hammer only, i.e. with pressure wave transition time T always higher than the valve opening time t_z. The experiment was performed at an average temperature of 281 K (Puntorieri. P. 2017).

The values of the forces impacting the components of the system were evaluated as follows:

1. In the first step, the forces were measured by a means of dynamometers (for a detailed description of the measurements and the results obtained, see Malesinszka A. (2015). Figure 26 shows only the relationship between the measured forces and the pressure in the cross-section in which the forces were measured.

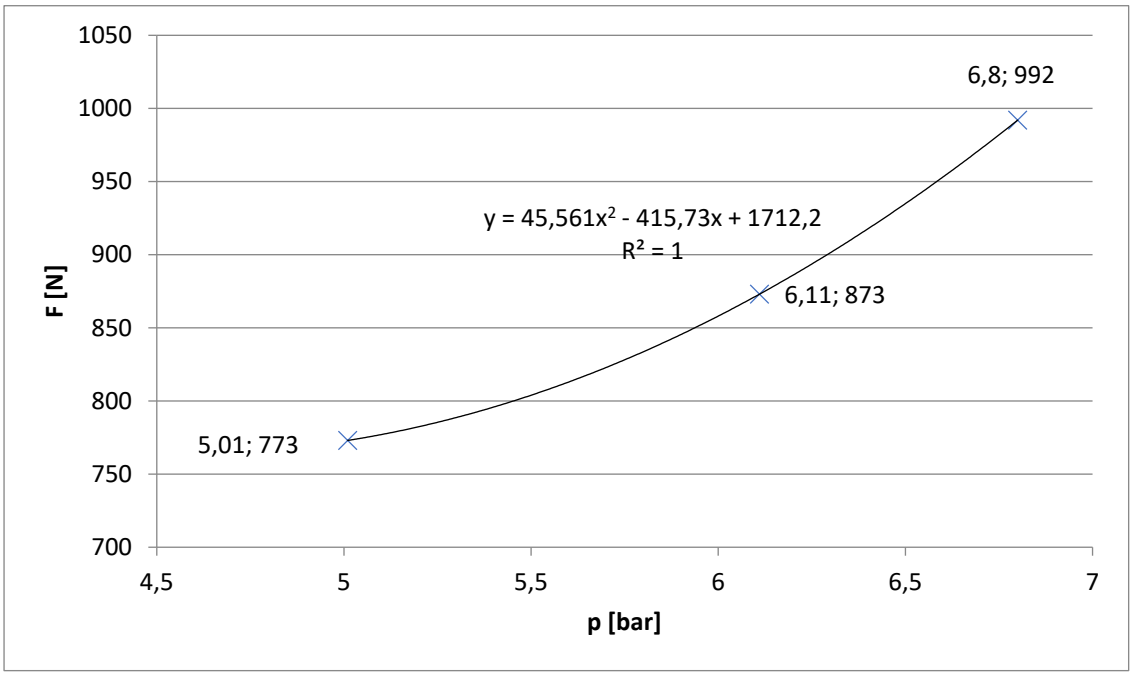

Figure 26 Relationship between the measured forces and the pressure in the cross-section in which the forces were measured

2. Then, in the same section after removing the dynamometers, a fixed support was installed, constructed from a special clamp hung on an 80 cm threaded, see Figure 27. On this threaded pipe, after special preparation, a strain gauge was attached, which then allowed the stress measurements to take place, see Figure 28. This fixed support is working as a cantilever beam with a point mass suspended at its end. The threaded pipe is considered as a cantilever beam, and the steel pipe with water as a suspended mass.

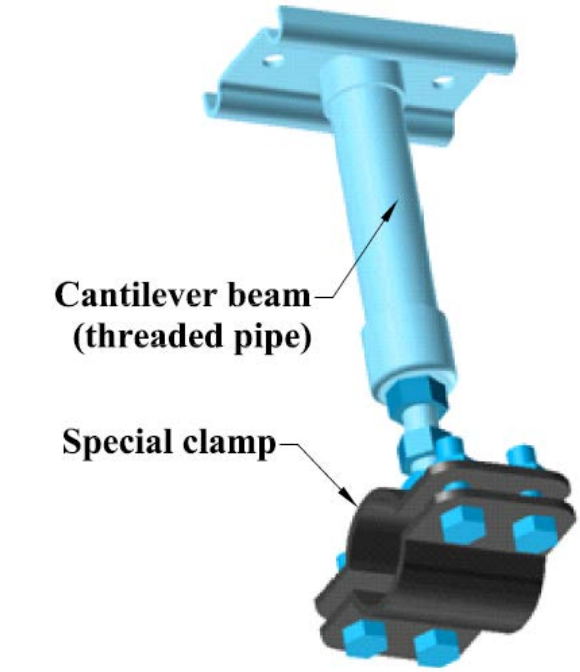

Figure 27 Scheme of a fixed support on which the model was suspended.

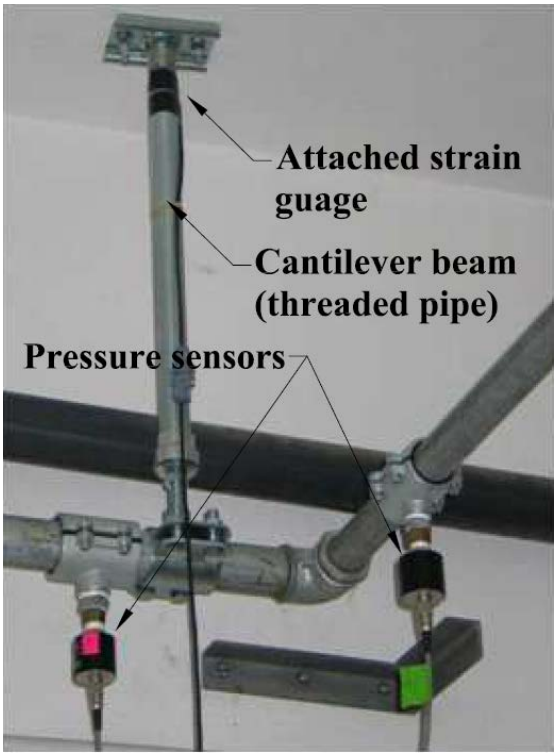

Figure 28 Fixed support with strain gauges attached

In addition, measurement involved the concurrent measuring of a pressures and flow rate, and also the opening time of the feed valve. This measurement guaranteed a comparison of the water hammer phenomenon for the same (or very similar) boundary conditions. The valve opening time was closely linked to the valve opening angle. The measurement of voltage obtained from the potentiometer, mechanically coupled with the valve hand wheel, was used to register the changes during the opening angle of the feed valve. This procedure ensured a voltage proportional to the angle of rotation of the valve hand wheel. The turbine flow meter type TUV-1210, which could record the counted flow units, was used for flow measurement.

All the recorded values were recorded using a computer that was equipped with software that controlled the measurement process and all further processing. The basic software was developed in the *"C"* language, using *"Turbo C"* program for compilation and subroutine statements. Two versions of the software were designed: a version used to record the measurements, and a version used to analyze the measurement results and the recorded value outputs.

CASE STUDY

The analysis included three work variants of the examined installation in the laboratory. Variant 1 – one nozzle opened, variant 2 – two nozzles opened, and variant 3 – three nozzles opened.

Strain gauges installed on the cantilever beam of the fixed support allowed the calculation of the mass that was suspended on the beam, and then using the equation of oscillatory motion, the beam displacement was calculated for the suspended installation.

Before any measurements were taken, the strain gauges attached to the cantilever beam of the fixed support was calibrated, and the basic strength characteristic of the applied cantilever, which was necessary for calculation of the mass suspended on the beam, was determined.

Two wire strain gauges with the following parameters were attached to the beam:

- nominal resistance R_{nom} = 600 Ω,
- transformation constant K = 2.62,
- active length l = 10 mm

Both strain gauges were combined in a "half-bridge" system. The half-bridge system was used due to the measured parameter. In this system, one strain gauge was under compression and the other under tension. The strain gauges were attached to the previously prepared surface (the surface was leveled and cleaned). The place of attaching the strain gauges is shown in Figure 28. The strain gauges were attached as close as possible to the place where the beam was fastened, so as to minimize

the effect of changing the length of the bent beam on the accuracy of strain gauge measurements. On the diagonal of the bridge to obtain the change in voltage *ΔU*, which depended on the resistance change *ΔR/R*:

$$\frac{\Delta U}{U} = \frac{1}{2}\frac{\Delta R}{R}$$

Equation 7

where:
U = voltage of bridge powering [V],

$$\Delta R = R_{nom} K \varepsilon$$

Equation 8

E = relative elongation of strain gauges in the range of elastic strains, *ε* = 0.001, thus:

$$\frac{\Delta U}{U} = \frac{1}{2} * 2.62 * 0.001 = 0.0013$$

Equation 9

With the bridge powered by a voltage *U* of 5V, a strain gauges bridge input signal imbalance is obtained, and is equal to:

$$\Delta U = 5 * 0.0013 = 0.0065 \text{ V} = 6.5 \text{ mV}$$

Equation 10

By strengthening the direct current, having for example an amplification of *L* = 1000, it is possible to obtain an input signal of 6.5 V with 1 kN of force applied to the end of the cantilever beam in question.
Strain gauges calibrating was carried out by applying a force of known value [kN], and then reading the values of voltage [mV] corresponding to these known force values and their corresponding voltage changes. Since the relationship presented is linear, a best fit of the variability function was determined by the least squares method Figure 29.

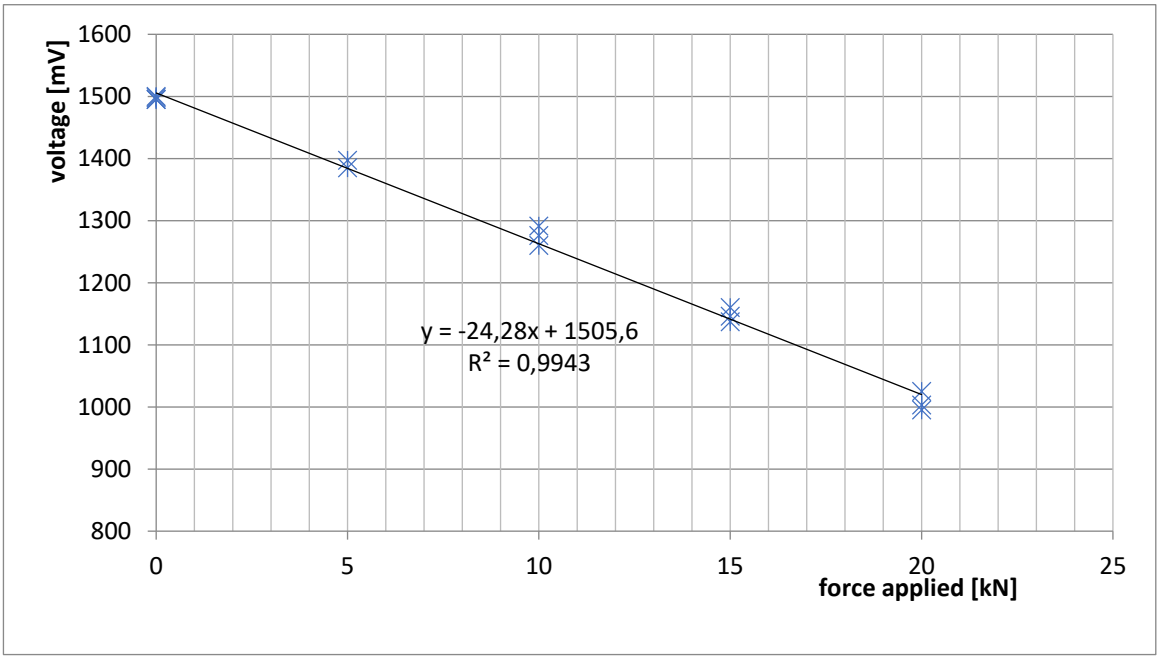

Figure 29 Strain gauges calibrating, readout of voltage value for known applied force value.

To calculate the strength parameters of the cantilever threaded pipe beam of the fixed support, it is necessary to know the basic geometrical and material parameters of the beam:

- inner diameter d = 33 mm,
- outer diameter D = 39 mm (below the thread),
- beam length L = 80 cm,
- elastic modulus for steel $E = 2.09*10^5$ MPa.

Beam strength parameters were then calculated based on the above data values:

- moment of inertia for beam cross-section:

$$J = \frac{\pi}{32}(D^4 - d^4) = 11.069\ cm^4$$

Equation 11

- cross-section modulus:

$$W = \frac{\pi}{16}\left(\frac{D^4 - d^4}{D}\right) = 5.677\ cm^3$$

Equation 12

– beam cross-section:

$$A = \frac{\pi}{4}(D^2 - d^2) = 3.39\ cm^2$$

Equation 13

– with a beam length of L = 80 cm, 271 cm^3 of beam material net volume is obtained.

CALCULATION OF THE DEFLECTION OF THE CANTILEVER BEAM – STATIC FORCE APPLIED AT THE END OF THE CANTILEVER

The displacement of the end of the beam as a result of the static action of the concentrated force, F, according to the material mechanics theory can be calculated from the relationship:

$$f = \frac{FL^3}{3EJ}$$

Equation 14

where:
f = displacement of the end of the cantilever beam (deflection) [m], F = concentrated force [N], L = beam length [m], E = modulus of elasticity of the beam [Pa], J = modulus of inertia of the beam [m^4].
For the scheme presented in Figure 28, in the first stage of the test, the components of the force caused by the water hammer pressure wave were measured using dynamometers, given by Malesinszka A. (2015). The measured force components were used at this point to calculate the displacement of the beam end after the static force was applied at the end of the beam, i.e. the threaded pipe of the fixed support.
The cantilever beam was 80 cm long. For that particular beam length and the calculated strength parameters in Table 4, the deflection of the cantilever beam based on the calculated resultant forces was determined.
The calculations are shown in Table 4:

Table 4 Calculated deflections for the acting resultant forces

Variant	Force *F* [N]	Deflection *f* [cm]
I	773	0.57
II	992	0.73
III	873	0.64

USE OF THE EQUATION OF THE OSCILLATORY MOTION FOR MAXIMUM DEFLECTION DETERMINATION OF THE CANTILEVER BEAM

In the first step, the frequency of the natural oscillations of the pipe system not filled with water was measured in the laboratory. Oscillation inductions were forced by hitting with a soft pad. The oscillations constitute periodical motion in which all the points of the oscillating system, after a fixed time interval, would return to the initial value in a reproducible manner. This time interval is called the period of oscillation, and it is denoted by the letter *T*. The reciprocal of the period *1/T*= f is called the frequency of oscillations. The frequency of natural oscillations of beam + mass f [Hz] system was measured, which gives:

– angle velocity

$$\omega = 2\pi f \ [rad/s]$$

Equation 15

– angle velocity of beam with susceptibility *k*, and mass concentrated at the end of the beam

$$\omega = \sqrt{\frac{k}{m}}$$

Equation 16

thus

$$m = \frac{k}{\omega^2}$$

Equation 17

in order to obtain the characteristic of oscillations, two records of suppressed oscillations, *"dr1"* and *"dr2"*, were made.

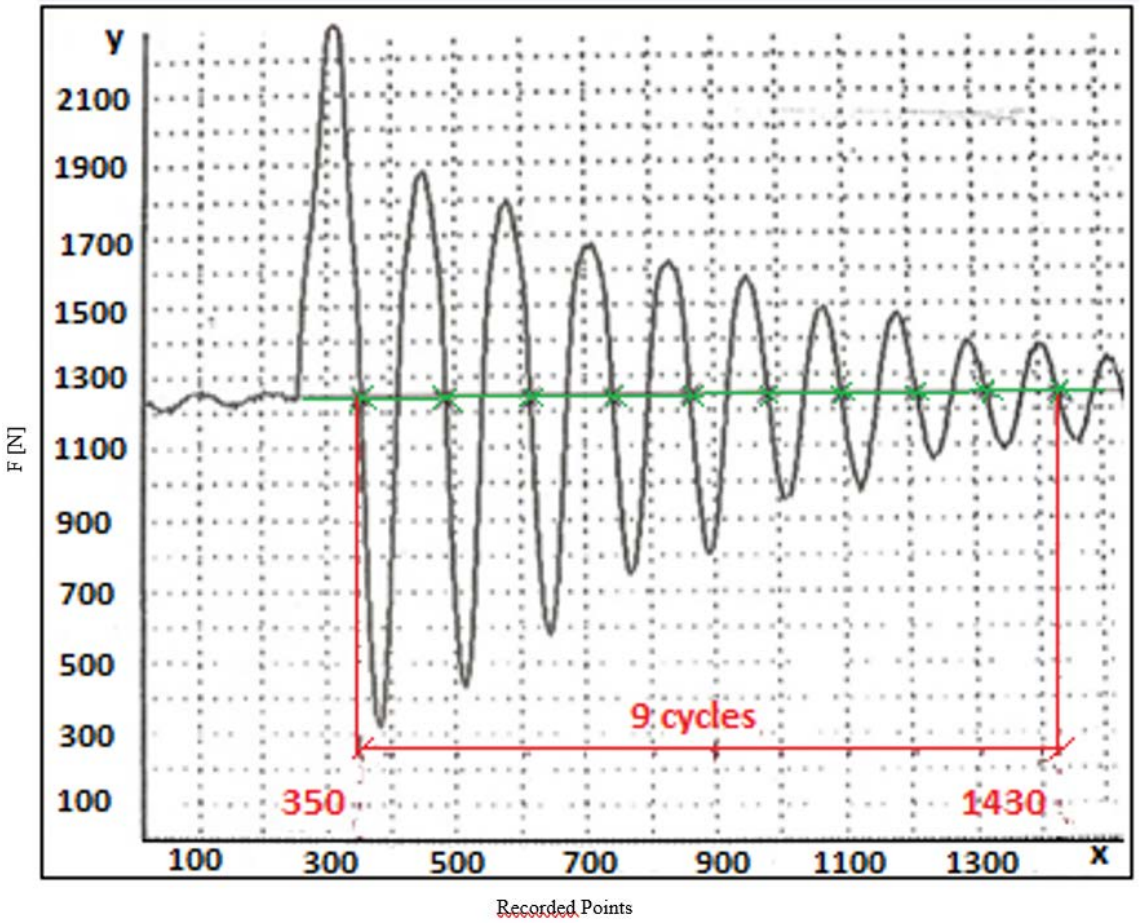

Figure 30 Course of forced oscillation for an empty pipe, "dr1"

To register "dr1" Figure 30, 9 cycles took 1430 - 350 = 1080 recorded points (x, y = counted non scaled impulses). Each registered point lasts 2 ms, thus 9 cycles lasted 2.16 seconds which corresponds to:

- oscillations period $T = 2.16/9 = 0.24$ [s],
- oscillations frequency $f = 4.17$ [Hz],
- angle velocity $\omega_0 = 26.17$ [rad/s].

On the basis of the course of the forced oscillation for the empty pipe, *"dr2"*, similarly to the first case *"dr1"*, 10 cycles were taken from the recorded characteristic, which took 1430 - 255 = 1175 registered points (x, y = counted non scaled impulses) 2.35 seconds, corresponding to:

- oscillation period $T = 2.35/10 = 0.235$ [s],
- oscillation frequency $f = 4.25$ [Hz],
- angle velocity $\omega_0 = 26.72$ [rad/s].

Mean value of angle velocity for the dry system is ω_{0avg} = 26.45 [rad/s]. Finally, it is possible to calculate the mass suspended on the cantilever beam assuming that the suspension is at its end point. Hence, the constant of beam susceptibility was calculated from $k = 3EJ/L^3$ [N/m], where L = beam length. According to the Equation 10we know that $m = k/\omega$^2 , where k = 135 [kN/m] and ω = 26.45 [rad/s] are the values calculated for the examined system. Thus, we obtain mass value m = 193 [kg].
In the same manner, using the measured characteristics, the following was established for the wet pipes:

- oscillation period T = 0.28 [s];
- oscillation frequency f = 3.57 [Hz];
- angle velocity ω = 22.4 [rad/s], calculated from Equation 8;
- mass m = 269 [kg], calculated from Equation 10.

As the value of the concentrated mass suspended at the end of the cantilever beam is known, it was possible to analyze the oscillations forced by a sudden application of force – a response of the system to the pressure wave propagation. Forcing the oscillating system motion is a certain process, and as known, its nature can be of an aperiodic process character, in particular the transition one.
Then the mathematical model of the system with suppressing takes the following form:

$$m\ddot{x} + c\dot{x} + kx = F(t)$$

Equation 18

where force $F(t)$ may be aperiodic, and also a discontinuous function. To determine the motion of the oscillating system affected by the action of aperiodic extortions, the response of the system on two elementary forces can be analyzed, i.e. the unit impulse and the unit step. The impulse is a measure of the impact of short-term forces, e.g. the closing and quick opening of the feeding valve. The step is a response to the force of the constant value suddenly applied to the physical system, e.g. a heat shock caused by a sudden temperature change.
In the case of the water hammer phenomenon, we are dealing with an applied instantaneous force. A measure of the impact of short-term forces is impulse S, i.e.

$$S = \int_{t_1}^{t_2} F(t)dt$$

Equation 19

When the time Δt of force F(t) operation is very short, as it is in the case of pressure wave propagation, it is an instantaneous force. The solution of the equation of suppressed oscillatory motion induced by instantaneous force, taking into account the subcritical suppression, is the following function:

$$x(t) = \frac{S}{m\omega_D} e^{-bt} sin\omega_D t$$

Equation 20

where:
x = displacement of the end of the cantilever beam in time
S = impulse caused by instantaneous force action, $S = F_0 \Delta t$,
m = mass, in this case calculated based on measured characteristics of mass value for a wet installation, m = 269 [kg],
ω_D = frequency of suppressed free oscillations (natural frequency),

$$\omega_D = \sqrt{\omega_0^2 - b^2}$$

Equation 21

ω_0 = natural oscillations frequency,
b = normalized suppression coefficient, $b = c/2m$,
c = viscous suppression coefficient, related to the suppressive properties of viscoelastic material,

$$c = \frac{gk}{\omega}$$

Equation 22

$$\omega = \omega_0$$

Equation 23

g = number characterizing the suppression properties of the beam,

$$g = ImE^*/ReE^*$$

Equation 24

ImE = imaginary part of complex elastic modulus,
ReE = real part of complex elastic modulus,
E = complex elastic modulus, i.e. variable over time,
k = number characterizing elastic properties of the beam,

$$k = AReE^*/l$$

Equation 25

On the basis of the experiments conducted, and by calculating certain values characteristic of the analyzed system, it is possible to derive an equation of suppressed oscillatory motion caused by the activity of the instantaneous force – pressure wave propagation.
In order to derive an equation of suppressed oscillatory motion, the relationship for T_D may be used, which is defined as the time interval between two successive peaks in the same direction. The T_D value is constant in time and can be calculated from the following relationship:

$$T_D = \frac{2\pi}{\sqrt{\omega_0^2 - b^2}}$$

Equation 26

Explanations are similar to those in Equation 14
Having the measured characteristics for the experiment, it is now possible to determine the value of T_D = 0.29 s. After converting the above relationship, it is possible to calculate the standardized suppression coefficient b = 5.69 [rad/s], and ω_D = 21.66 rad/s.
For the assumed unit impulse inducing system oscillation, the equation of the change of displacement versus time takes the form (h and x are the same parameters describing displacement of the end of the cantilever beam):

$$h(t) = \frac{1}{m\omega_D} e^{-bt} sin\omega_D t$$

Equation 27

m = 269 kg, b=5.69 rad/s,
ω_D = 21.66 rad/s,
T_D = 0.29 s

$$h(t) = 1.716 * 10^{-4} e^{-5.69t} sin21.66t$$

Equation 28

In the case of a water hammer, it was assumed that the concentrated force F was acting in infinite time. So, it is assumed that the impulse S is equal to the force F.
According to the equation of the oscillatory motion, the maximum displacement x_{max} is as follows:

$$x_{max} = \frac{S}{m\omega_D} e^{\frac{-b\pi}{2\omega_D}} \quad for \quad t = \frac{\pi}{2\omega_D} = 0.07\ s$$

Equation 29

Assuming $S = F$, x_{max} was calculated for the force values listed in Table 5.

Table 5 Calculated deflections for the acting resultant forces

F1 (N)	*X1* (cm)	*F2* (N)	*X2* (cm)	*F3* (N)	*X3* (cm)
773	8.78	992	11.26	873	9.91

Knowing the function describing end of the cantilever beam displacement, the pipe of the installation displacement is known as well.

MATLAB PACKAGE IMPLEMENTATION

To calculate the change in displacement of the end of the supporting beam for unit impulse versus time, the MATLAB package was used. For this purpose, the following *oscillation* function was created: function [x, t] = oscillation (S, m, omega0, Td, figure), which requires the following input parameters:

S = value of unit impulse [N],
m = mass concentrated at the end of beam [kg],
omega0 = angular velocity [rad/s],
Td = contractual period [s],
figure = parameter specifying whether or not to create a figure.

The function returns two output values:

x = the value of maximum displacement [cm],
t = time, after which the value of maximum displacement occurred.

To solve the problem, all of the values needed for equation 26 must be calculated. Based on the ω_0 and T_d parameters, the value of the normalized suppression coefficient (*b*) is determined. Then, by using this value, the value of ω_D is calculated. After calculating all the necessary values, the symbolic variable *t* is created, and equation 26 is built using the provided and calculated values.

The built equation is solved to find the global minimum using the `GlobalSearch` class and the corresponding settings for the optimization problem of one variable, from Barton N. (2013).
Finally, the graph of the function is plotted, and the maximum value found (the minimum value determined by the above optimization problem) is marked on the graph, and the two output parameters are returned from the function.
The function block diagram is shown in Figure 31.
Example of a function call:

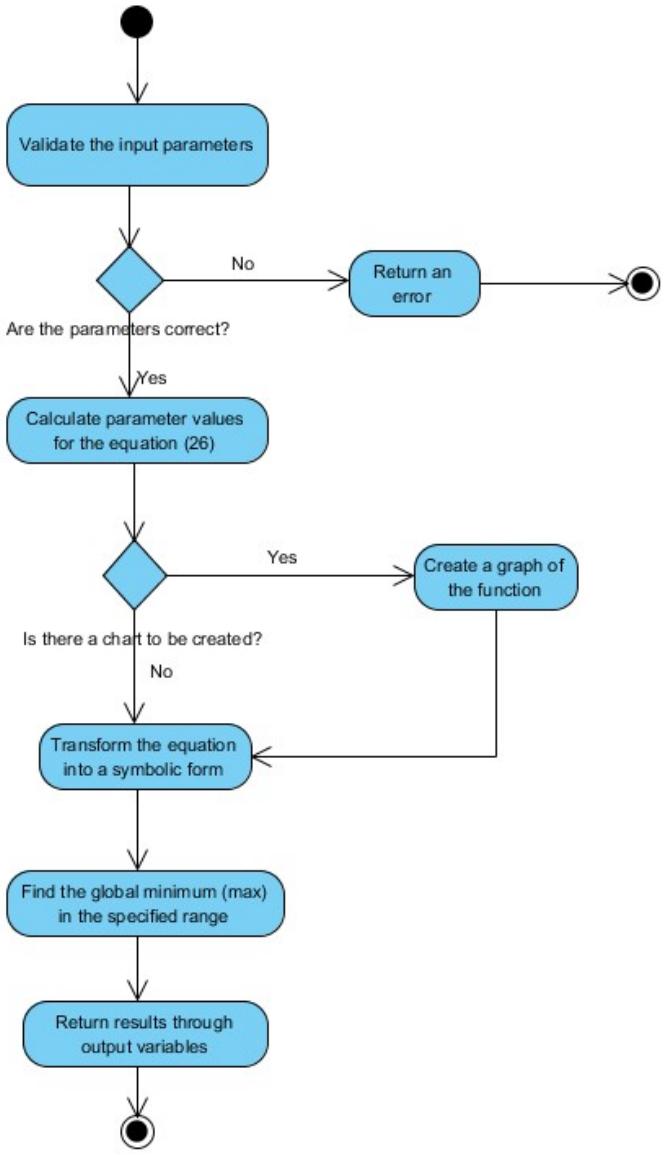

Figure 31 Function block diagram

For the following input parameters: S = 992 N, m = 269 kg, ω_0 = 22.4 rad/s, T_d = 0.29 s output parameters were obtained: x = 11.661 cm, t = 0.060653 s and the graph of the function was as Figure 32.

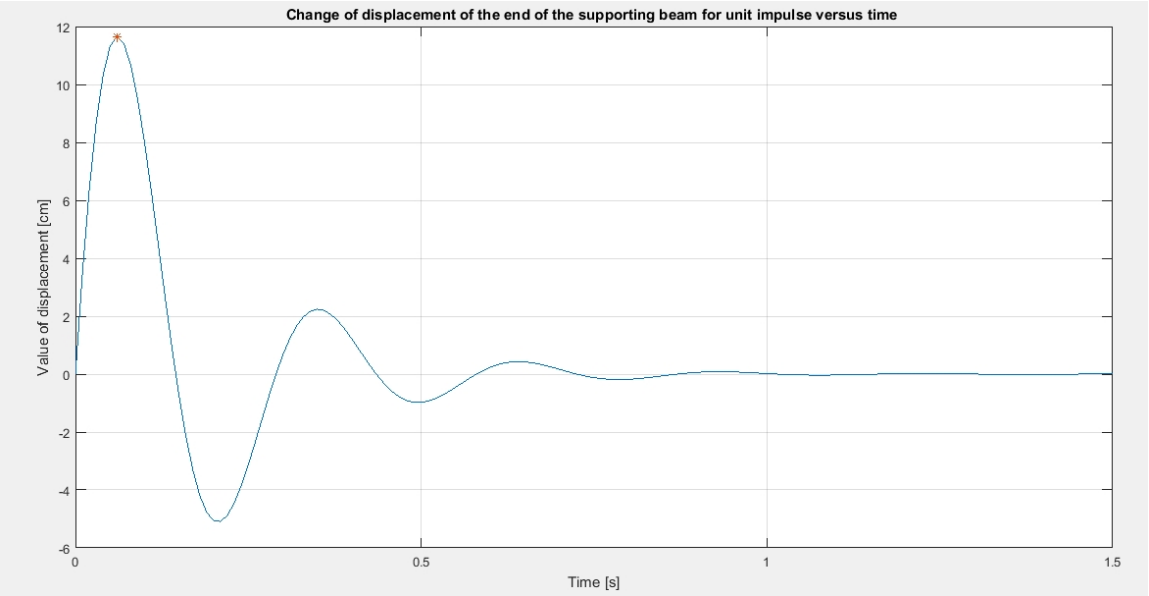

Figure 32 Change of displacement for unit impulse versus time

Chapter 4
EQUIVALENT CELERITY IN WATER HAMMER FOR SERIALLY CONNECTED PIPELINES

This thesis presents the results of research on a physical model that confirms the dissimilarity of celerity values for pipes of different diameters and considers the relationship of diameter size changes with the length of the combined sections. In the case of piping systems, instead of computing the celerity c, the equivalent celerity c_e must be determined. For this purpose, an equation for natural vibration analysis has been proposed as a simple and fast method for computing the equivalent celerity of piping systems.

The analytically computed values were compared with values obtained from actually measured characteristics.

In this way, the satisfactory compliance of the compared values, and thus the validity of applying derived equations for a simple estimation of the equivalent celerity in piping systems, can be confirmed.

This allows the computation of the maximum pressure increase in the system.

Using natural vibration analysis to calculate the equivalent celerity, it is possible to estimate the basic parameters of water hammer in a fast and easy way, and among other things, the expected maximum pressure increase without having to use complex computer programs to simulate water hammer.

This in turn can translate into a fast verification of the assumed parameters and pipe configuration in the rebuilt or modernized network for estimating the water hammer phenomenon as a function of connected pipes of different diameters, different lengths and different material compositions.

To facilitate the use of the equations, an algorithm implemented in MATLAB has been presented that allows the specification of the value of the celerity c_e for any number of connected pipes.

This work was presented at the WIT Transactions on Engineering Sciences conference in Prague (2018) and is being published in the ASCE journal.

LINEAR ANALYSIS METHODS

To simulate the water hammer phenomenon, linear analysis methods can be used, provided that the pulsing in the relevant system is a periodic motion. This is confirmed by harmonic analysis of the phenomenon, using the classical oscillation equations, and limiting it to the case of damped natural vibrations. Vibrations are periodic movements in which all points of the vibrating system repeatedly return to the initial state after a fixed time interval. The simplest vibrating motion is the harmonic motion. Any periodic vibration can be formed by the superposition of the basic harmonic vibrations of the same period and, in a limited case, from an infinite number of higher harmonic vibrations of appropriately selected amplitudes and phases. Vibrations triggered by the action of a single pulse are natural vibrations. An example of this type of vibration is the water hammer formed under the influence of a single pulse, such as, for example, the sudden closure of a valve.

In an attempt to predict certain parameters of the water hammer phenomenon, one can use a theory based on the natural vibrations of the system utilizing the equations of fluid mechanics.

Often, when using equations governing the variable flow of liquid in the pipeline system, the solution reduces to a function of time. Thus, the analysis is limited only to a temporary state or the method of triggering this state. According to harmonic analysis of the water hammer phenomenon, a variable flow may sometimes be referred to as periodically pulsing or showing its own vibration. With such a description of the phenomenon, the solution of the equations allows the frequency to be determined (i.e. one can search for solutions directly specifying a steady pulsation cycle). In this case, achieving a uniform rate of the pulsation cycle is important.

Frequency-dependent factors, such as friction or wave celerity, have a major impact on the dynamic behaviour of liquids in pulsating conditions as a result of extraordinary energy dissipation or due to fluctuations of wave celerity.

Borrowing methods from the theory of linear vibrations requires reducing the equations describing the course of the phenomenon to a linear form Pipes (1958). To this end, the differential equation of motion and continuity is adopted in simplified form, i.e. it is assumed that the average flow parameters are "constant". Thus, their derivatives are both zero, and the friction is reduced to a linear form. This way, a particular solution of equations is obtained - a solution resulting in algebraic equations related to the pipeline parameters and boundary conditions.

Simplified equations of motion and continuity take the following form, Wylie (1993):

$$\frac{\partial H}{\partial x}+\frac{1}{gQ}\frac{\partial Q}{\partial t}+\frac{\lambda Q^n}{2gDA^n}=0$$

Equation 30

$$\frac{\partial Q}{\partial x}+\frac{gA}{c^2}\frac{\partial H}{\partial t}=0$$

Equation 31

The use of these equations in the linear vibration analysis after the introduction of the hyperbolic functions allows the derivation of equations describing the amount of pressure and flow as a function of position in the pipeline:

$$H(x)=H_U cosh\gamma x-Z_C Q_U sinh\gamma x$$

Equation 32

$$Q(x)=-\frac{H_U}{Z_C}sinh\gamma x+Q_U cosh\gamma x$$

Equation 33

Equation 29 and Equation 30 are equations of pressure and flow transfer. Using the above equations allows the computation (after appropriate substitutions and transformations) of the equivalent celerity thanks to the linking of pipe properties (A_i, c_i, L_i) with the natural frequency of the system. As will be shown, the use of the method of natural vibration provides a simple solution to this problem. Further discussion will focus on the serial connection of two and three pipes made of different materials and for different ratios of diameters and lengths of connected sections.

For the correct solution of the issue, a correct definition of the boundary conditions of system operation is important.

Figure 33 shows an example of a serial connection of two pipes. According to the presented scheme, the boundary conditions are as follows:

$$H_{D1}=H_{U2}\ and\ Q_{D1}=Q_{U2}$$

Equation 34

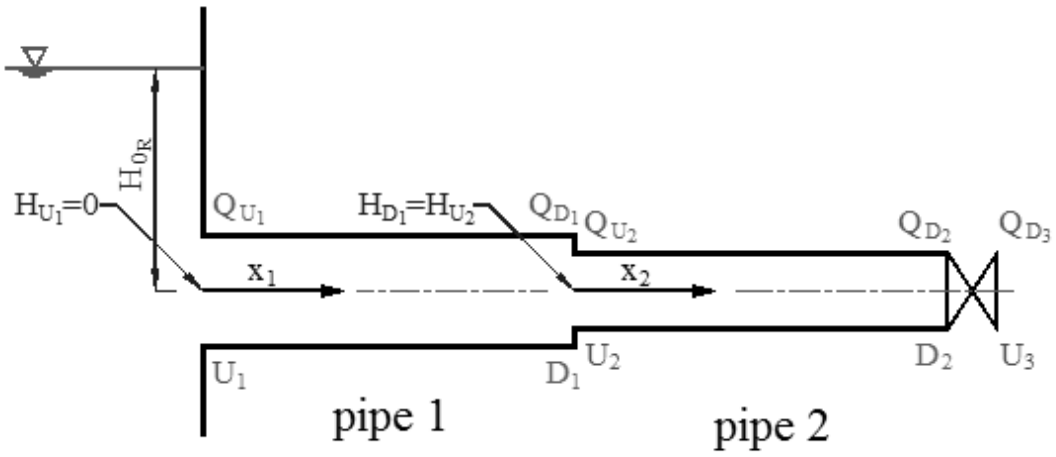

Figure 33 Scheme of a serial connection of two pipes.

For any point of the pipe, an equation for the transfer of pressure and flow can be written as given in Equation 29 and Equation 30.
Using the boundary conditions and the fact that the pipes are serially connected, the following equation can be obtained:

$$-\frac{Z_{c1}}{Z_{c2}} tanh\gamma_1 L_1 tanh\gamma_2 L_2 = 1$$

Equation 35

To obtain only the dependencies between geometric parameters of the connected pipes and the vibration frequency of the entire system from the equation above, adequate substitutions for Z_C and γ must be made. For this purpose, it should be noted that if the vibration pulsation has a regular amplitude at each point x of the hydraulic system, the size of the real part of s must be zero. The propagation constant thus takes the following form:

$$\gamma = \sqrt{C\omega(-\omega L_b + iR)}$$

Equation 36

The proper impedance is:

$$Z_C = -\frac{i\gamma}{C\omega}$$

Equation 37

For a system without friction:

$$\gamma = \sqrt{-C\omega^2 L_b} = \omega i\sqrt{CL_b}$$

Equation 38

Substituting C and L_b with dependencies, $C = gA/c^2$and $L_b = \zeta/(gA)$ (Brown 1969), ((Zielke 1972), the following is obtained:

$$\gamma = \frac{\omega i}{c}$$

Equation 39

$$Z_c = \frac{c}{gA}$$

Equation 40

Substituting the dependencies Equation 36 and Equation 37 into Equation 32, it follows:

$$tanh\frac{\omega L_1}{c_1}i \cdot tanh\frac{\omega L_2}{c_2}i = -\frac{c_2 A_1}{c_1 A_2}$$

Equation 41

Using the generalized Euler's formula:

$$\tanh zi = \frac{\sinh zi}{\cosh zi}$$

Equation 42

where:

$$\sinh zi = i\sin z \ , \cosh zi = \cos z$$

Equation 43

The relation Equation 38 can be written as follows:

$$i\left(tan\ \frac{\omega L_1}{c_1}\right)i\ \left(tan\ \frac{\omega L_2}{c_2}\right) = -\frac{c_2 A_1}{c_1 A_2}$$

Equation 44

$$tan\ \frac{\omega L_1}{c_1}\ tan\ \frac{\omega L_2}{c_2} = \frac{c_2 A_1}{c_1 A_2}$$

Equation 45

Solving the equation above with regard to ω, the equivalent celerity of the pressure wave c_e for the entire pipeline can be determined. Because the entire period of a complete cycle, $2T$, amounts to:

$$2T = \frac{4L}{c_e} = \frac{2\pi}{\omega}$$

Equation 46

hence:

$$c_e = \frac{2}{\pi} L\omega$$

Equation 47

where $L = L_1 + L_2$, is the length of the entire pipeline.
It should be noted that using the dependency Equation 42 substantially simplifies and speeds up the computation of the equivalent celerity of pressure oscillation changes upon reaching the natural vibrations of the system. Equation 42 is only true for a system consisting of two pipes. The analysis of natural vibration oscillations for three pipes connected in series requires the introduction of a new dependency in accordance with the scheme described above. Using Equation 29 and Equation 30 for computation purposes requires the knowledge of pressure distribution in sequential cross-sections of the analysed pipe system, which would be quite problematic to obtain.
For the system consisting of 3 pipes, as shown in Figure 34, one must correctly determine the boundary conditions and then, proceeding similarly as for the system consisting of 2 pipes, derive a new dependency.

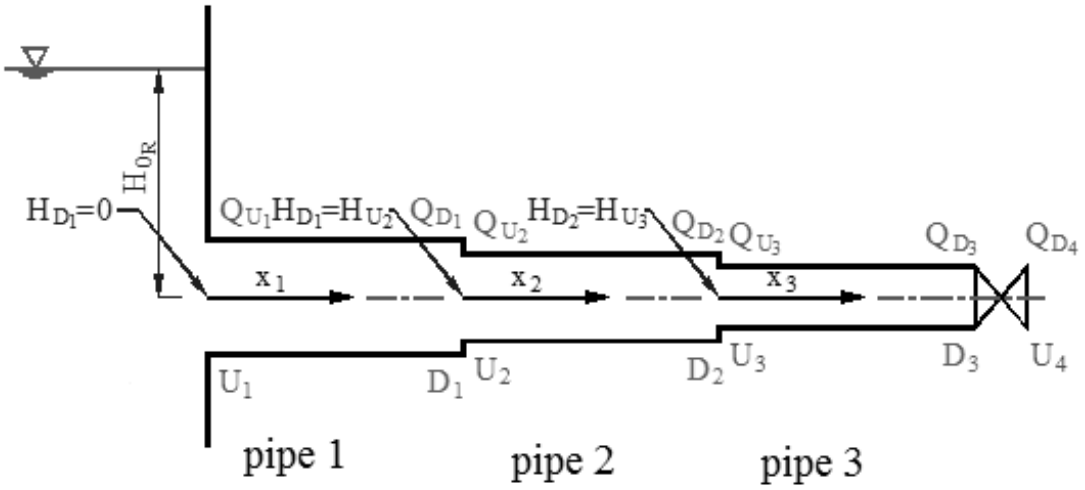

Figure 34 Scheme of a serial pipe connection.

Finally, for the system consisting of three pipes, the following equation is obtained:

$$\frac{c_1 A_2}{c_2 A_1}\tan\frac{\omega L_1}{c_1}\tan\frac{\omega L_2}{c_2}+\frac{c_1 A_3}{c_3 A_1}\tan\frac{\omega L_1}{c_1}\tan\frac{\omega L_3}{c_3}+\frac{c_2 A_3}{c_3 A_2}\tan\frac{\omega L_2}{c_2}\tan\frac{\omega L_3}{c_3}=1$$

Equation 48

Similarly, as was the case with two pipes, the solution of the equation with respect to ω allows for the computation of the equivalent celerity c_e.

MATERIALS AND METHODS

To validate the use of the natural vibration method to determine the equivalent celerity in water hammer research, a series of tests on the measuring station as shown in Figure 35 has been conducted.

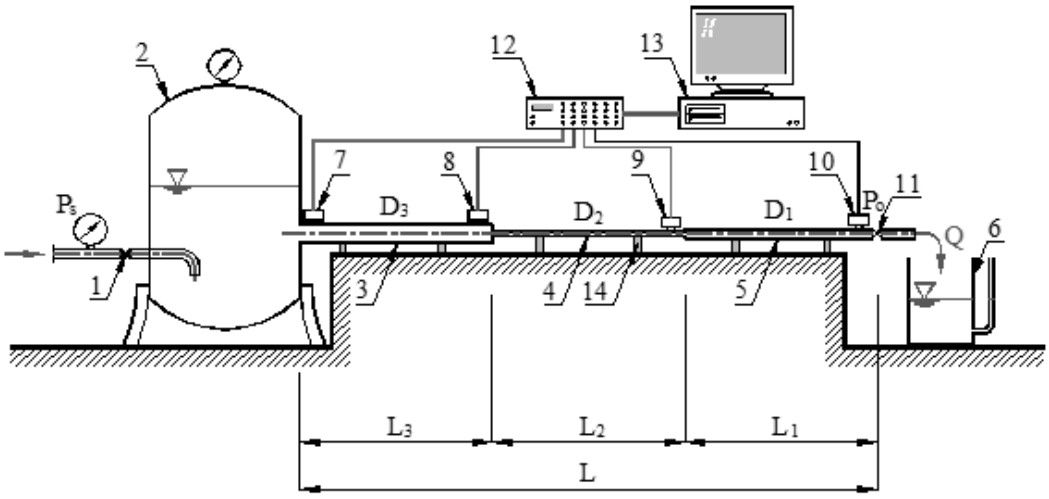

Figure 35 Measuring station for the research of water hammer 1 – reducing valve; 2 – hydrophore tank; 3, 4, 5 – tested pipes with variable geometric parameters (diameter, length of tested section); 6 – measuring vessel; 7, 8, 9, 10 – pressure sensors; 11 – shut-off valve with closing time meter, 12 – amplifier; 13 – PC with analog card; 14 – regulated pipe clamped to the ground.

For testing purposes, pipes of geometric parameters as listed in Table 6 have been used.

Table 6 Properties of pipes used for testing.

No.	Symbol of pipe used for testing	D_0	e	C
		[mm]	[mm]	[m/s]
Polyethylene MDPE pipes				
1	P1	50 (1.97 in.)	4.6 (0.18 in.)	390 (1,279.5 fps)
2	P2	40 (1.57 in.)	3.7 (0.14 in.)	390 (1,279.5 fps)
3	P3	32 (1.26 in.)	3.0 (0.12 in.)	390 (1,279.5 fps)
4	P4	25 (0.98 in.)	2.3 (0.09 in.)	390 (1,279.5 fps)
Steel pipes				
5	S1	48 (1.89 in.)	3.0 (0.12 in.)	1,280 (4,199.5 fps)
6	S2	42 (1.65 in.)	3.5 (0.14 in.)	1,280 (4,199.5 fps)
7	S3	33.5 (1.32 in.)	3.5 (0.14 in.)	1,280 (4,199.5 fps)
8	S4	27 (1.06 in.)	3.0 (0.12 in.)	1,280 (4,199.5 fps)

The closing time of the ball valve with adjustable spindle angle was determined by an electronic meter with an accuracy of 10^{-3} s. Depending on the type of measured pipe, the closing time of the ball valve varied: for steel pipes, t_z = 0.016 - 0.023 s; for polyethylene pipes, t_z = 0.025 - 0.035 s (depending on the initial opening degree of the ball valve).

Measurements and analysis of the results apply only to a simple water hammer, i.e. one in which the time of the pressure wave T is always greater than the bar closing time $t_z < T$. In addition, the bar closing time t_z is always shorter than the returning time t_r of the first reflected pressure wave to the outlet side $t_z < t_r$.

The experiment was performed at a constant temperature of 8°C± 2% (46.4°*F*). Maintaining a fixed temperature was especially important for polyethylene pipes due to the effects of temperature on their mechanical properties, given by Janson (1995).

The characteristics of the water hammer pressure *p(t)* were defined in the three measuring points of the pipeline. The pressure sensors have been tarred so that the voltage value for the known pressure p0 is zero. The measuring range of the sensors (12 - 20 *bar* ± 0.1 bar (174.04 - 290.06 *psi*)) has been selected according to the stream velocity v_0 of uniform flow and the expected maximum pressure at the measuring points.

The water stream pressure before the water hammer was measured at the outlet of the pipeline. The pressure was 4.5 - 5.0 bar± 0.1 bar (65.26 - 72.51 psi). The average velocity v_0 of fixed flow (determined in the calculation section of the pipeline and the section at the end of the pipeline) and the pressure p_0 were chosen so as to prevent the occurrence of cavitation during water hammer.

The study was conducted for five variants of connected pipes, see Figure 36.

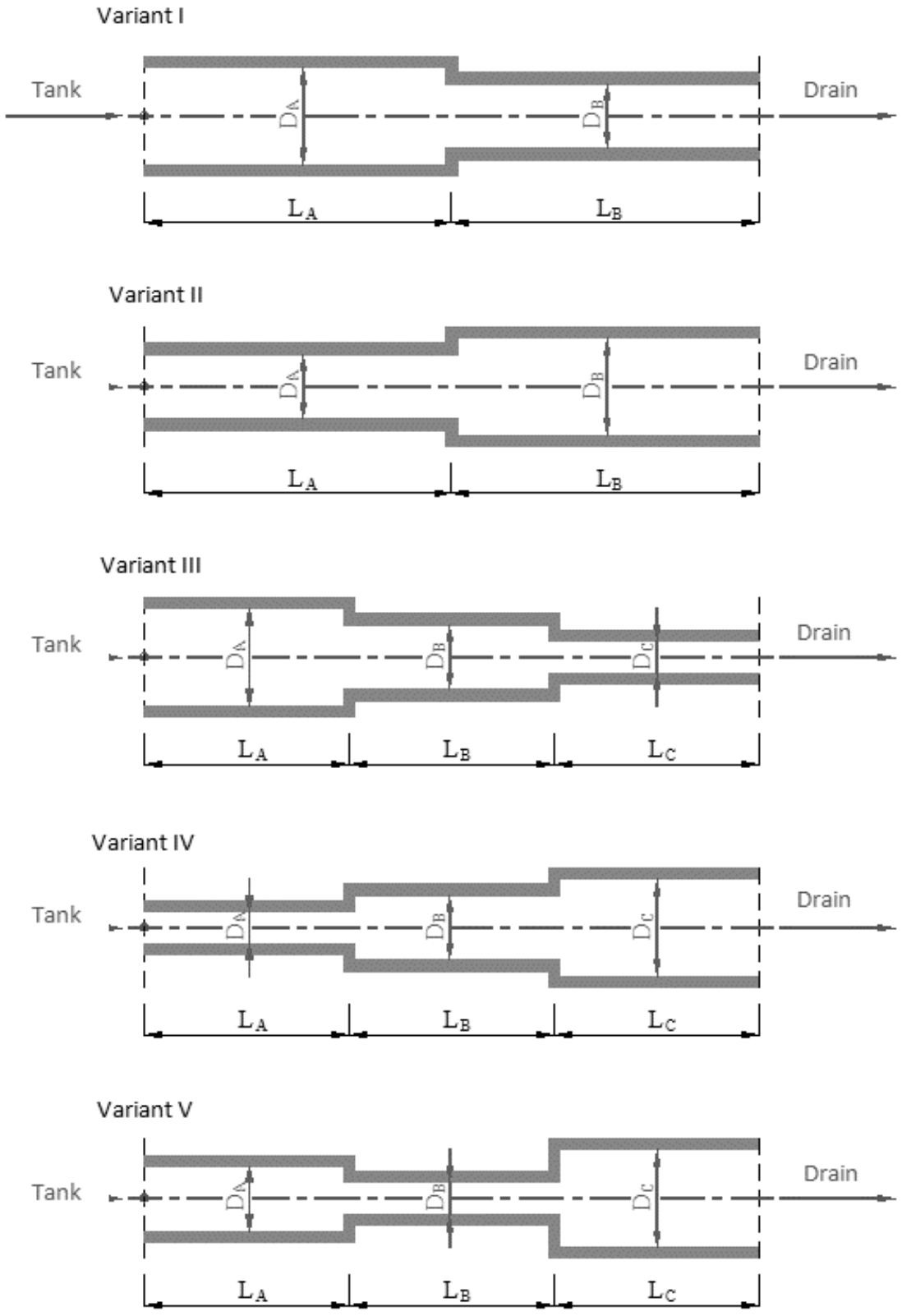

Figure 36 Different variants of tested piping systems connected in series.

RESULTS AND DISCUSSION

In the conducted measurements, a number of pressure characteristics for different variants of connected pipes were registered, see Figure 36. In addition, the impact of the length of individual sections was taken into consideration.

Based on experimentally acquired pressure characteristics, the celerity c_e of pressure disturbance propagation was calculated for the measured period T of resultant vibrations, and the total length L of the pipeline

$$c\_e = 2L/T$$

Equation 49

The period T is calculated as the arithmetic average of 10 initial phases of water hammer (example characteristics with marked period *2T* are shown in Figure 37 Figure 38 Figure 39 Figure 40).

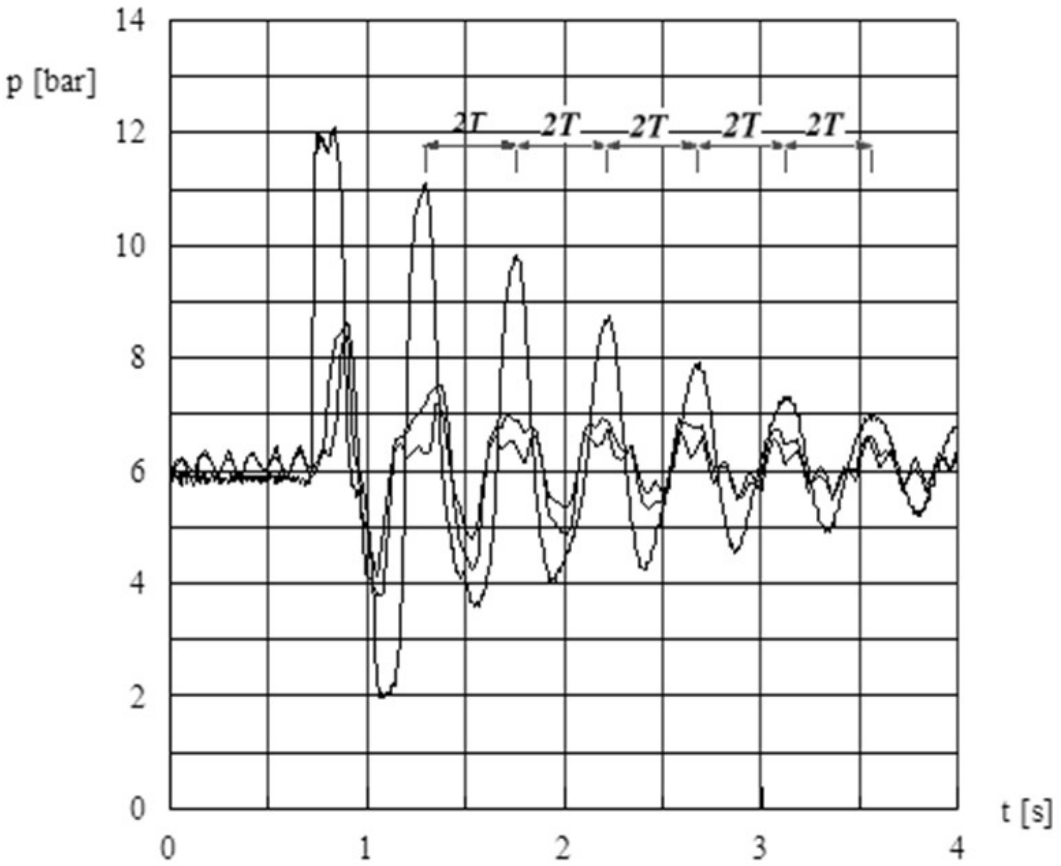

Figure 37 Pressure characteristics for three measuring sections (sections of pressure sensor locations) for a polyethylene pipe P1P4 (D_1= 40.8 mm (1.61 in.), L_1= 24.25 m (79.56 ft), D_4= 20.4 mm (0.80 in.), L_4= 25.0 m (82.02 ft)).

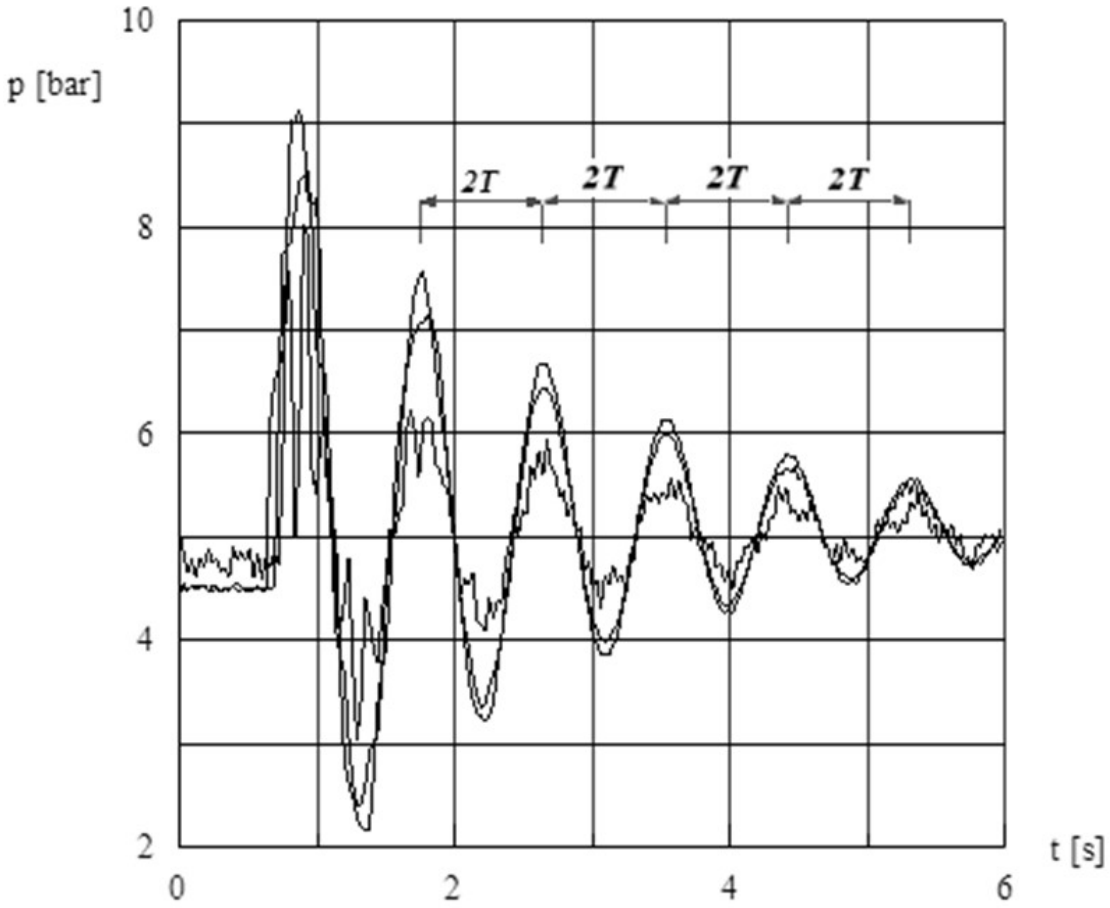

Figure 38 Pressure characteristics for three measuring sections for a polyethylene pipe P4P1 (D1= 42 mm (1.65 in.), L1= 26.45 m (86.78 ft); D4= 20.4 mm (0.80 in.), L4= 25.0 m (82.02 ft).

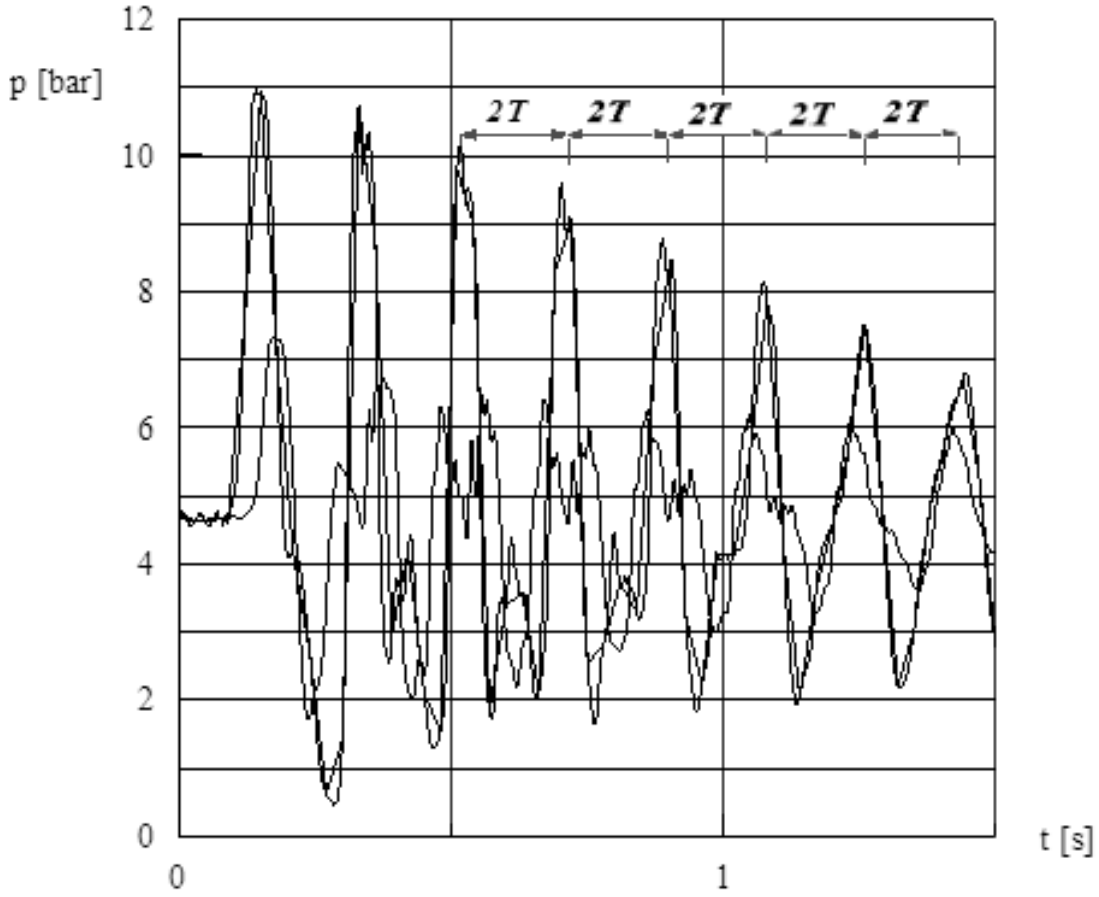

Figure 39 Pressure characteristics for three measuring sections for a steel pipe S1S4 (D_1= 42 mm (1.65 in.), L_1= 26.45 m (86.78 ft), D_4= 21 mm (0.83 in.), L_4= 24.60 m (80.71 ft).

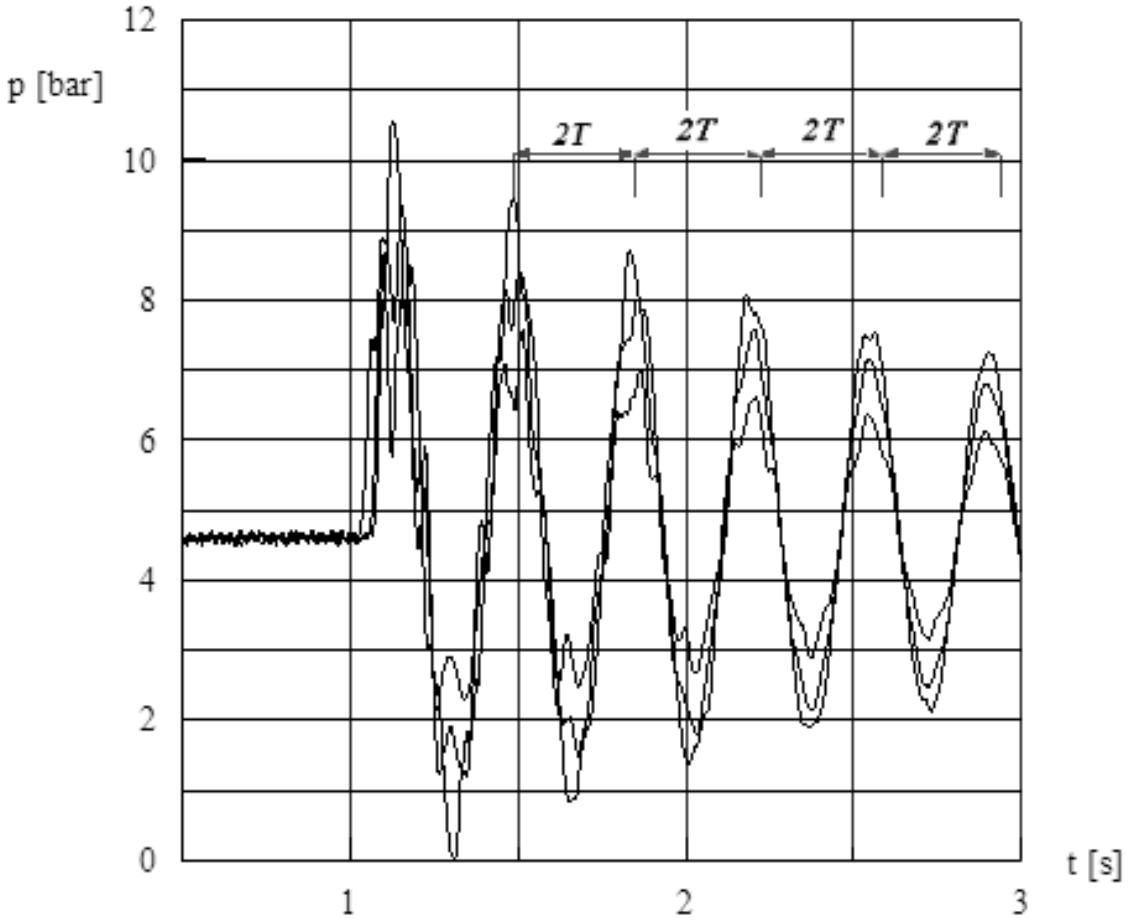

Figure 40 Pressure characteristics for three measuring sections for a steel pipe S4S1 (D_1= 42 mm (1.65 in.), L_1= 26.45 m (86.78 ft), D_4= 21 mm (0.83 in.), L_4= 24.60 m (80.71 ft)).

Empirical values of equivalent celerity pressure disorders c_e were calculated with an uncertainty of ± 1.5% for the estimated measurement error of length *L* and period *T*.

Then, based on Equation 42, Equation 44, and Equation 45, the equivalent celerity values for the analysed systems were computed. Exemplary calculation results of the equivalent celerities are summarized in Table 7, Table 8, Table 9, and Table 10; including both compared methods and different variants of pipe connections in systems of two and three sections.

Table 7 Two thick polyethylene MDPE pipes – pipe parameters, comparison of the equivalent celerity of the pressure wave obtained experimentally and analytically for different variants of connections.

Thick polyethylene MDPE pipes							
Geometric parameters of pipes				Variant	c_e experimentally	c_e analytically	c_e numerically
					m/s	m/s	m/s
D1(mm)	D2(mm)	D3(mm)	D4(mm)	**P1P2**	435 (1,427 fps)	445 (1,460 fps)	445.2 (1,461 fps)
40.8 (1.61 in.)	32.6 (1.28 in.)	26.0 (1.02 in.)	20.4 (0.80 in.)	**P2P1**	350 (1,148 fps)	335 (1,099 fps)	334.7 (1,098 fps)
				P1P3	473 (1,552 fps)	498 (1,634 fps)	498.2 (1,635 fps)
L1(m)	L2(m)	L3(m)	L4(m)	**P3P1**	280 (919 fps)	281 (922 fps)	281.7 (924 fps)
24.25 (79.56ft)	24.00 (78.74ft)	24.85 (81.53ft)	25.00 (82.02ft)	**P1P4**	523 (1,716 fps)	550 (1,804 fps)	549.6 (1,803 fps)
				P4P1	225 (738 fps)	232 (761 fps)	230.2 (755 fps)

Table 8 Two steel pipes – pipe parameters, comparison of the equivalent celerity of the pressure wave obtained experimentally and analytically for different variants of connections.

Steel pipes							
Geometric parameters of pipes				Variant	c_e experimentally	c_e analytically	c_e numerically
					m/s	m/s	m/s
D1(mm)	D2(mm)	D3(mm)	D4(mm)	**S1S2**	1,320 (4,331 fps)	1,425 (4,675 fps)	1,425 (4,675 fps)
42.0 (1.65 in.)	35.0 (1.38 in.)	26.5 (1.04 in.)	21.0 (0.83 in.)	**S2S1**	1,150 (3,773 fps)	1,135 (3,724 fps)	1,134 (3,720 fps)
				S1S3	1,590 (5,216 fps)	1,635 (5,364 fps)	1,633 (5,358 fps)
L1(m)	L2(m)	L3(m)	L4(m)	**S3S1**	940 (3,084 fps)	919 (3,015 fps)	920.3 (3,019 fps)
26.45 (86.78ft)	21.20 (69.55ft)	21.20 (69.55ft)	24.60 (80.71ft)	**S1S4**	1,720 (5,643 fps)	1,800 (5,905 fps)	1,802 (5,912 fps)
				S4S1	760 (2,493 fps)	768 (2,520 fps)	755.97 (2,480 fps)

Table 9 Three thick polyethylene MDPE pipes – pipe parameters, comparison of the equivalent celerity of the pressure wave obtained experimentally and analytically.

Thick polyethylene MDPE pipes						
Geometric parameters of pipes			Variant	c_e experimentally	c_e analytically	c_e numerically
				m/s	m/s	m/s
D1(mm)	D2(mm)	D3(mm)	**P1P2P3**	458 (1,503 fps)	489 (1,604 fps)	489.4 (1,605 fps)
40.8 (1.61 in.)	32.6 (1.28 in.)	26.0 (1.02 in.)				
L1(m)	L2(m)	L3(m)	**P3P2P1**	288 (945 fps)	298 (978 fps)	297.8 (977 fps)
12.0 (39.37ft)	12.0 (39.37ft)	12.0 (39.37ft)				

Table 10 Three steel pipes – pipe parameters, comparison of the equivalent celerity of the pressure wave obtained experimentally and analytically.

Steel pipes						
Geometric parameters of pipes			Variant	c_e experimentally	c_e analytically	c_e numerically
				m/s	m/s	m/s
D1(mm)	D2(mm)	D4(mm)	**S1S2S4**	1,690 (5,545 fps)	1,730 (5,676 fps)	1,734.2 (5,690 fps)
42.0 (1.65 in.)	35.0 (1.38 in.)	21.0 (0.83 in.)				
L1(m)	L2(m)	L4(m)				
13.30 (43.63ft)	14.15 (46.09ft)	12.20 (40.03ft)				

To better illustrate the effect of the lengths of the connected pipes on the equivalent celerity, studies have been conducted for different ratios of connected sections for a system of two pipes. The results obtained experimentally and analytically are shown in diagrams (from Figure 41 to Figure 46).

They show the change of celerity c_e as a function of the share of length of the individual sections in the total length of the system. The length ratio is expressed as the share of the length of the second section *L2* of the total length of the system. This means that *L2/L = 0*, when only the first pipe of length *L1* is being analysed. In turn, *L2/L = 1*, when only the second pipe of length *L2* is being analysed. Intermediate values *L2/L* correspond to a respective share of the length *L1* and *L2* in the entire system.

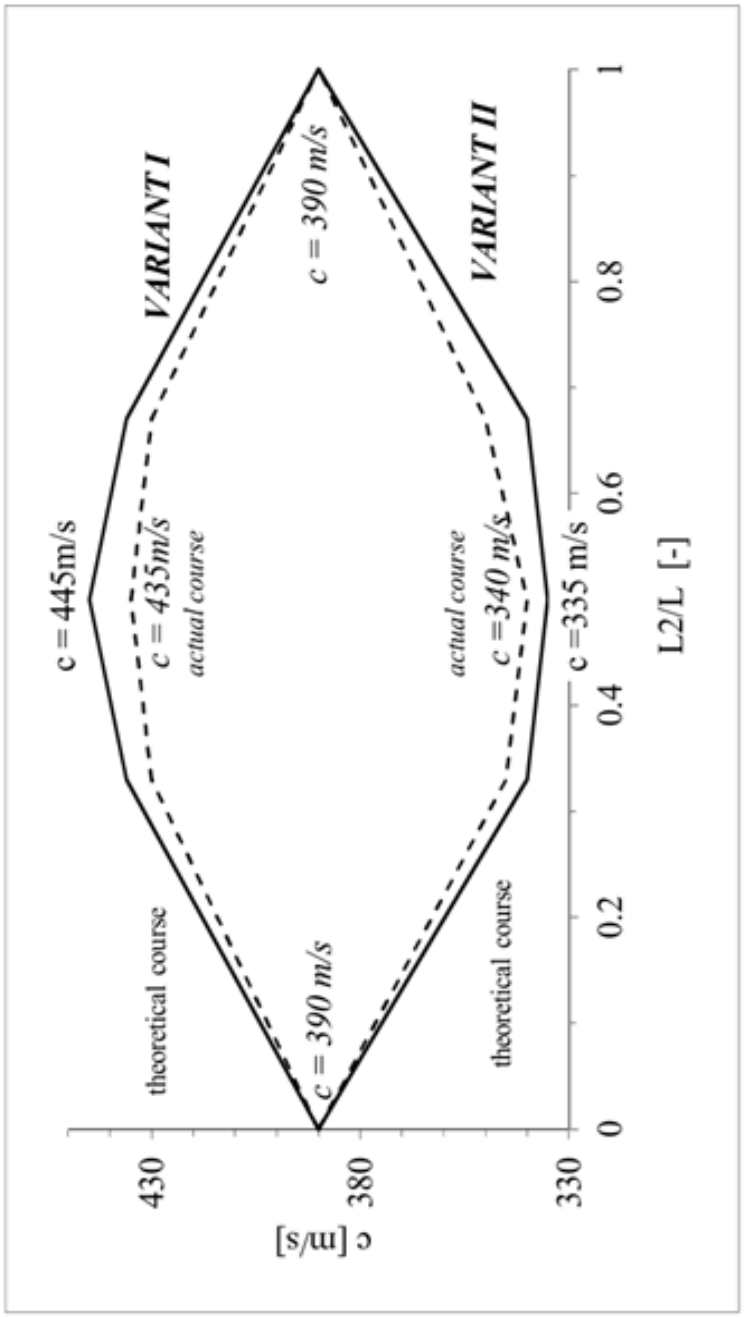

Figure 41 Characteristics of the celerity of pressure oscillation – equivalent pressure wave in a pipeline composed of two thick polyethylene MDPE pipes of sections D_1= 40.8 mm (1.61 in.) and D_2=32.65 mm (1.28 in.), (Variant I - P1P2, Variant II - P2P1).

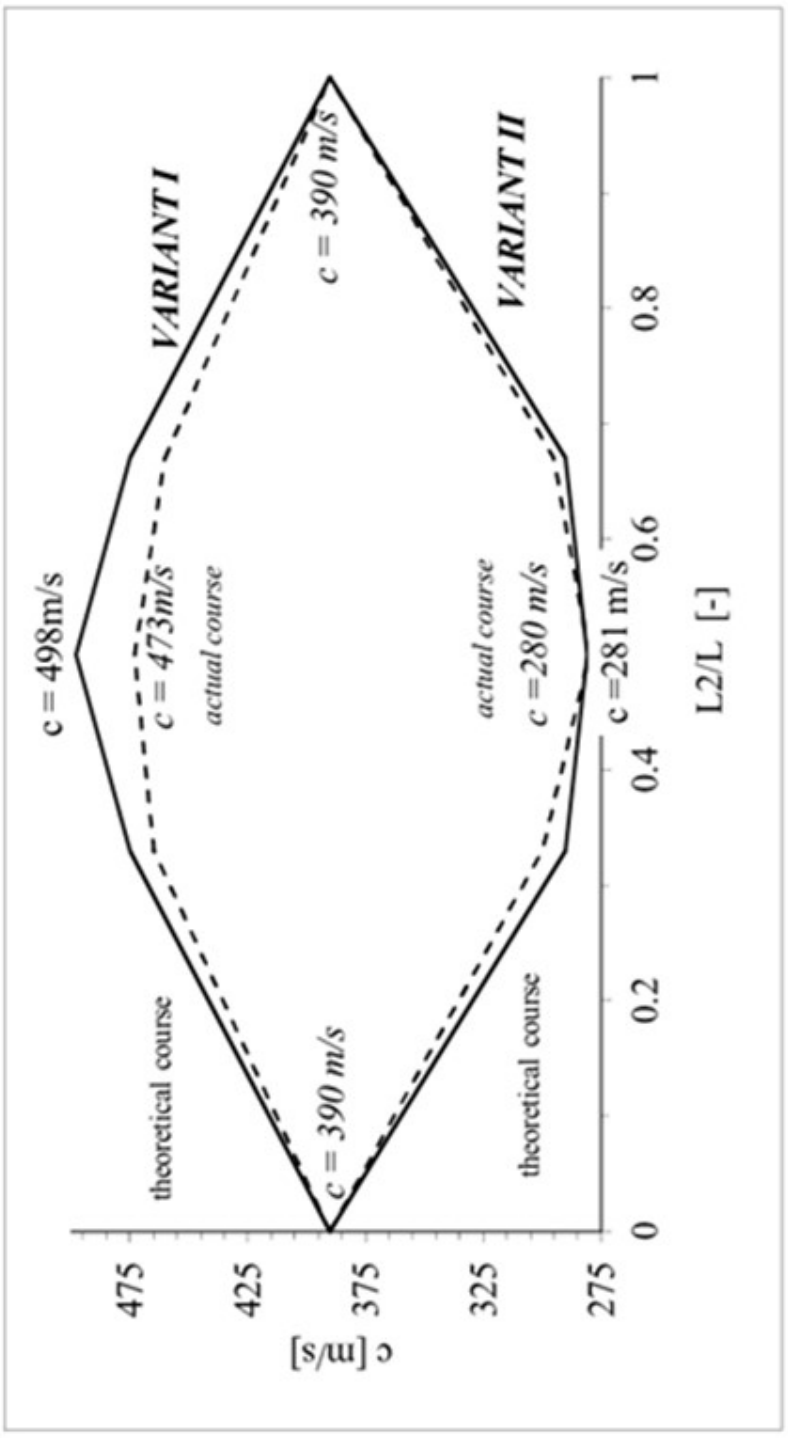

Figure 42 Characteristics of the celerity of pressure oscillation – equivalent pressure wave in a pipeline composed of two thick polyethylene MDPE pipes of sections D_1= 40.8 mm (1.61 in.) and D_3=26 mm (1.02 in.), (Variant I - P1P3, Variant II – P3P1).

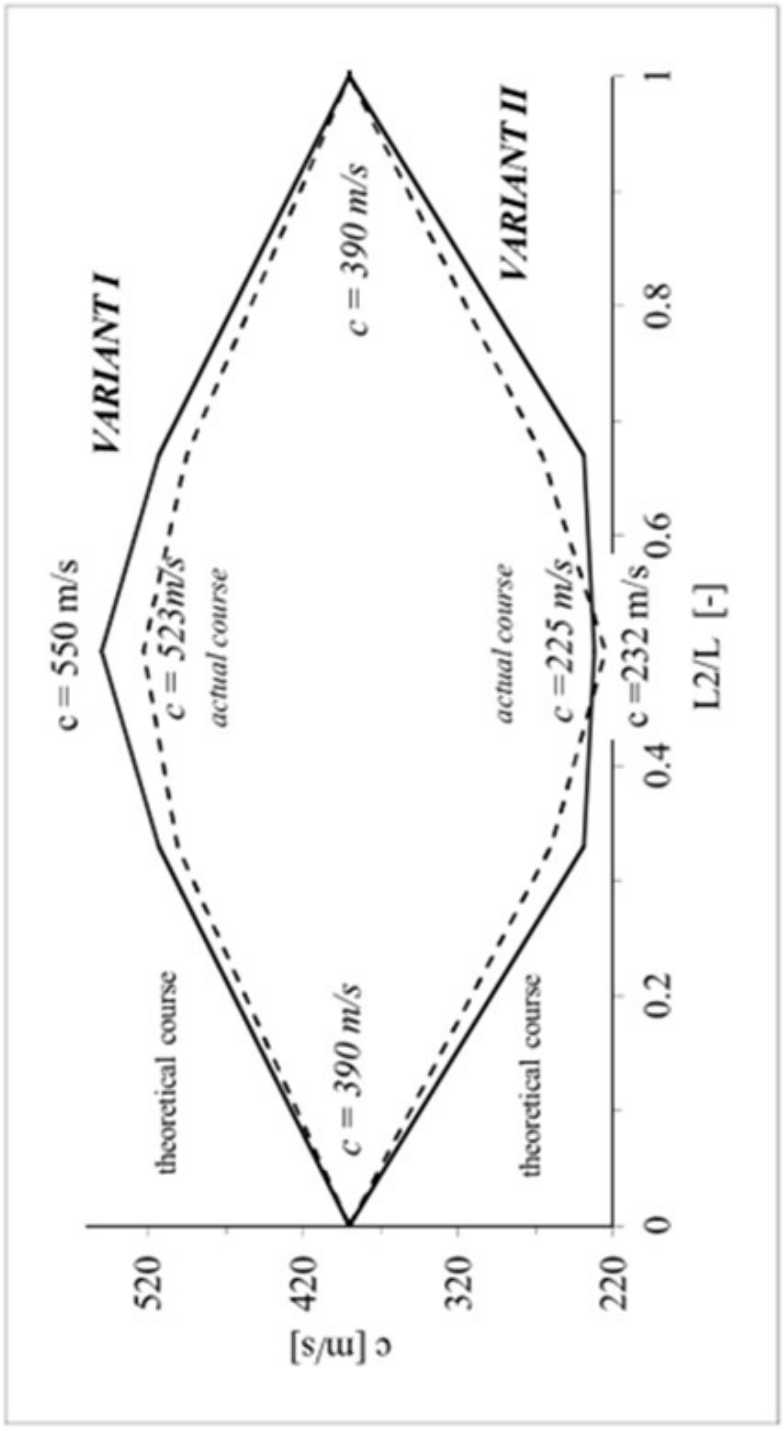

Figure 43 Characteristics of the celerity of pressure oscillation – equivalent pressure wave in a pipeline composed of two thick polyethylene MDPE pipes of sections D_1= 40.8 mm (1.61 in.) and D_4=20.4 mm (0.80 in.),(Variant I - P1P4, Variant II – P4P1).

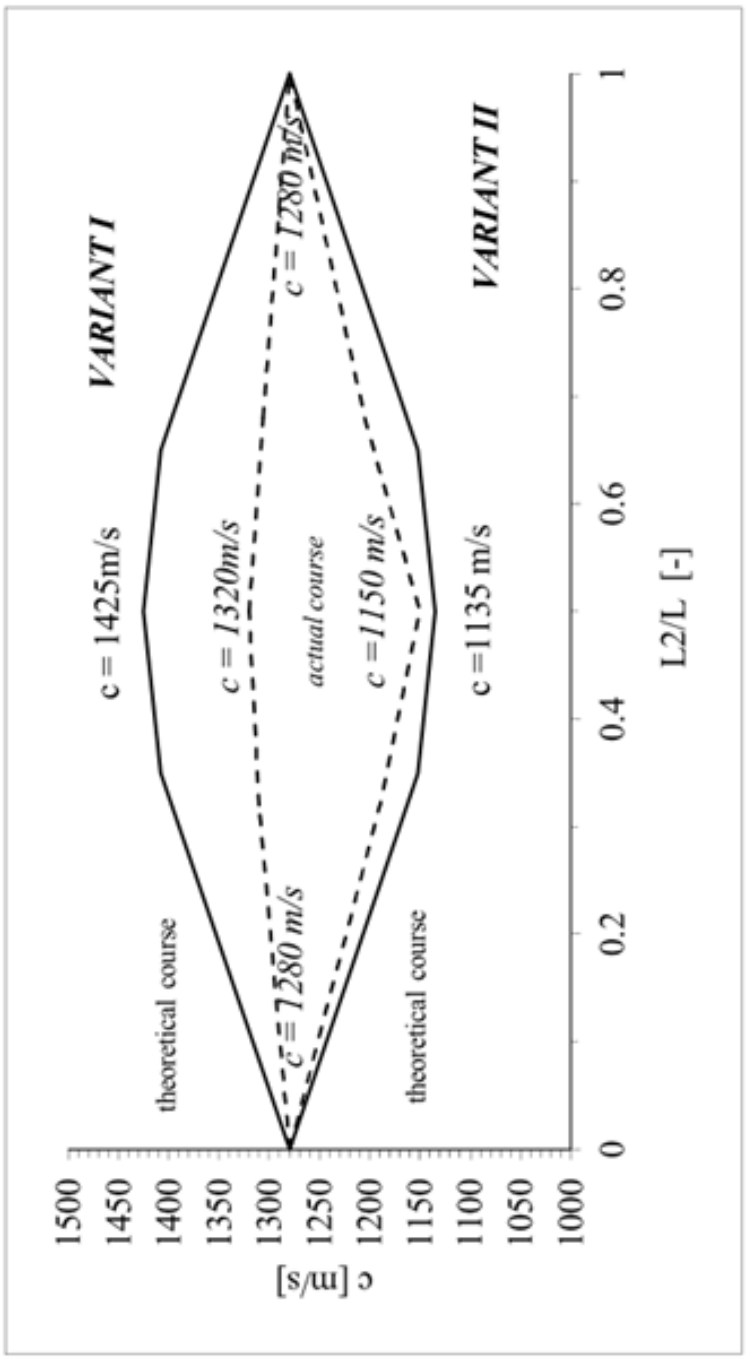

Figure 44 Characteristics of the celerity of pressure oscillation – equivalent pressure wave in a pipeline composed of two steel pipes of sections D_1= 42 mm (1.65 in.) and D_2=35 mm (1.38 in.),(Variant I - S1S2, Variant II - S2S1).

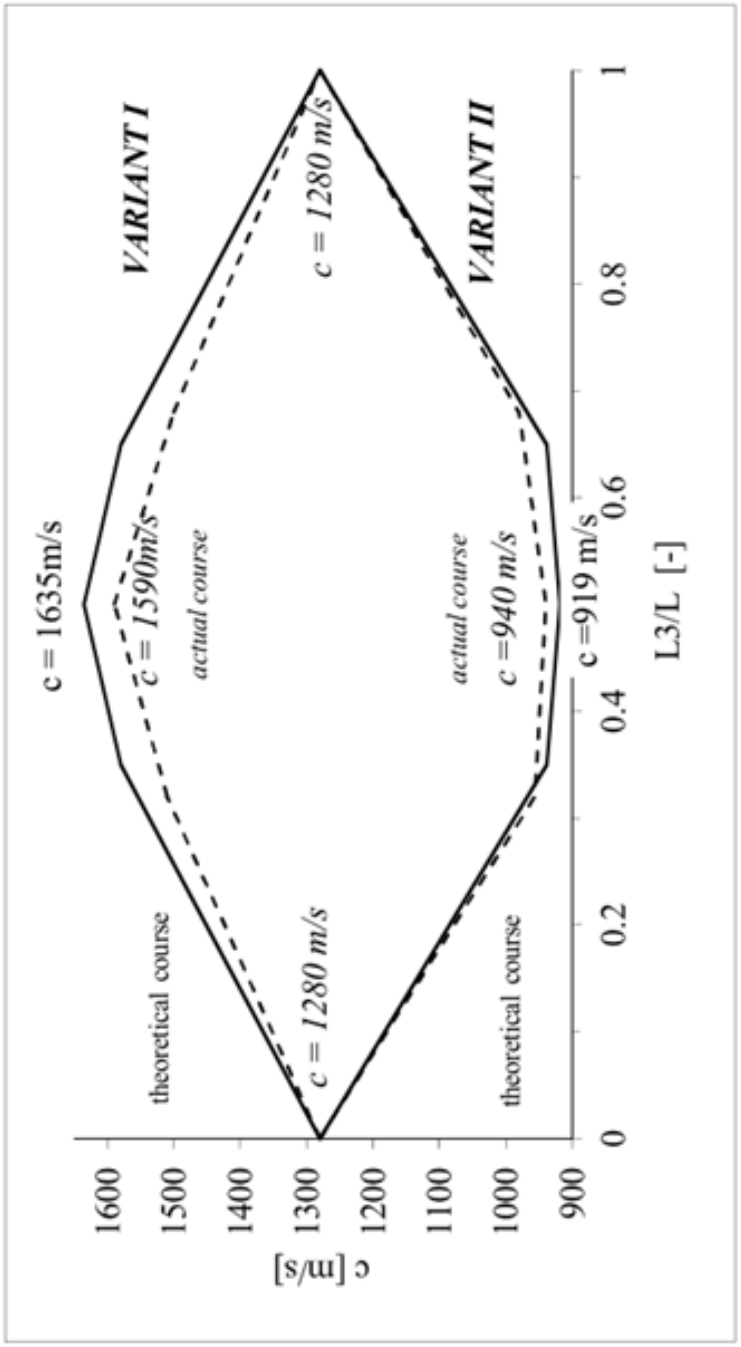

Figure 45 Characteristics of the celerity of pressure oscillation – equivalent pressure wave in a pipeline composed of two steel pipes of sections D_1= 42 mm (1.65 in.) and D_3=26.5 mm (1.04 in.), (Variant I - S1S3, Variant II – S3S1).

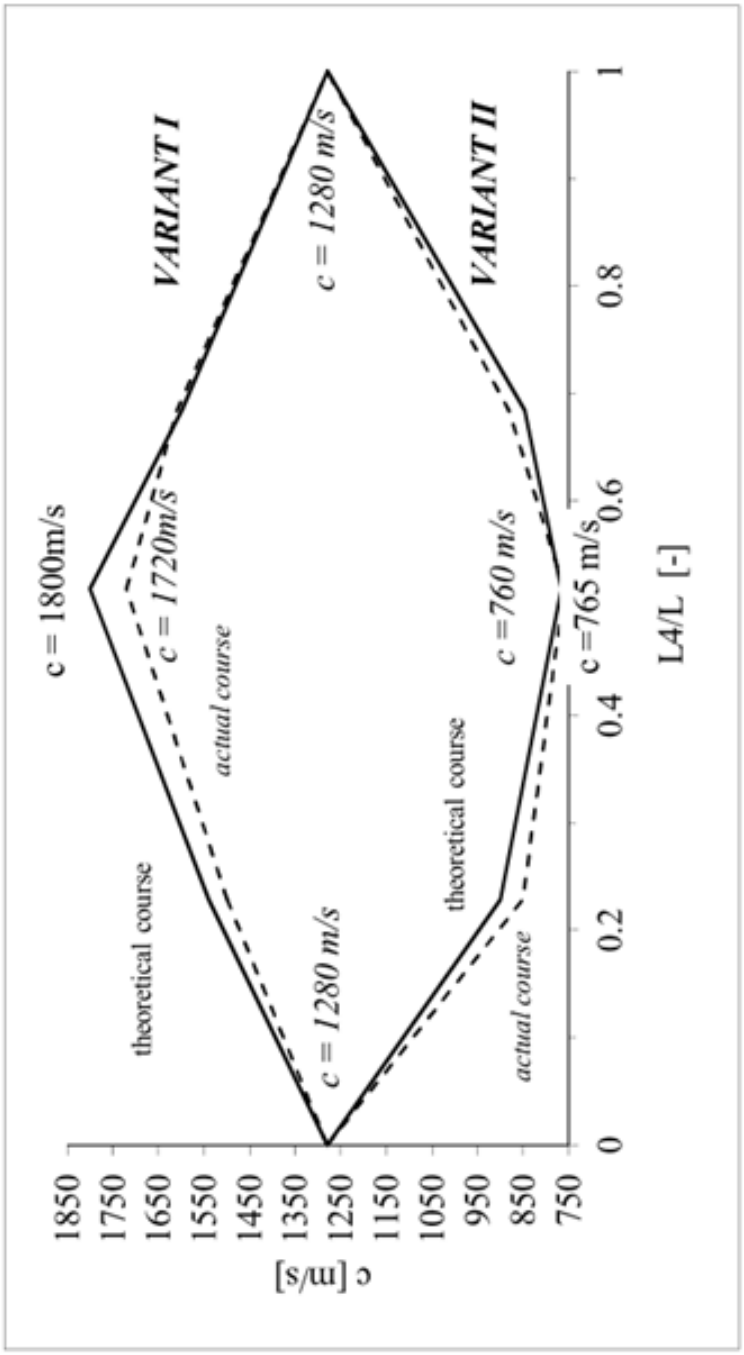

Figure 46 Characteristics of the celerity of pressure oscillation – equivalent pressure wave in a pipeline composed of two steel pipes of sections D_1= 42 mm (1.65 in.) and D_4=21 mm (0.83 in.),(Variant I - S1S4, Variant II – S4S1).

The upper curves correspond to variant I, wherein the pipe with a larger diameter is located on the tank side. The lower curves illustrate the change of value c_e for the reverse configuration.

The values of celerity c_e obtained for two pipes connected in series were the same for constant values of L_{s1}/L and L_{p1}/L and for the same order of pipe-laying (curve 1 or 2, from Figure 41 to Figure 46) independently of the overall length L of the connected pipes. For the proportion of the lengths of connected pipes L_{s1}/L and L_{p1}/L equal to 0.5, a maximum pressure wave celerity c_e (variant I) and minimum celerity c_e (variant II) have been recorded. This shows that the range of expected values of the pressure wave celerity c_e depends on the ratio of the cross-sections of connected pipes and their arrangement order.

Using the dependencies of Equation 43 and Equation 46, derived from the method of linear analysis of natural vibrations, the dependence of the equivalent celerity c_e of the pressure wave on the length ratios L_{s1}/L and L_{p1}/L can be obtained. For comparative purposes, the results obtained by analysis were applied to the celerity diagrams learned from experimental data.

As seen in Figure 41 to Figure 46, there is satisfactory consistency in results (the relative error falls within the range 0.3% - 7% and is usually not greater than 5%). Some differences arise from the fact that the classical theory ignores frequency-dependent factors, such as friction and wave celerity. For curves describing dependencies in connected pipes of variant I, the differences in the values obtained are higher. For this type of connection, the course of the water hammer phenomenon is more complex as a result of a greater number of disorders compared to variant II that accompany the phenomenon (in the form of reflected overlapping waves which constructively add together; compare the characteristics in Figure 37 and Figure 38, as well as Figure 39 and Figure 40. It should be noted that in variant I, the equivalent velocities of pressure disorders are higher, which may indicate a greater elasticity of the "pipe - liquid" system during the process of reaching the natural vibrations.

NUMERICAL VERIFICATION

To verify the experimental values and the possibilities of solving water hammer issues in pipelines comprised of multiple pipes of various parameters, the MATLAB software package (version 2016) has been used.

A function was implemented that allows the determination of ω (function [*omega*]) and the equivalent celerity of the pressure wave c_e (function [*C*]) for any number of pipes, based on pipe parameters. This function has the following form:

function [*omega, C*] = pipes(c, L, A, *start_fzero, script_name*)

In the first step, the size of vectors **c, L** and **A** is verified in order to determine the number of pipes (ref. N) composing the system. If the number of elements in individual vectors is not equal, the function returns an error.

The essential transformation is performed using symbolic computation (*syms* package, Symbolic MATLAB Toolbox). First, a starting point in the form of two equations is assumed:

$$H_{D1} = -Q_{U1}Z_{C1}sinh\gamma_1 L_1$$

Equation 50

$$Q_{D1} = Q_{U1}cosh\gamma_1 L_1$$

Equation 51

with symbolic variables H_{D1} and Q_{D1}.

Then, iteratively for steps *k=2 … N-1*, new symbolic variables and substitutions are made:

$$H_{Uk}=H_{Dk-1}$$

Equation 52

$$Q_{Uk} = Q_{Dk-1}$$

Equation 53

$$H_{Dk} = H_{Uk}cosh\gamma_k L_k - Q_{Uk}Z_{Ck}sinh\gamma_k L_k$$

Equation 54

$$Q_{Dk} = -\frac{H_{Uk}}{Z_{Ck}}sinh\gamma_k L_k + Q_{Uk}cosh\gamma_k L_k$$

Equation 55

The last step (N) includes the creation of further symbolic variables and final substitutions:

$$H_{UN}=H_{DN-1}$$

Equation 56

$$Q_{UN} = Q_{DN-1}$$

Equation 57

$$Q_{DN} = -\frac{H_{UN}}{Z_{CN}} sinh\gamma_N L_N + Q_{UN} cosh\gamma_N L_N$$

Equation 58

In this manner, the expression Q_{DN} is obtained, containing one variable. Using *matlabFunction(),* the expression is converted into a handle, which is then used in function *fzero()* with the parameter *start_fzero*. The function *fzero()* finds the closest zero of a function relative to the starting point *start_fzero*.
After determining the zero of a function, the additional parameter *C* returned by the function as well as the determined value of *omega* is calculated.
The flowchart of the resolving algorithm is shown in Figure 47.

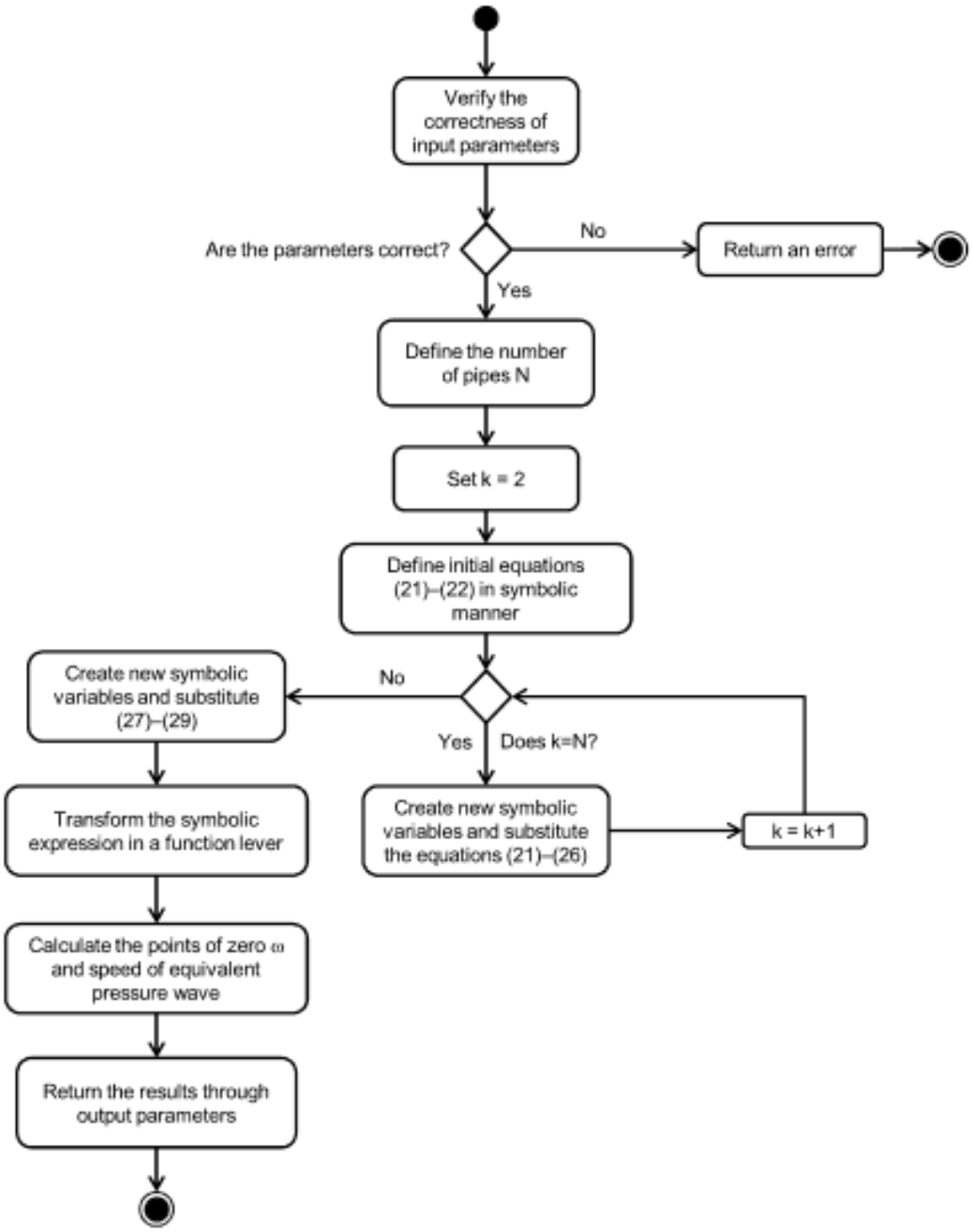

Figure 47 The flowchart of the resolving algorithm.

Example of calling the function:

```
c=[390 390 390 390];
L=[20 20 20 20];
A=[0.007853981633974484    0.005026548245743669
0.003216990877275948 0.001963495408493621];
[omega, C]=pipes(c,L,A,1,pipes4.m');
```

The created function has been used to find solutions for the following configurations summarized in Table 11, Table 12, Table 13, Table 14 Table 15 and Table 16, described by Malesinska A. (2018).

Table 11 Introduced parameters for MDPE pipes with thick walls

Pipe symbol	D_0 [mm]	Theoretical c [m/s]	L1 [m]	L2 [m]
P1	50.0 (1.97 in.)	390 (1,279.5 fps)	20 (65.62ft)	20 (65.62ft)
P2	40.0 (1.57 in.)	390 (1,279.5 fps)	20 (65.62ft)	50 (164.04ft)
P3	32.0 (1.26 in.)	390 (1,279.5 fps)	20 (65.62ft)	10 (32.81ft)
P4	25.0 (0.98 in.)	390 (1,279.5 fps)	20 (65.62ft)	70 (229.66ft)

Table 12 Introduced parameters for MDPE pipes with thin walls

Pipe symbol	D_0 [mm]	Theoretical c [m/s]	L1 [m]	L2 [m]

C1	50.0(1.97 in.)	310 (1,017 fps)	20 (65.62ft)	50 (164.04ft)
C2	40.0(1.57 in.)	310 (1,017 fps)	20 (65.62ft)	50 (164.04ft)

Table 13 Introduced parameters for steel pipes

Pipe symbol	D_0 [mm]	Theoretical c [m/s]	L1 [m]	L2 [m]
S1	48.0 (1.89 in.)	1,280 (4,199.5 fps)	20 (65.62ft)	20 (65.62ft)
S2	42.0 (1.65 in.)	1,280 (4,199.5 fps)	20 (65.62ft)	50 (164.04ft)
S3	33.5 (1.32 in.)	1,280 (4,199.5 fps)	20(65.62ft)	10 (32.81ft)
S4	27.0 (1.06 in.)	1,280 (4,199.5 fps)	20(65.62ft)	70 (229.66ft)

Table 14 Calculation results

Configuration of connections	For length L1		For length L2	
	ω	c [m/s]	Ω	c [m/s]
P1P2P3P4	10.50221112152479	534.87322 (1,754.8334 fps)	5.54304328329149 7	529.32164 (1,736.6196 fps)
P4P3P2P1	5.167824591083589	263.19514 (863.5011 fps)	2.73007875085016 6	260.70331 (855.3258 fps)
P1P3P2P4	9.220684109756455	469.60558 (1,540.7007 fps)	5.33137275294544 9	509.10859 (1,670.3038 fps)

P4P2P3P1	5.408930689494223	275.47457 (903.7880 fps)	2.769177948964361	264.43701 (867.5755 fps)
P1C1P3P4P2	6.737833398136067	428.94379 (1,407.2959 fps)	3.047041487098698	387.96137 (1,272.8391 fps)
C1P1P4P3C2	5.506723162255213	350.56888 (1,150.1604 fps)	2.497031088462339	317.93187 (1,043.0836 fps)
S1S2S3S4	33.02175168144384	1,681.7840 (5,517.6640 fps)	17.656268331295225	1,686.0494 (5,531.6582 fps)
S4S3S2S1	18.07107514224697	920.35229 (3,019.5285 fps)	9.442600304925012	901.70190 (2,958.3396 fps)
S2S4S1S3	22.38505375321479	1,140.0614 (3,740.3590 fps)	12.556887077531622	1,199.0943 (3,934.0367 fps)
P1S2C1C2	6.862010290845349	349.47931 (1,146.5857 fps)	3.081942802698400	333.54437 (1,094.3057 fps)
P1C1S2C2	8.308183872173458	423.13233 (1,388.2294 fps)	3.883364073194765	420.27847 (1,378.8664 fps)

Computations for real pipeline network map data:

Table 15 Input parameters for steel pipes

Pipe symbol	D_0 [mm]	Theoretical c [m/s]	L [m]
S1	100 (3.94 in.)	1,280 (4,199.5 fps)	120 (393.70ft)
S2	150 (5.90 in.)	1,280 (4,199.5 fps)	200 (656.17ft)
S3	200 (7.87 in.)	1,280 (4,199.5 fps)	180 (590.55ft)
S4	250 (9.84 in.)	1,280 (4,199.5 fps)	160 (524.93ft)

Results for configuration S4S3S2S1: ω =4.35568 and c_e = 1,830.12203 [m/s], (6,004.3373 fps).

Table 16 Input parameters for MDPE pipes

Pipe symbol	D_0 [mm]	Theoretical c [m/s]	L [m]
P1	150 (5.90 in.)	390 (1,279.5 fps)	150 (492.12ft)
P2	200 (7.87 in.)	390 (1,279.5 fps)	150 (492.12ft)
S3	200 (7.87 in.)	1,280 (4,199.5 fps)	400 (1,312.33ft)
P4	150 (5.90 in.)	390 (1,279.5 fps)	550 (1,804.46ft)
P5	100 (3.94 in.)	390 (1,279.5 fps)	100 (328.03ft)
S6	200 (7.87 in.)	1,280 (4,199.5 fps)	380 (1,246.72ft)

Results for configuration S6P5P4S3P2P1: ω =1.26143 and c_e = 1,389.2801 [m/s], (4,558.0056 fps).

MAXIMUM PRESSURE INCREASE ESTIMATION IN WATER HAMMER

However, not only equivalent celerity is important for designers, engineers or users of the pipe network, but, above all, possible maximum pressure increase caused by water hammer. The pressure increase can be easily calculated by using equivalent celerity.
The Joukowski equation can be used for the calculation of pressure increase, given by Wylie (1993):

$$\Delta p = \pm \rho ce \Delta v$$

Equation 59

Dimensions: F=Force, L=Length, M=Mass, T=Time
ce = equivalent celerity [L/T].
ΔP = Maximum pipe pressure increase in water hammer phenomenon [F/L2].
Δv = Change in velocity in water hammer [L/T].
ρ = Fluid density [M/L3].
To confirm validity of numerical calculations of equivalent celerity, compliance of calculated pressure increases series of measurements was done. In the section some schemes were shown, see Table 17.

Table 17 Schema examples (S – steel pipes; P – PVC).

Schemas	Seria	L1 [m]	L2 [m]	D1 [mm]	D2 [mm]	
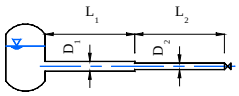	S1S2	26.45	21.20	42.0	35.0	
	P1P2	24.00	24.00	40.8	32.6	
	P1P4	24.25	25.00	40.8	20.4	
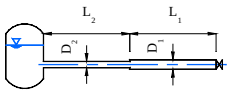	S2S1	26.45	21.20	35.0	42.0	
	P2P1	24.00	24.00	40.8	32.6	
	P4P1	24.25	25.00	40.8	20.4	
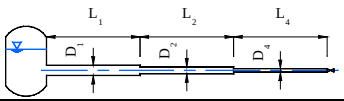	P1P2 P3	All pipes have the same length L = 12.00 m		D1 [mm]	D2 [mm]	D4 [mm]
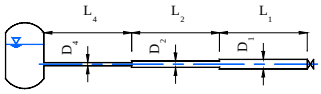	P3P2 P1			42	35	21

The measurements were conducted for straight pipes of various lengths, diameters, and material configurations. Each time, the pipes were fixed to the base in a way that prevented any displacement.
The measurements were conducted in accordance with the following assumptions:

1. Measurements and analysis were concerned with a simple water hammer
2. The experience was performed at 281°K
3. The pressure characteristics were measured in four measuring sections on the pipeline: at the downstream near the ball valve,

at the change of the cross-sections area of the connected in series pipes; as a control point, pressure was also measured in the middle of the pipeline just behind the tank

4. Pressure was measured by using a system consisting of a strain gauge set, extensometers amplifier (ZEP-101) and a computer with AD/DA.
5. Pressure values were measured with a time step of 5μs
6. Pressure gauges have linear operating characteristics with a correlation coefficient of more than 0.999
7. Measurement range of gauges 1.2 MPa and 2 MPa
8. Steady motion parameters before the water hammer appears were also measured
9. The initial pressure was chosen to prevent the occurrence of cavitations during a water hammer
10. Each measurement had calculated measurement error.

As a result of the experiments, the characteristics of the pressure change caused by water hammer wave propagation were obtained and recorded.

Only two example characteristics for two configuration of the same pipes are shown below (Figure 48 and Figure 49).

On the charts presented, the following symbols were adopted:

Δ p	first pressure increase caused by water hammer;
Pż	pressure increase calculated based on the Joukowski formula;
Δ pmax	maximum pressure increase observed during water hammer phenomenon.

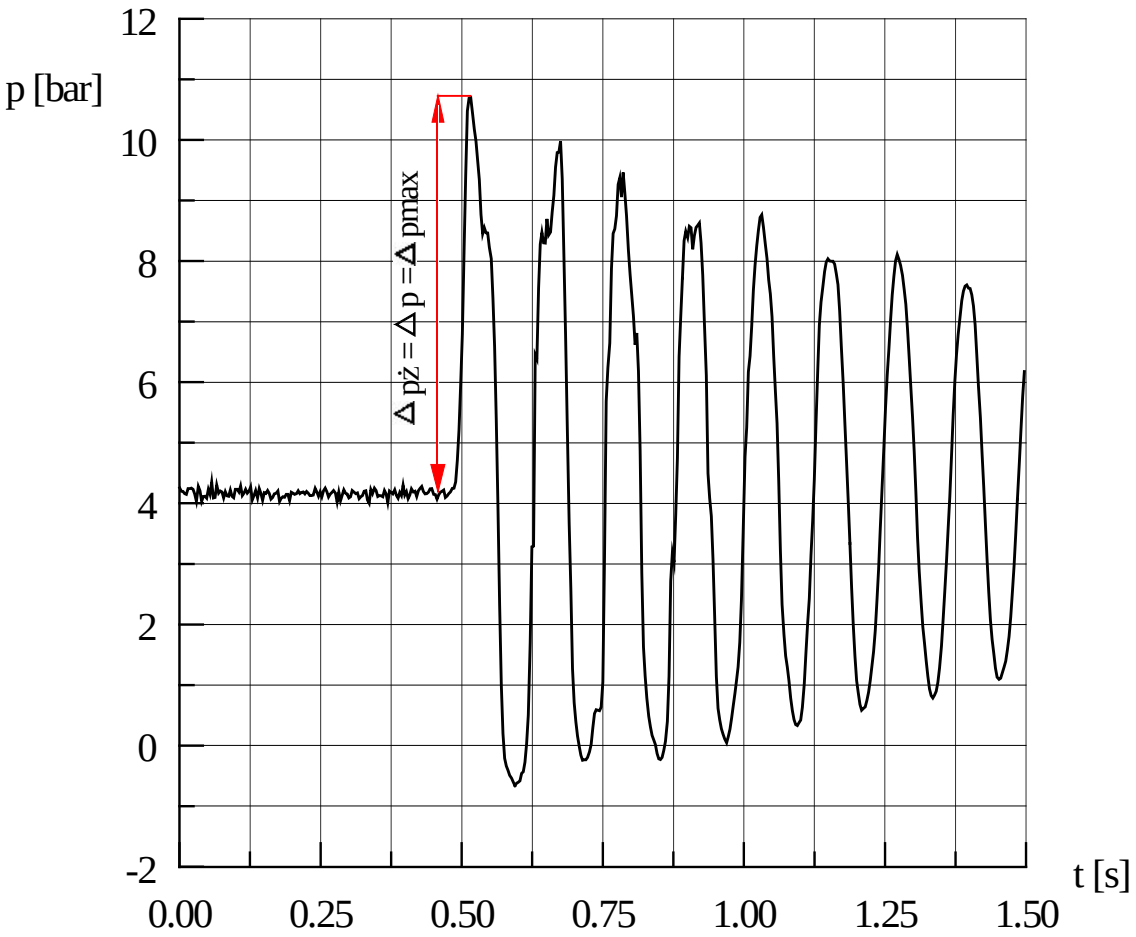

Figure 48 Pressure characteristics for three measuring sections for a steel pipe S1S2.

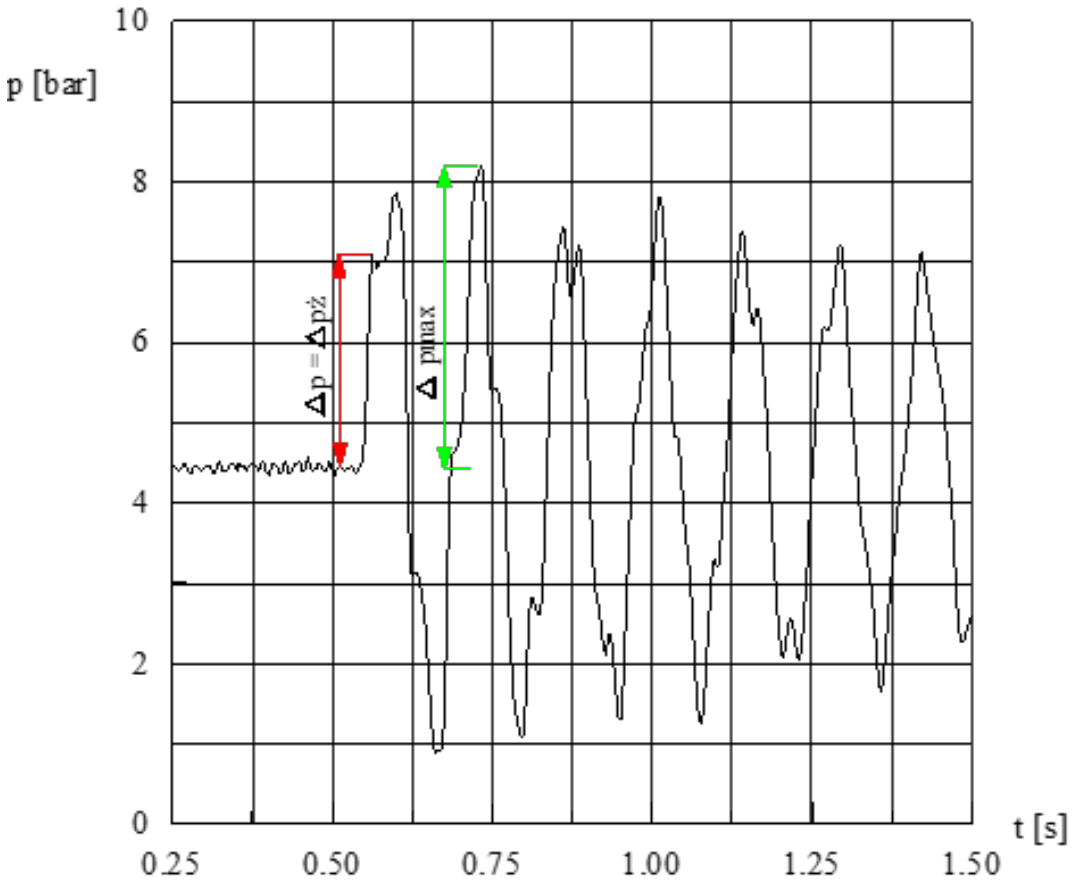

Figure 49 Pressure characteristics for three measuring sections for a steel pipe S2S1.

For the investigated schemes, the equivalent celerity ce was calculated using the MATLAB algorithm and then the pressure increase was calculated according to Equation 59. Calculated pressure values were compared with values obtained with the real characteristics. In addition, the maximum recorded pressure increase was read from the real characteristics. The results are summarized in Table 18.

Table 18 Summary of calculated and measured parameters.

Series	c_e [m/s]	t_Z [s]	V_o [m/s]	Δp [bar]	Δp_{obl} [bar]	Δp_{max} [bar]
S1S2	1320	0.020	0.520	6.80	6.86	6.80
P1P2	435	0.034	1.160	5.06	5.04	5.06
P1P4	523	0.031	1.390	7.25	7.27	7.25
S2S1	1155	0.021	0.203	2.27	2.34	3.94
P2P1	350	0.033	0.950	3.30	3.32	4.35
P4P1	225	0.035	0.810	1.80	1.83	5.60
P1P2P3	458	0.028	0.917	4.20	4.19	4.20
P3P2P1	288	0.033	1.200	3.50	3.47	6.50

where: ce – equivalent celerity; tz – closing time of the ball valve; Vo – average velocity for steady flow; Δp- pressure obtained from the real characteristics; Δpobl - Pressure calculated for the equivalent celerity from the eqn (22); Δpmax- maximum pressure obtained from the real characteristics.

As can be seen, a satisfactory correspondence between the values of Δp calculated from the Equation 59 by using the equivalent celerity and the pressure increase obtained from the real pressure characteristic (Figure 48 and Figure 49). The case, for which the diameters are set in ascending order, is noteworthy. The calculated value Δp is equal to the measured value, but this is not the maximum recorded pressure increase, see Figure 49.

Chapter 5
CONCLUSION

EXPERIMENTAL CAMPAIGN

The present work is the result of three years of experiments concerning the water hammer phenomenon in two different laboratories.

1) The first experimentation was carried out at the Laboratory of Hydraulics and Environment at the Department of Civil Engineering, Architecture and Georesources, in the Instituto Superior Técnico, Lisbon, Portugal.
2) The second and third experimentations were carried out at the Warsaw University of Technology, Warsaw, Poland.

CONCLUSIONS OF THE FIRST EXPERIMENT

The experiment conducted in Lisbon had the objective of understanding with experimentation the transient flow phenomena using measurements carried out in the laboratory pipe-rig, as well as confirming that the classic water hammer theory is not always valid in the presence of cavitation, presented in Puntorieri (2017).

Initial discharges are analysed with different closure positions, in steady state conditions.

To improve the results of the numerical modelling, the valve manoeuvres need to be adjusted to fit the experimental data.

In this research behaviour of the system is analysed, in steady state flow, for different positions of the valve closure and it compares collected data for different transient events.

The results carried out in the laboratory confirmed that the classic water hammer theory is not always valid, described by Brunone (2000) and Ghidaoui (2005). The sudden transient pressure drops and, subsequently, the transient cavitation occurs only for flow rates higher than 523.1 l/h; this phenomenon is increasingly evident with the increasing of the initial flow rate.

Chapter 2 shows that the interaction which arises between the valves and the flow in a pipe system is complex and not linear since the behaviour of the flow remains almost constant in all three cases for a degree of closure higher than 55º.

After this threshold, through minor movements of the valve, the flow drastically decreases to zero.

Engineers should be aware of this risk and should make proper use of modern techniques and software to ensure that these water hammer problems are dealt with adequately, described by Puntorieri (2017) and Bwire (2015).

CONCLUSIONS OF THE SECOND EXPERIMENT

The first experiment conducted at Warsaw University had the objective the study of water hammer phenomena on a physical model in combinations of two and three pipelines connected in series. The combined pipelines were made of steel and polypropylene. Pipelines made of one material type were connected in series in different configurations of diameter ratios and lengths of connecting sections. The obtained results were used to verify the value of the equivalent celerity calculated from equations derived using linear analysis of natural vibrations of the system. For verification of the equations, an algorithm in MATLAB has been developed that allows the calculation with ease of the equivalent celerity, ce, for N pipelines connected in series with varying diameter, length and material composition, given by Malesinska A. (2018).

One of the factors affecting the reliability of an installation is its proper suspension to the structure of the building or other supporting components. This is especially important for installations which are exposed to dynamic loads. An example of an installation with the required high reliability exposed to dynamic loads is a fire protection system. The selection of fastening elements for a given type of installation depends on the force that the fastener can carry. Unfortunately, it is usually assumed that the force is applied statically. The thesis presents the values of installation displacement calculated traditionally for the static system *(f)*. These values were compared with the displacements obtained with the use of the oscillation equation *(x or h)*. Such calculations were possible thanks to the results of research conducted on a physical model in the laboratory. It was not possible to measure displacements at this stage of the research. Installed strain gauges were used to measure the quantities necessary to determine the natural frequency of the system. The displacement values obtained from the oscillation equation were on average ten times larger than the displacements calculated from the static system, by Ferras (2017). The order of magnitude of the displacements calculated on the basis of the oscillation motion theory was consistent with the eye observations carried out directly on the model during the measurements. The next stage of the research will be the recording of the displacements of the system by means of a camera with software for the recording of fast-changing phenomena. This will allow real displacement functions to be obtained and validation of the use of equations of oscillation motion (taking into account the natural frequency of the system) for the

description of the phenomenon, assuming $S = F$. The obtained measurement results will allow for a possible correction of the equations used. Based on current knowledge, it is well known that the coefficient of compressibility (the inverse of the bulk modulus) of a liquid is meaningful when analysing a water hammer phenomenon. However, from the material mechanics point of view, the bulk modulus of the liquid is negligibly small (e.g. 2.2 GPa for water compared to 160 GPa for steel). Nevertheless, according to the authors, the bulk modulus of the liquid together with the coefficient of elasticity of the pipe walls has an influence on the suppression rate, and thus on the size of displacements caused by transient phenomena.

CONCLUSIONS OF THE THIRD EXPERIMENT

The second experiment conducted at Warsaw University had the objective to measure dynamic forces and associated displacements recorded on the model caused by transient flow conditions. For measured forces the displacements of the pipe was also calculated by using the oscillation motion equations. Force measurements and displacement analysis were carried out in laboratory on the model of a simple fire protection system equipped with three nozzles. The measurement results and calculations were used to calibrate a mathematical model created using MATLAB software Malesinska A (2018).The maximum values of the equivalent celerity measured for two pipes were reached by the system with a length ratio $L1/L = 0.5$. The measured values, max c_e, both for polyethylene pipes and steel pipes are a function of the exponent *A1/A2* cross-section (where *A1* is the area on the pipe outlet, and A2 is the cross-section of the intake pipe).

Changing the relative celerity of oscillation c_{emax}/c_i as a function of the ratio of pipeline cross-sections *A1/A2* is essentially the same for both considered pipelines (steel and polyethylene). Figure 50 presents the results obtained analytically for both polyethylene pipes as well as steel pipes as a graph of a continuous function. Almost full compliance of the course of both functions could be observed. The graph also includes a marked trend line that is much in agreement with the course of two analytic functions ($R2 = 0.9993$), along with its equation. In addition, in order to verify compliance of the analytic course with the physical picture of the phenomenon, the values of equivalent velocities (c_{emax}/c), obtained as a result of measurements on the physical model, have been marked (● - points from measurements of polyethylene pipes, ■ - points from measurements of steel pipes). The difference in the measured and calculated values of equivalent celerity ranged from 1% to 7% for steel pipes and from 0.3% to 5% for polyethylene pipes.

The change of the equivalent celerity in relation to the individual celerity for a particular type of material has a consistent process for both tested materials, see Figure 50. The increase or decrease of the equivalent celerity is closely linked to the proportion of connected pipes and their lengths. Therefore, the equivalent celerity rate in the duct system can be easily assessed. Knowing the cross-sections of the connected pipes, the cross-section ratio A1/A2 must be calculated.

Knowing this ratio allows one to read the increasing or decreasing multiplier of the individual celerity for a given material from the graph, see Figure 50. In addition, for example, knowing that the cross-section ratio *A1/A2* = 2, it can be seen that c_e/c = 0.79. This allows one to calculate the equivalent celerity for steel c_e = 0.79*1,280 = 1,011 m/s (3,316.93 fps), as well as for polypropylene c_e = 0.79*390 = 308 m/s (1,010.50 fps).
This algorithm allows for the quick and easy determination of the important parameters describing the course of the water hammer phenomenon in a system of pipes connected in series.

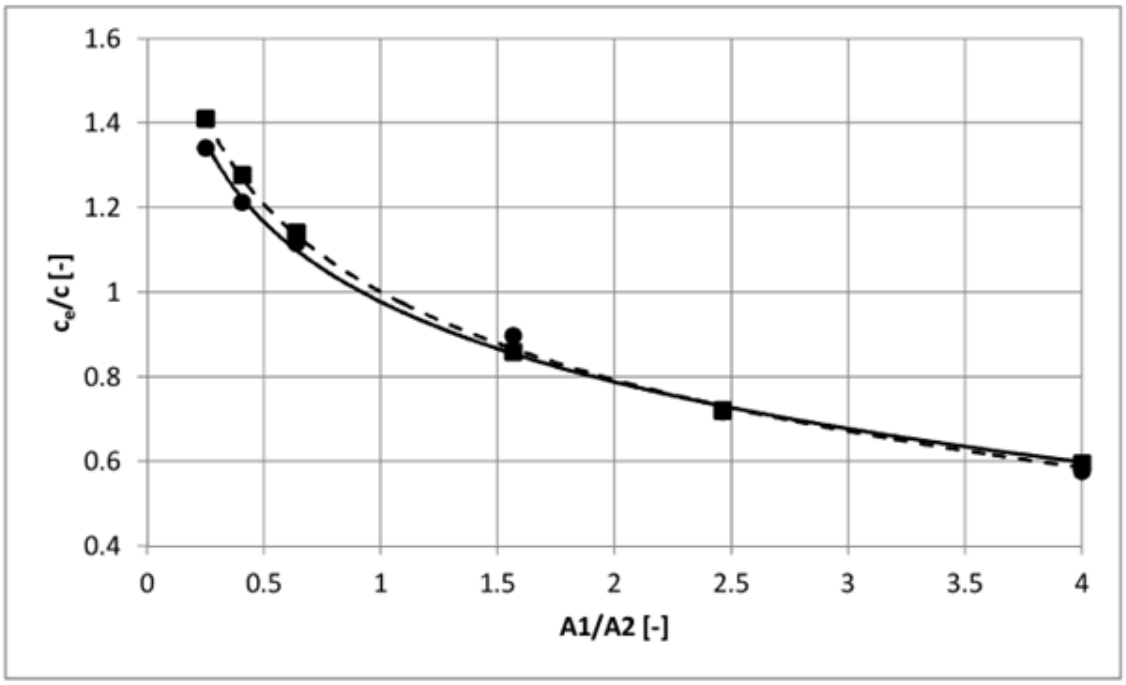

Figure 50 The ratio of the maximum pressure oscillation celerity versus wave celerity in a single (uniform) pipeline for steel and polyethylene pipes as a function of the pipe cross-section coefficient**.**

The natural vibration analysis equations can also be used for a quick estimation of the equivalent celerity for a piping system made of different materials. The equations presented in this thesis include two and three pipe systems connected in series. For the calculations of any number of serially connected pipes of varying diameter, length, and material composition, a MATLAB algorithm has been presented. To calculate the equivalent celerity in any mixed system of serially connected pipes, it is enough to know the individual celerity for a given material, diameter, length and alignment sequence of the connected

pipes. The accuracy of the obtained computations falls within common accuracy limits of engineering computation. Using the analysis of natural vibrations, one can create, in an analogous manner, an algorithm for a series of connected pipes with disbursements along the way. Using the algorithm will speed up the design process and facilitate the supervision of safety control water supply systems, such as those for fire prevention purposes (and many more).

The presented algorithm makes it possible to calculate the maximum pressure increase in water hammer for any number of serially connected pipes of any diameters, lengths and materials. It should be noted, however, that the presented equations were derived for the integer lengths of pipes L, which allows the determination of the pressure increase in the section of the gate valve. However, knowing the boundary conditions, such as the location of gate valves, pumps or pipe branching, the pressure increase in any cross-section x, without the need to refer to differential equations, can be calculated by modifying the presented equations. Equations for a parallel connected pipe system can be derived in a similar way. The presented equations are limited to positive pressure increases, unfavourable low pressures cannot be analysed (e.g. negative pressure or vapor pressure) by Malesinska A. (2018). The limit of this model is the number of elements that can be processed by the algorithm. The algorithm in MATLAB allows an easy calculation of the equivalent speed of the water hammer wave for any configuration of the series of connected pipes: diameter, length, material (for a maximum of 5 variables). For this reason, considering that in water networks (fire system, irrigation ...) there are more complex configurations than those analysed, the objective is to implement the numerical model and to exceed the limit of the 5 variables.

GENERAL CONCLUSIONS

It can be said that this work provides researchers, designers and testers with useful tools for a better evaluation of the water hammer phenomenon (especially fire protection systems).

In short, this work has been set up in order to communication, in the style of a "report", that which has been done and produced in these 3 doctoral years.

From Chapters 2,3 and 4 we see a progression in research and analysis of the water hammer. The first years were dedicated to a greater exploration of this phenomenon and to the interaction that it can have with other phenomena, such as cavitation. Subsequently, the forces and displacements in fire-fighting systems were analysed. In concluding the work, the equivalent celerity in pipes with different diameters, materials

and lengths has been studied. This last part of the research has allowed a numerical model to be obtained that can calculate and homogenize the equivalent celerity for pipelines with different diameters, lengths and materials (up to a maximum of 5 variabilities). This numerical model was successfully compared with a physical model at the Warsaw Polytechnic Laboratory. Making the homogeneous equivalent celerity for different pipelines allows a calculation to be obtained of pressures generated by the most correct water hammer.

This work has been published in major scientific journals and at international conferences, gaining interest from numerous researchers. The next step will be to implement the algorithm for the calculation of the equivalent celerity.

Notation

A – pipeline cross-section area,
C – constant, passive capacitive reactance,
D – pipeline diameter,
D_0 – outer diameter of the pipe,
E – water compressibility module,
H – difference of ordinates of the system endings, power level of the liquid column, H_D – upstream end of the pipe, H_U – downstream end of the pipe,
H_{0R} – static pressure in the tank,
L – length,
L_b – passive inertial resistance,
Q – volumetric flow rate, Q_D – upstream end of the pipe, Q_U – downstream end of the pipe,
R – resistivity of the pipeline per unit of length,
T – measured period,
Z_C – proper impedance determined for the liquid in a specific pipeline, resistivity
c – wave head celerity in water hammer [m/s],
c_e – equivalent wave head celerity in water hammer,
e – wall thickness of the pipe,
g – acceleration due to gravity,
n – power exponent,
p – pressure, Δp – change of pressure,
p_0 – initial pressure,
p(t) – characteristics of the water hammer pressure,
s – permanent, complex frequency (Laplace transform) $s = \sigma + i\omega$, σ – real part, iω – imaginary part,
t – valve closing time,
v – velocity before closing the valve,
x – any position in the pipeline,
t_r – returning time of the first reflected pressure wave to the outlet side of the pipe,
t_z – bar closing time,
v_0 – stream velocity,
γ – propagation constant of disturbance
ζ – factor depend on Reynolds number,
H – viscosity,
λ – multiplication factor of the friction element,
ρ – density,
ω – circular frequency.

BIBLIOGRAPHY

Agnieszka Malesińska, Ph.D., Mariusz Rogulski, and Pierfabrizio Puntoreiri, Giuseppe barbaro Beata Kowalska. “Equivalent celerity in water hammer for serially connected pipelines.” *ASCE's Journal of Pipeline Systems - Engineering and Practice*, 2018.

Al-Khomairi, A., & Ead, S.,. “Sizing of a plastic chamber with air-filled balls for water hammer control.” *Advances in Fluid Mechanics VIII Conference.* 2010.

Allievi, L. “General theory of the variablemotion of water in pressure conduits.” *Annali della Società degli In-gegneri ed Architetti Italiani*, 1902: 285–325.

Anderson, A. “Celebrations and challenges—Waterhammer at thestart of the 20th and 21st centuries.” *Proc., 8th Int. Conf. on PressureSurges, , BHR Group.* Cranfield, U.K, 2000. 317–322.

Barton N, Parry A. “Using CFD to understand multiphase gas measurement. .” *Measurement and Control (United Kingdom)*, 2013: 50-57.

Batterton, Shawn. *Water Hammer: An Analysis of Plumbing Systems, Intrusion, and Pump Operation.* Blacksburg Virginia, 2006.

Brown, F.T., Margolis, D.L., Shah, R.P. “Small Amplitude Frequency Behavior Fluid Lines with Turbulent Flow.” *J.Basic Eng., Tran. ASME*, 1969 : 678-693.

Bruce, S., and David, S. Water Hammer:. “Water Hammer: Practical Solutions.” *Butterworth-Heinemann, London*, 1995.

Brunone, B., Karney, B., Mercarelli, M., Ferrante, M. “Velocity Profiles and UnsteadPipe Friction in Transient Flow. Journal of Water Resources Planning and Management.” *ASCE*, 2000: 236-244.

Bwire B., Onchiri R., Mburu N. “Simulation Of Pressure Variations Within Kimilili Water Supply System Using Epanet.” *International journal of civil engineering & technology (IJCIET)*, 2015: 28-38.

Cauchy. “Oeuvres Complétes.” Paris, 1890.

Christopher E. “Cloud cavitation: observations, calculations and shock waves.” *Multiphase Science and Technology*, 1998: 303-321.

Donghyuk, K. & Kazuhiko, Y. “Analytical Study of Cavitation Surge in a Hydraulic System. .” *ASME J. of Fluids Eng* , 2014.

Edwards JE, Otterson DW,. “Tech talk: (7) Floe measurement basics (Part 2). .” *Measurement and Control (United Kingdom)*, 2015: 115-121.

Euler. *De la Propagation du Son" Mérnoiresde l' Acad.* 1759.

Ferras D, Manso P, Schleiss A, Covas D,. “Fluid-structure interaction in straight pipelines with different anchoring conditions.” *Journal of Sound and Vibration*, 2017: 348-365.

Frizell, J. P. “Pressures resulting from changes of velocity ofwater in pipes.” *Trans. Am. Soc. Civ. Eng*, 1898: 819, 1–18.

Gale, J., Tiselj, I., Horvat, A. “Two-fluid model of the WAHA code for simulations of water hammer transients. .” *Multiphase Science and Technology*, 2008: 291-322.

Ghidaoui M, Zhao M, McInnis D, Axworthy D. “A Review of Water Hammer Theory and Practice.” *ASME*, 2005.

Ghidaoui, M. S., Zhao, M., McInnis, D. A., & Axworthy, D. H. “A Review of Water Hammer. Theory and Practice. .” *Applied Mechanics Reviews*, 2005: 49-76.

http://www.valvemagazine.com/magazine/sections/back-to-basics/8418-water-hammer.html. n.d.

Janson, L.E. “Plastics Pipes for Water Supply and Sewage Disposal.” *Borealis, Sweden*, 1995.

Joukowsky, N. “On the hydraulic hammer in water supply pipes.” *Mémoiresde l’Académie Impériale des Sciences de St.-Pétersbourg*, 1898.

Kries, J. “On the relations between pressure and veloc-ity, which exist in the wavelike motion in elastic tubes.” 1883.

Lagrange. *MecaniqueAnalytique*. 1788.

Lescovich, Joseph, E.,. “The Control of Water Hammer by Automatic Valve.” *American Water Works Association*, 1967: 632-644.

Libraga, J, Ribeiro R, Covas, D, et al. “Experimental and Numerical Analysis of Water Hammer in a Metal Pipe Rig. .” *11th International Conference on Computing and Control for the Water Industry, Exeter, UK*. Exeter, UK., 2011.

Malesinska A., Rogulski M., Puntorieri P., Barbaro G., Kowalska B. “Displacements of the pipe system caused by a transint phenomenon using the dynamics forces measured in the laboratory.” *Measurement and control*, 2018: in press.

Malesinska A., Wojciech M., Puntorieri P., Barbaro G., Kowalska B. E. “Equivalent celerity in water hammer for serially connected pipelines.” *ASCE's Journal of Pipeline Systems - Engineering and Practice. In press*, 2018.

Malesinszka A. “Experimental study of water hammer-induced forces and deformations in dry pipe fire protection systems.” *Fire Safety Journal*, 2015: 16-24.

Meniconi S, Brunone B, Ferrante M. “Water-hammer pressure waves interaction at cross-section changes in series in viscoelastic pipes. .” *Journal of Fluids and Structures*, 2012: 33, 44-58.

Pipes, L.A. “Applied Mechanics for Engineers and Physicists.” New York: McGraw-Hill, 1958.

Psrmiakian. *Waterhammer Analysis*. 1963.

Puntorieri, P., Barbaro, G., Martins, N., Covas, D., Vincenzo, F.. “Hydraulic Transient Experimental Study In A Copper Pipe.” *9th International WIT Conference on Computational & Experimental Methods in Multiphase & Complex Flow.* TALLIN: WIT, 2017.

Puntorieri. P., Barbaro G., Fiamma V. “EXPERIMENTAL STUDY OF THE TRANSIENT FLOW WITH CAVITATION IN A COPPER PIPE SYSTEM.” *International Journal of Civil Engineering and Technology (IJCIET)*, 2017.

Rankine, W. J. M. “On the thermodynamic theory of waves offinite longitudinal disturbance.” *Philos. Trans. R. Soc. London,* , 1870: 160,.

Shamloo H., Mousavifard M. “Numerical simulation of turbolent pipe flow for water hammer.” *ASME journal of Fluids*, 2015: 137(11).

Soares, A., Martins, N. & Covas, D. “Investigation of Transient Vaporous Cavitation: Experimental and Numerical Analyses.” *Procedia Engineering*, 2015: 119, (235–242).

Tijsseling, Arris S. “Johannes von Kries and the History of Water Hammer.” *JOURNAL OF HYDRAULIC ENGINEERING © ASCE* , 2007 .

valvemagazine. n.d.

Wood. “Hystory of water hammer.” Report, 1970.

“Fluid Transient in System.” By E.B., Streeter, V.L. Wylie. New York.: Prential Hall. Inc., Englewood Cliffs, 1993.

Zielke, W., Hack, H.P. “Resonance frequencies and associated mode shapes of pressurized piping systems.” *International Conference on Pressure Surge.* 1972. 6-8.

INDEX OF FIGURES

LIST OF TABLES

LIST OF EQUATIONS